

Diagnosing the Characteristic Interaction between the Polar and Subtropical Jet Streams during North American Jet Superposition Events

Andrew C. Winters

Daniel Keyser and Lance F. Bosart

University at Albany, SUNY

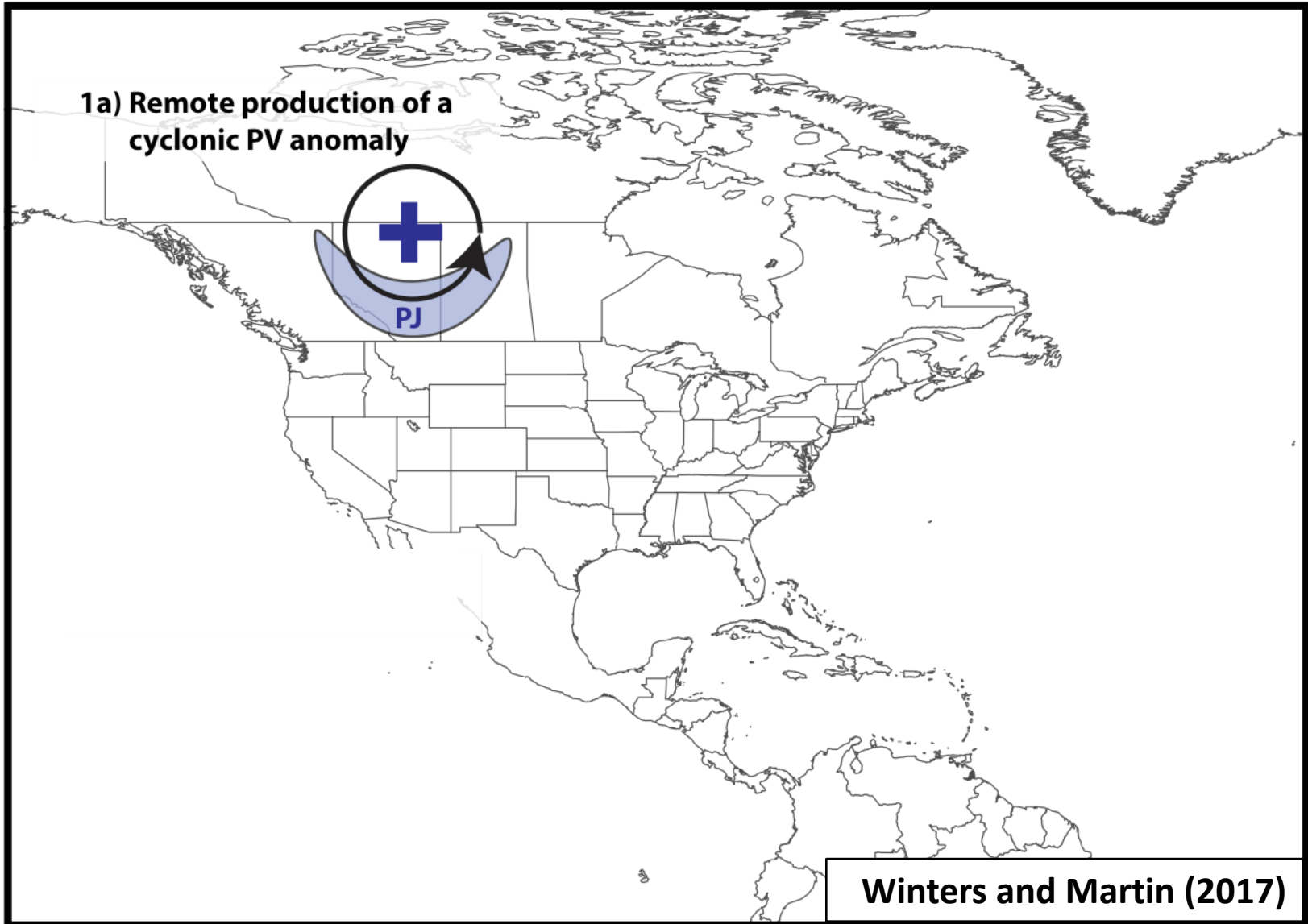


99th AMS Annual Meeting
32nd Conference on Climate Variability and Change
Phoenix, AZ

8 January 2019

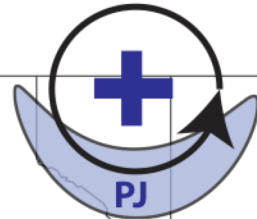
This work is funded by an NSF-PRF (AGS-1624316)

Jet Superposition Conceptual Model



Jet Superposition Conceptual Model

1a) Remote production of a cyclonic PV anomaly

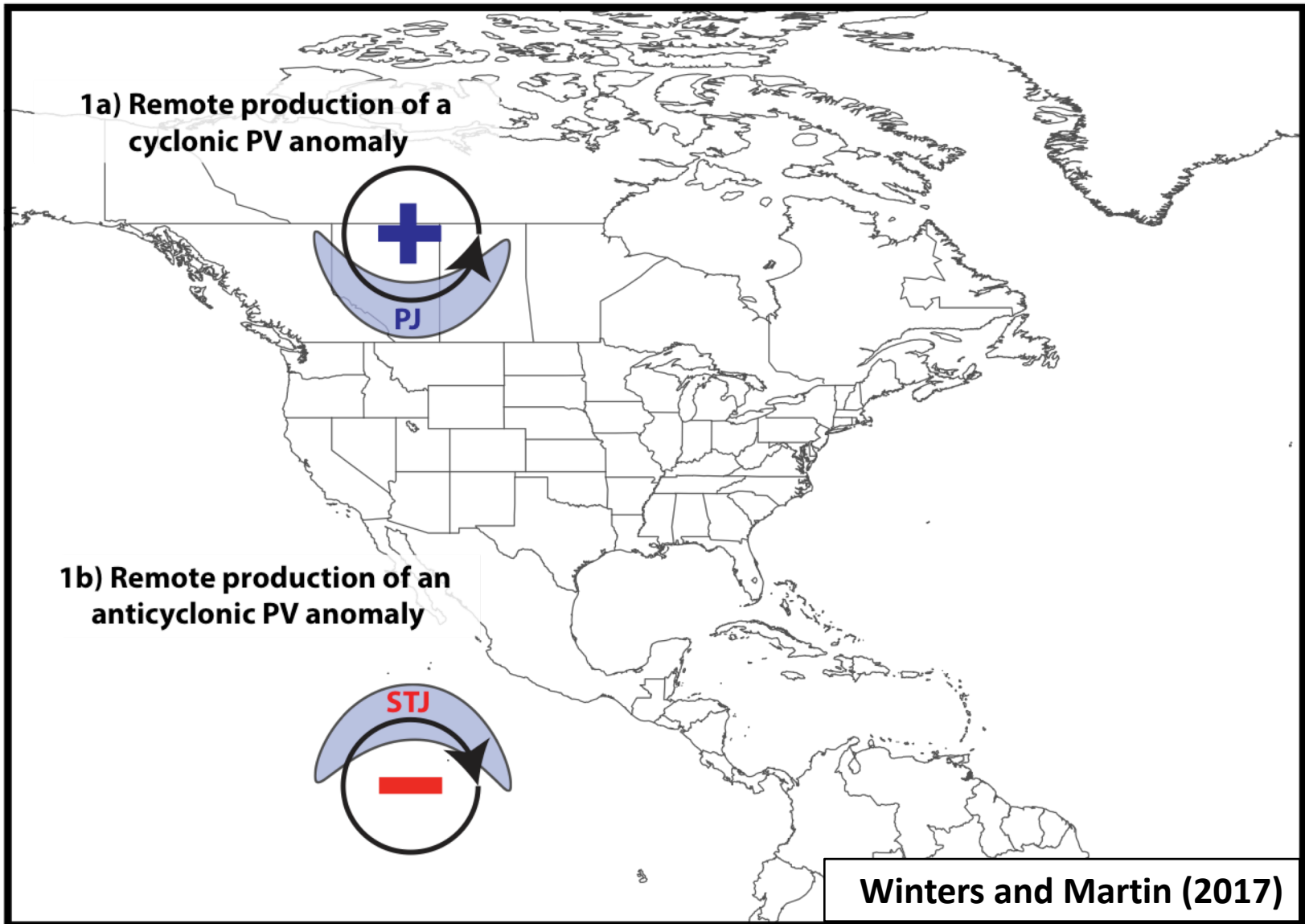


Polar cyclonic PV anomalies:

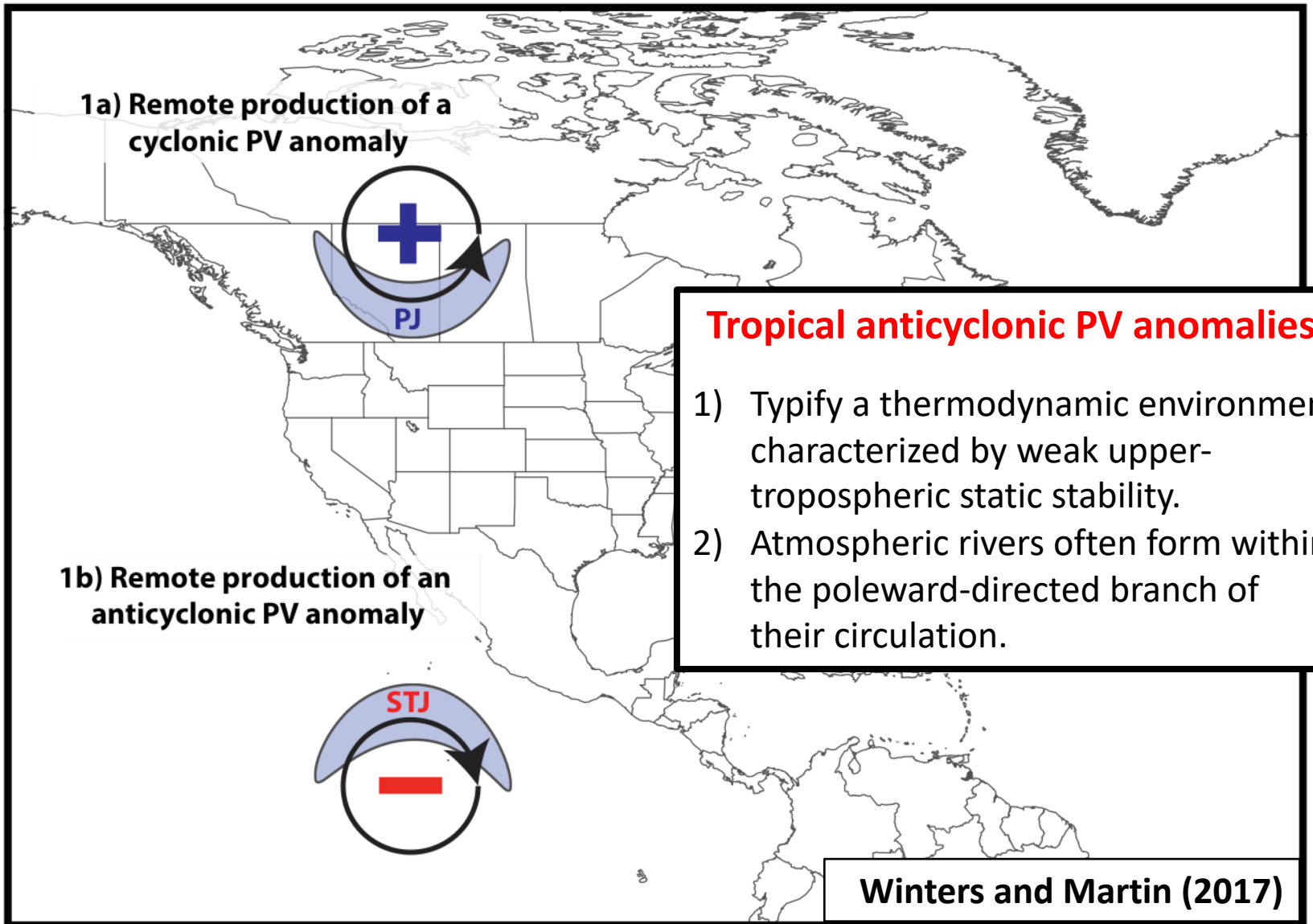
- 1) Often referred to as coherent tropopause disturbances (Pyle et al. 2004) or tropopause polar vortices (Cavallo and Hakim 2010).
- 2) Typify a dynamical environment conducive to midlatitude cyclogenesis.

Winters and Martin (2017)

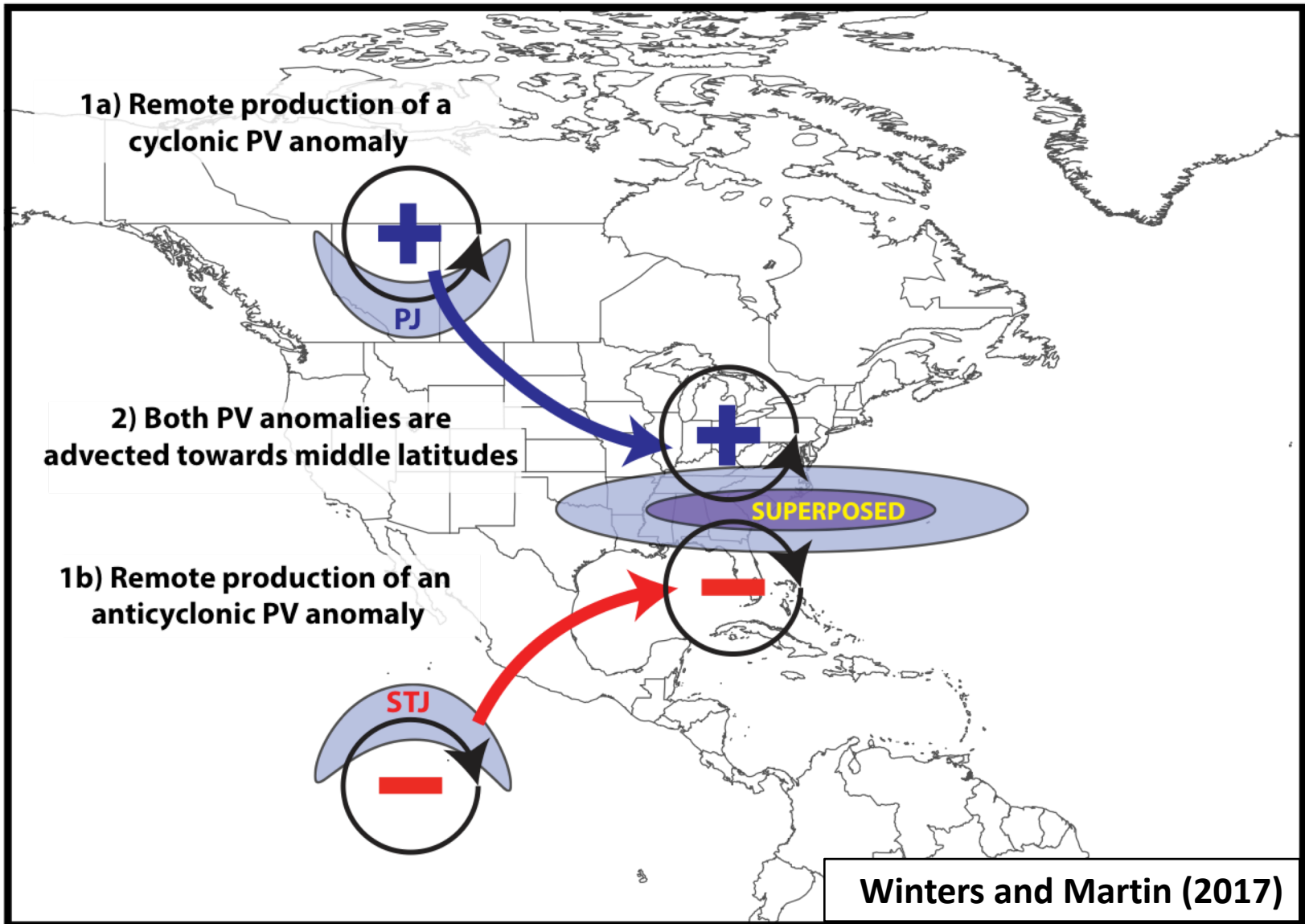
Jet Superposition Conceptual Model



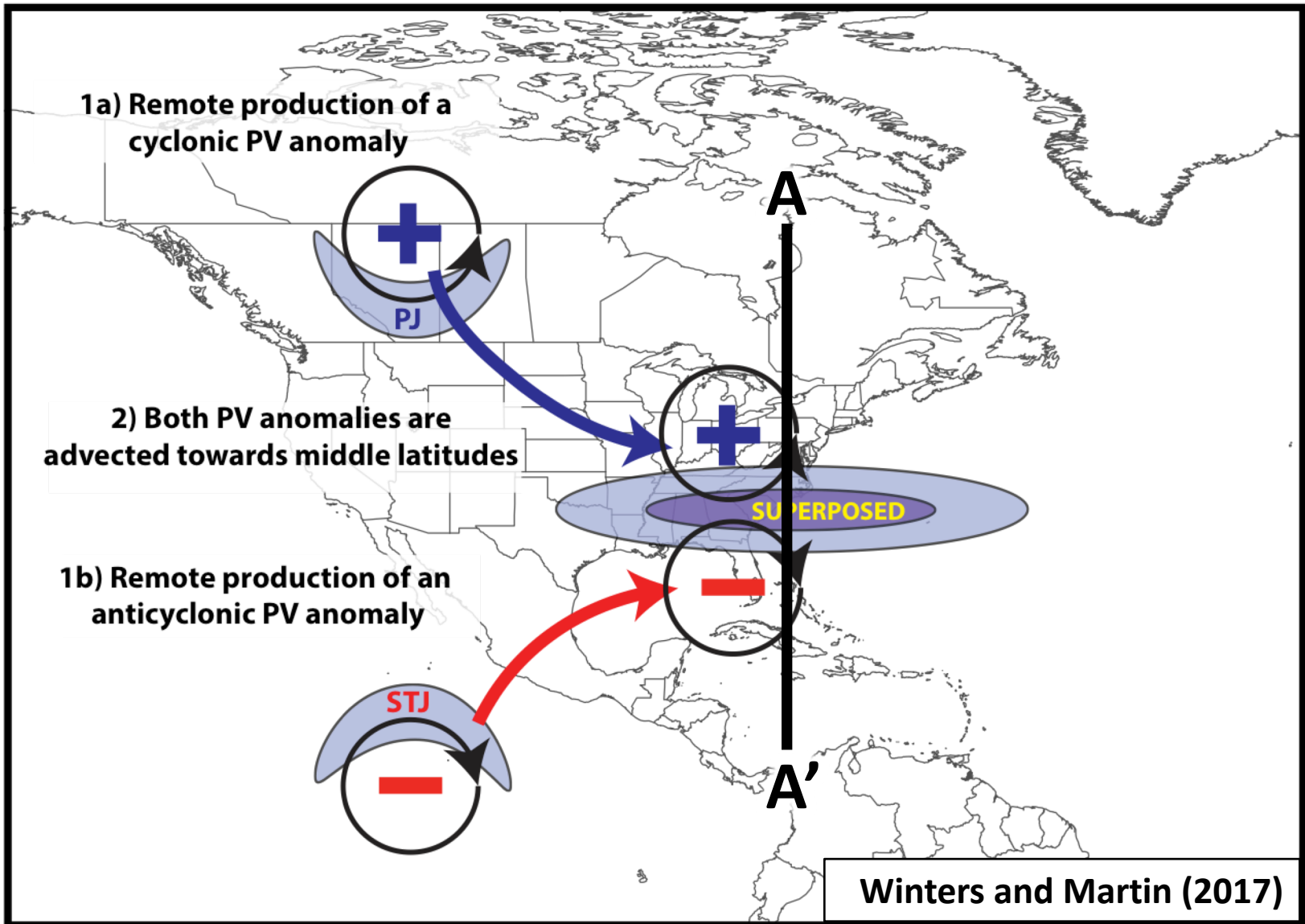
Jet Superposition Conceptual Model



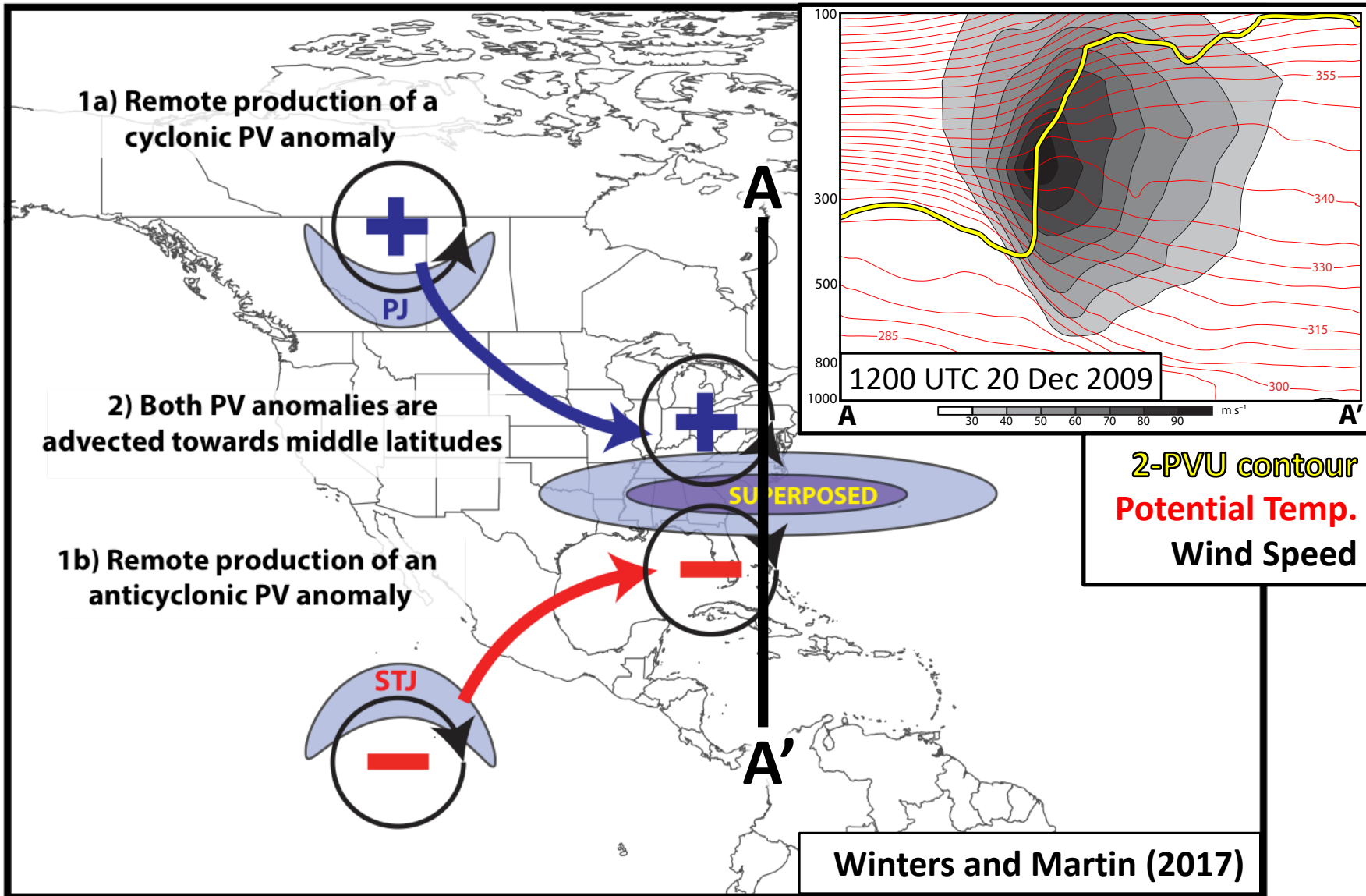
Jet Superposition Conceptual Model



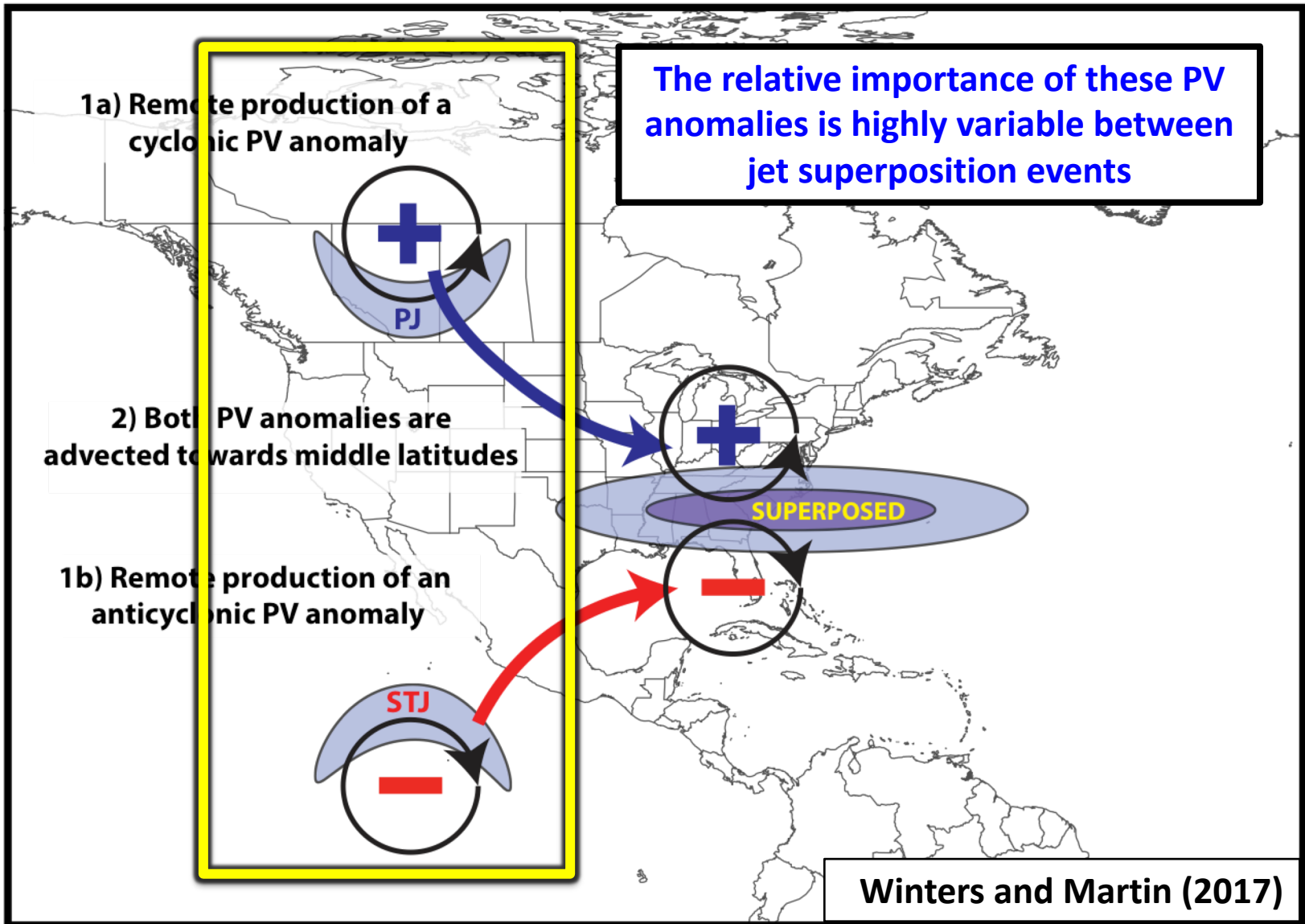
Jet Superposition Conceptual Model



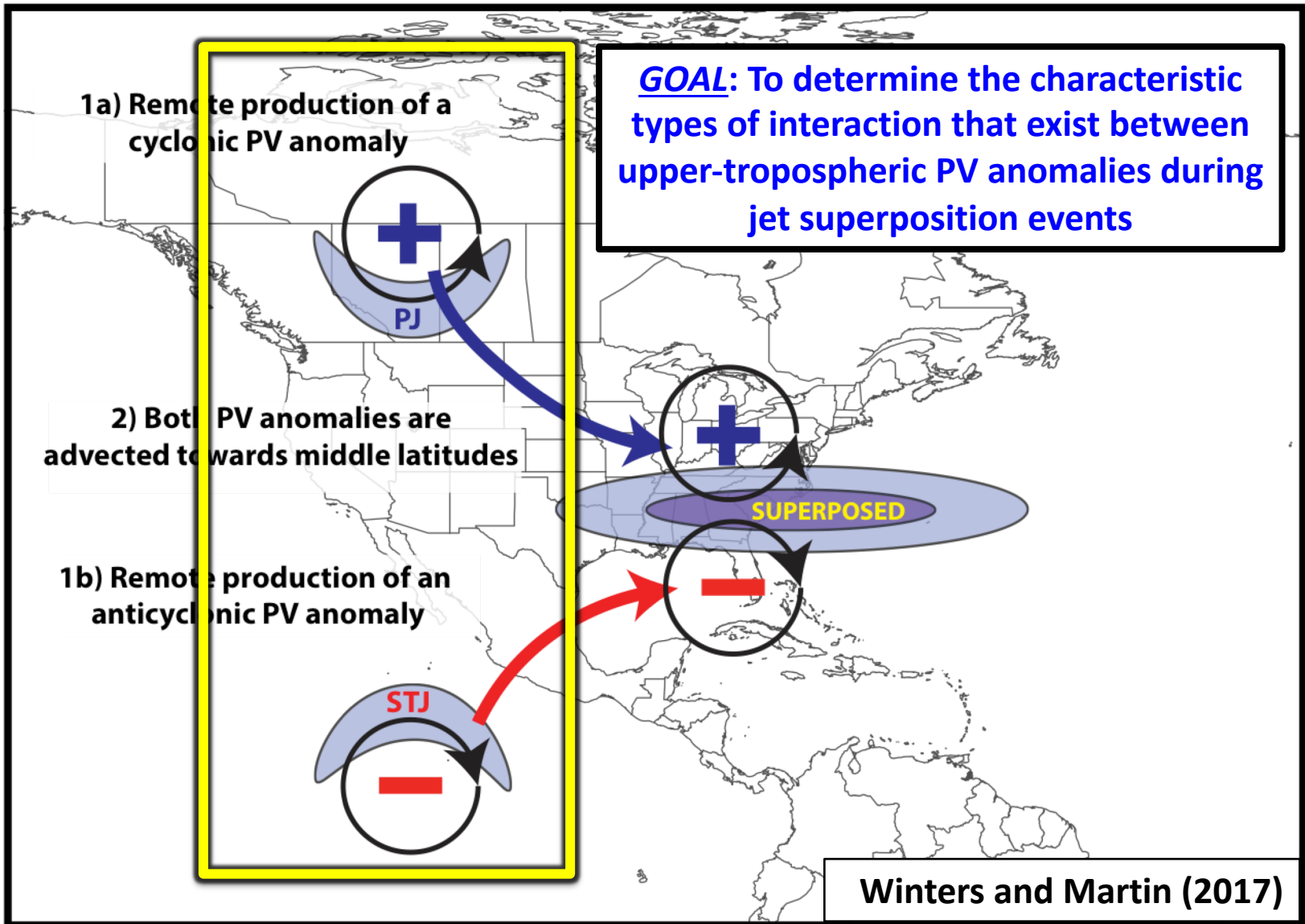
Jet Superposition Conceptual Model



Jet Superposition Conceptual Model



Jet Superposition Conceptual Model



Jet Superposition Event Identification and Classification

Jet Superposition Event Identification

- Isolated NCEP CFSR (Saha et al. 2014) grid points over North America characterized by a jet superposition during Nov.–Mar. 1979–2010 using the Christenson et al. (2017) scheme.
- Retained analysis times that rank in the top 10% in terms the number of grid points characterized by a jet superposition.
- Filtered retained analysis times to group together jet superpositions that are < 30 h and < 1500 km apart.

326 unique jet superposition events

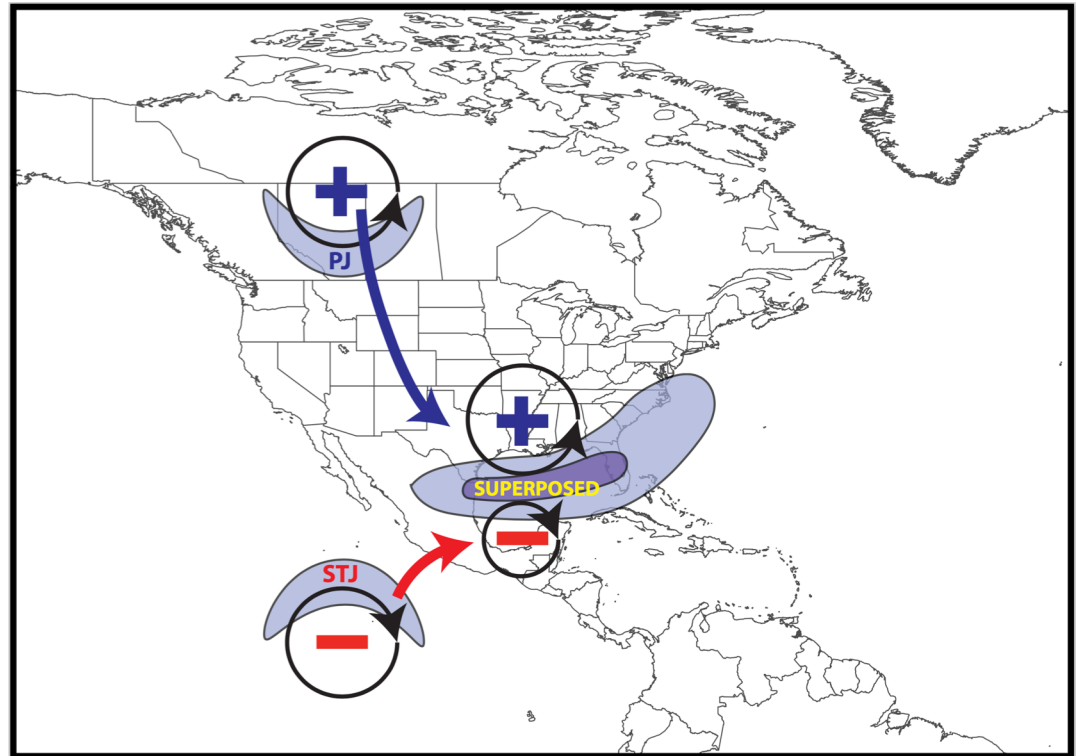
Jet Superposition Event Classification

- Classified jet superposition events into event types based on the deviation of the polar and subtropical jets from their respective climatological latitude bands at the time of jet superposition.

Jet Superposition Event Classification

- Classified jet superposition events into event types based on the deviation of the polar and subtropical jets from their respective climatological latitude bands at the time of jet superposition.

1) Polar Dominant (N=80)

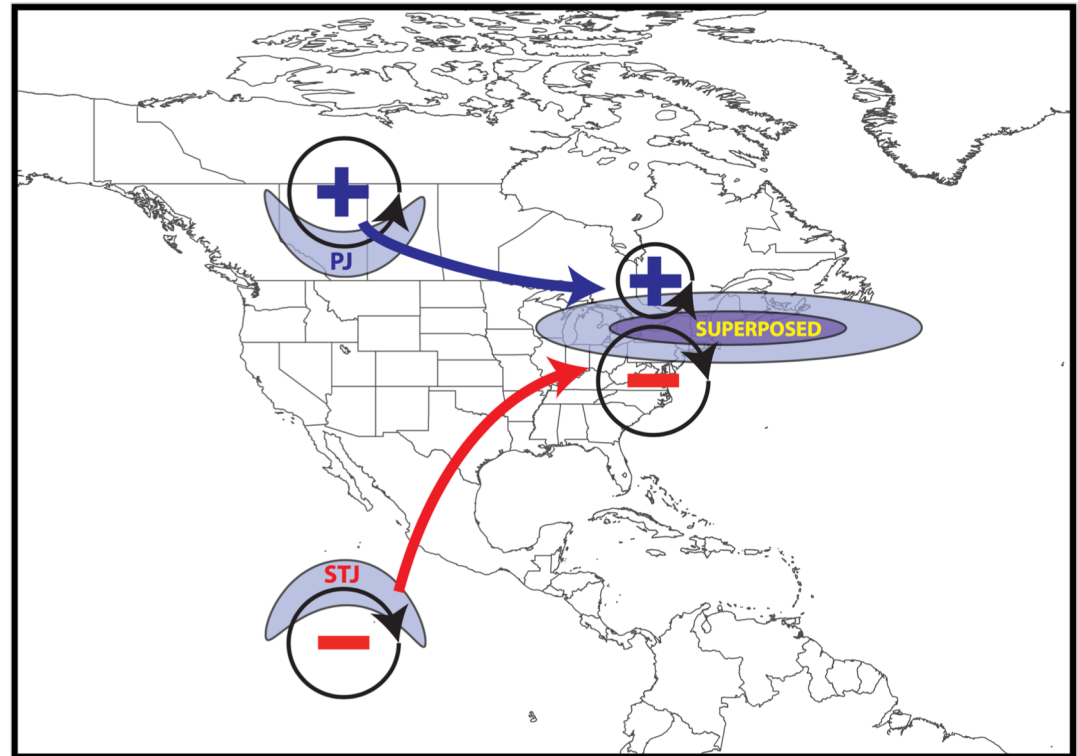


Jet Superposition Event Classification

- Classified jet superposition events into event types based on the deviation of the polar and subtropical jets from their respective climatological latitude bands at the time of jet superposition.

**1) Polar Dominant
(N=80)**

**2) Subtropical
Dominant (N=129)**



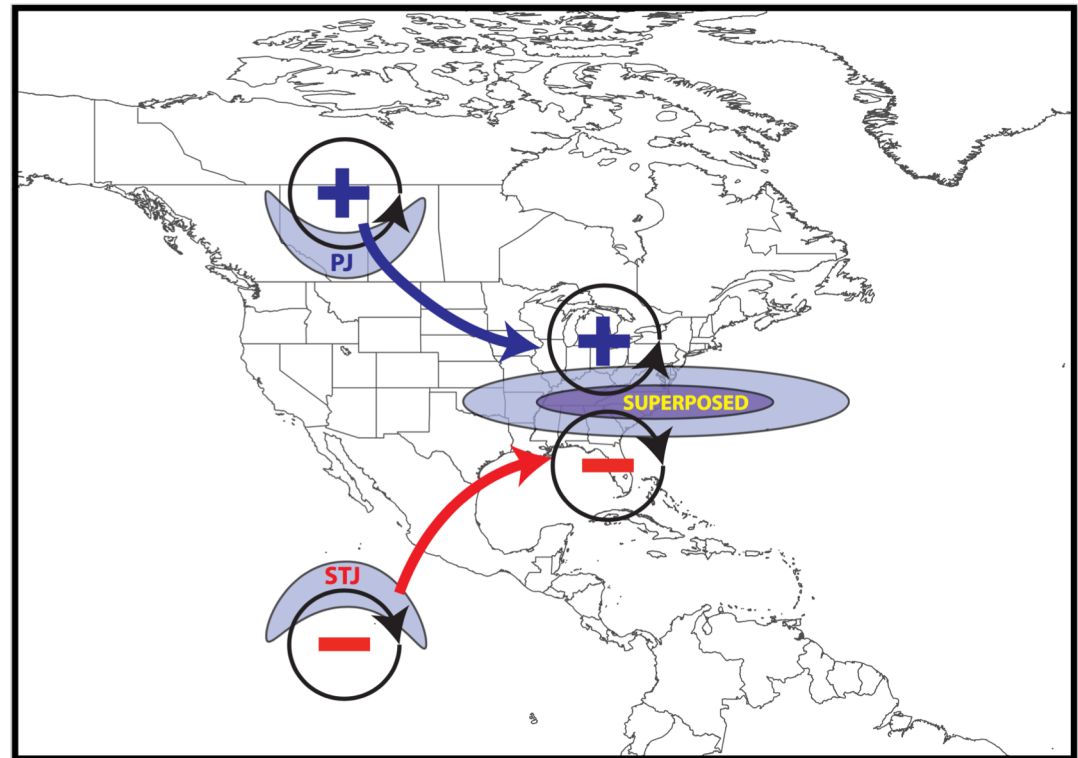
Jet Superposition Event Classification

- Classified jet superposition events into event types based on the deviation of the polar and subtropical jets from their respective climatological latitude bands at the time of jet superposition.

1) **Polar Dominant**
(N=80)

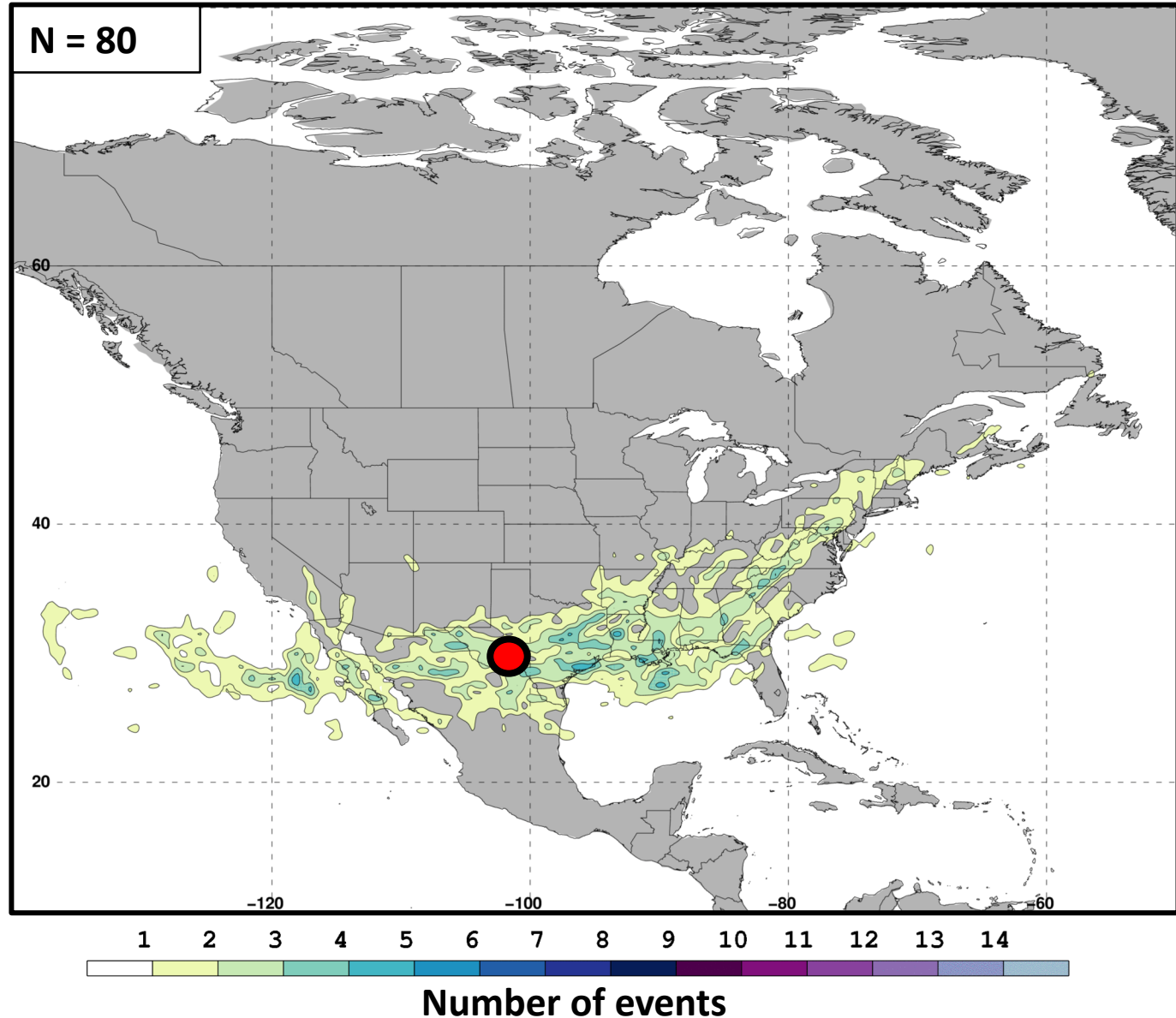
2) **Subtropical Dominant** (N=129)

3) **Hybrid** (N=117)



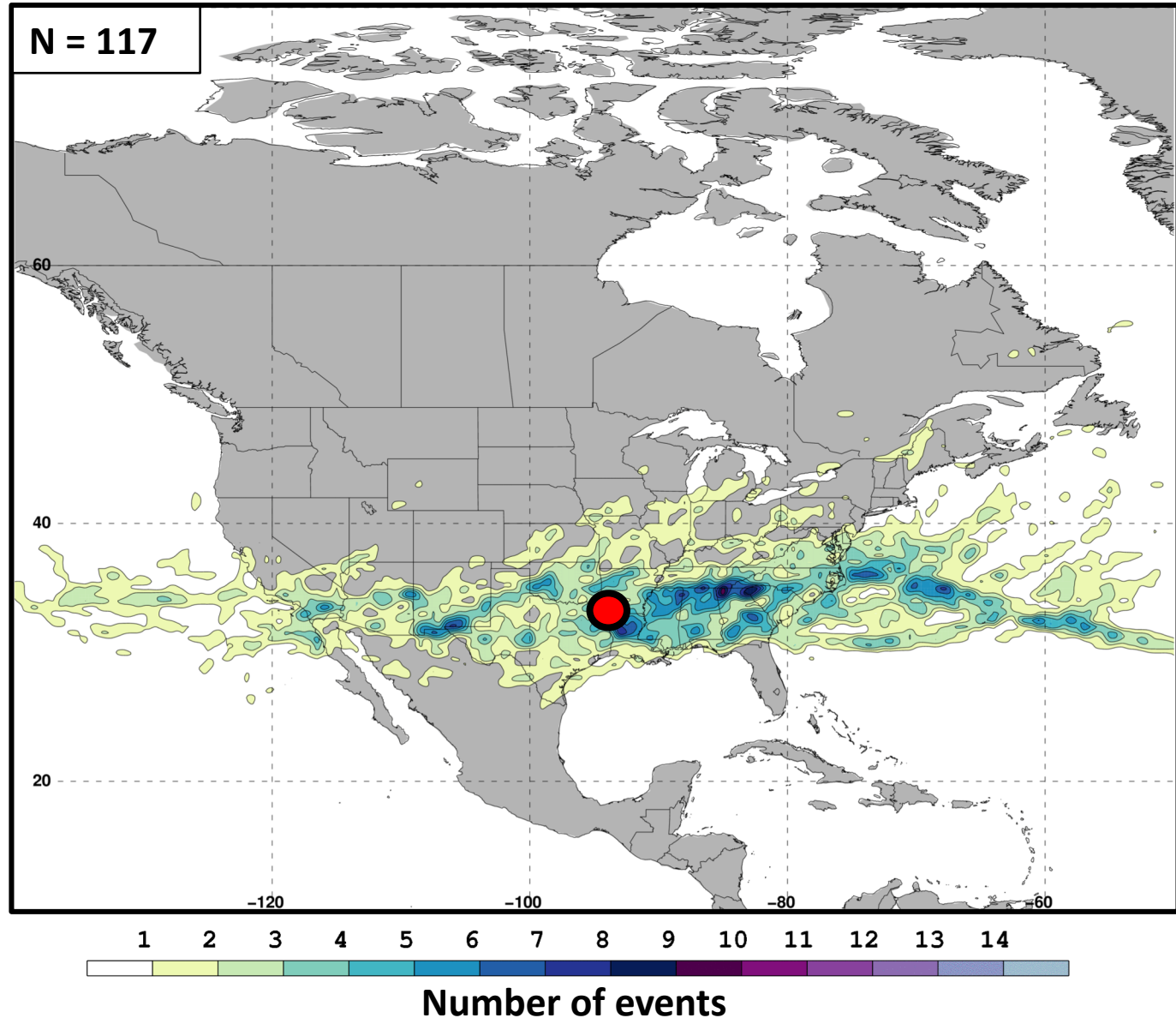
Jet Superposition Event Classification

Frequency of
Polar Dominant
Jet
Superposition
Events



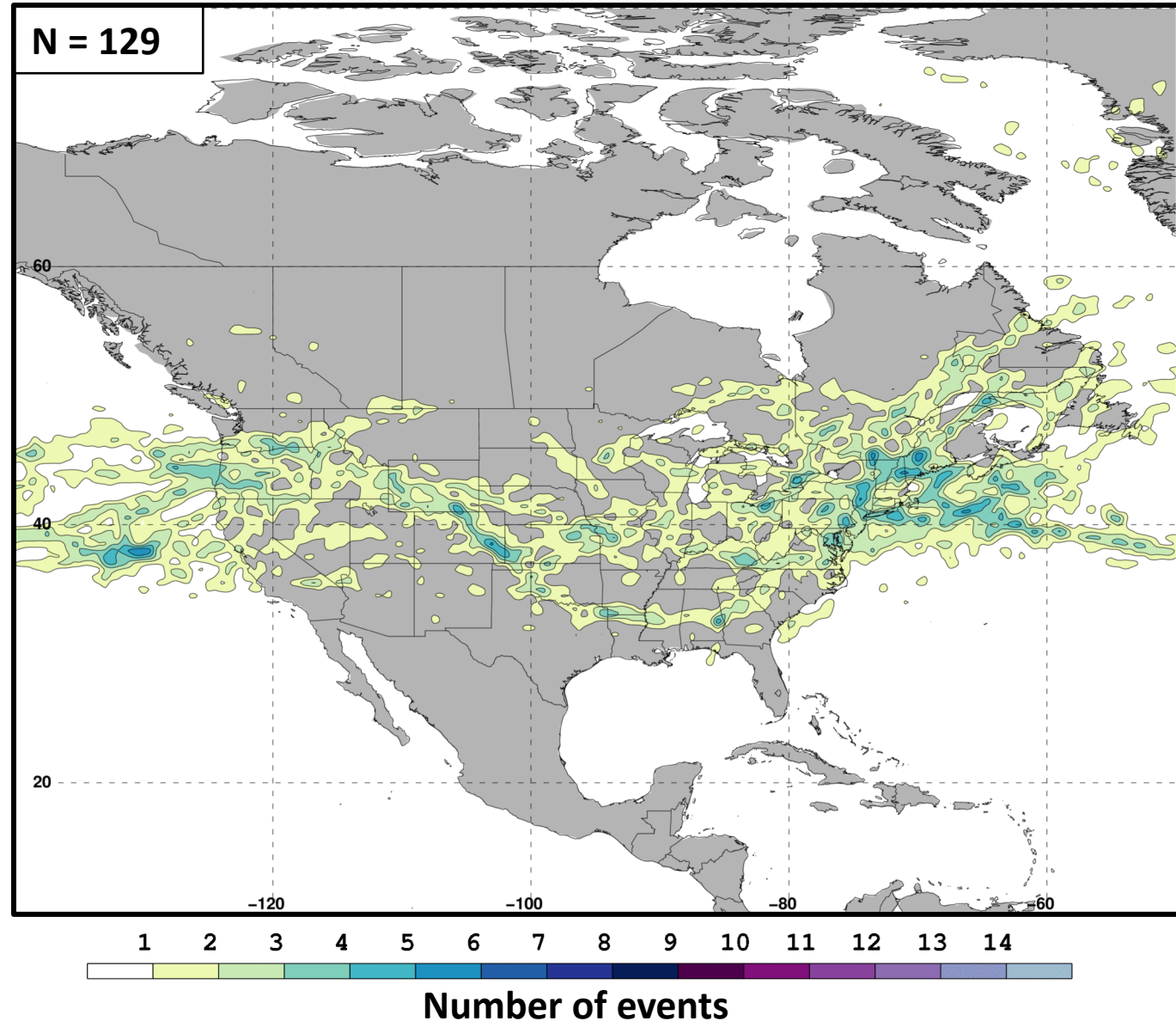
Jet Superposition Event Classification

Frequency of
Hybrid
Jet
Superposition
Events



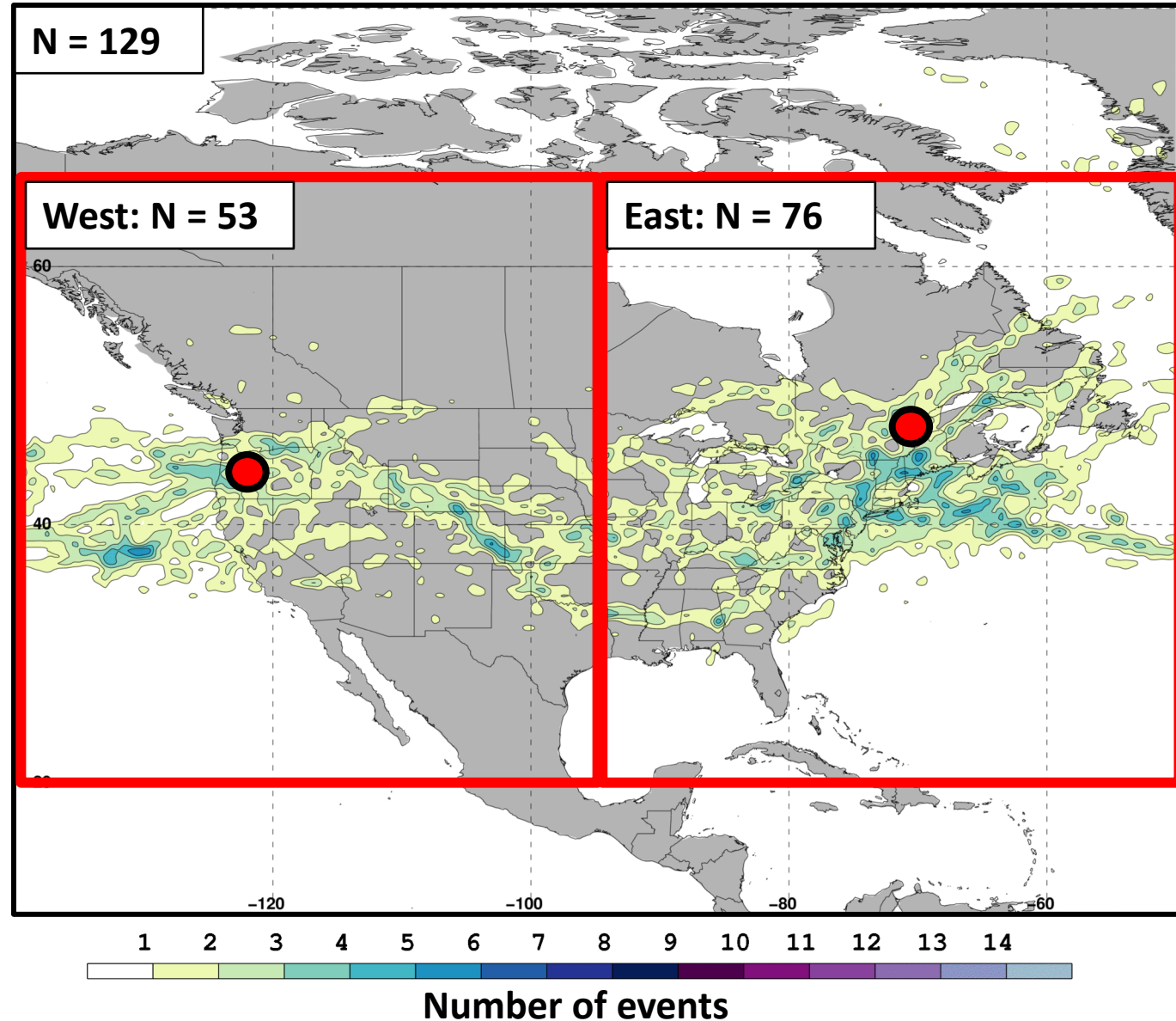
Jet Superposition Event Classification

Frequency of
**Subtropical
Dominant Jet
Superposition
Events**



Jet Superposition Event Classification

Frequency of
**Subtropical
Dominant** Jet
Superposition
Events



**Jet Superposition Event
Composites:**

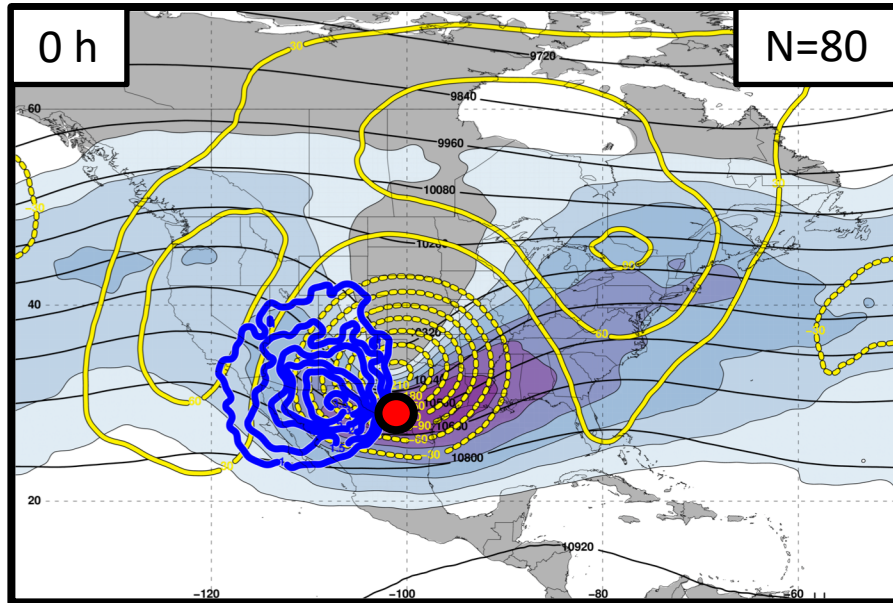
Polar Dominant

vs.

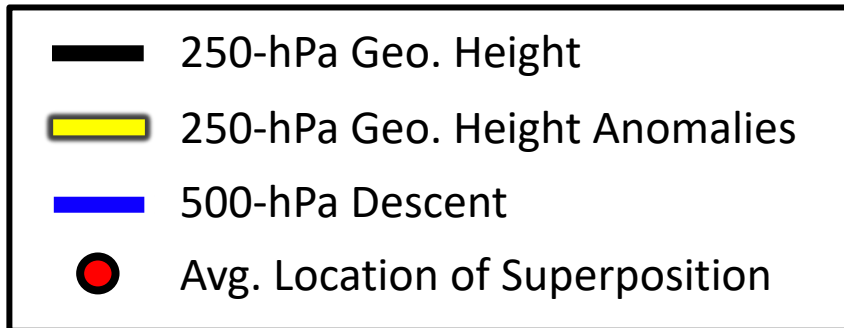
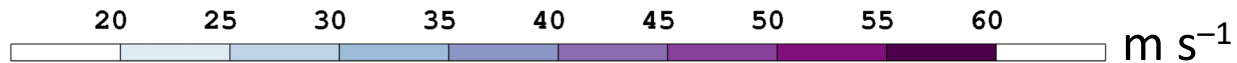
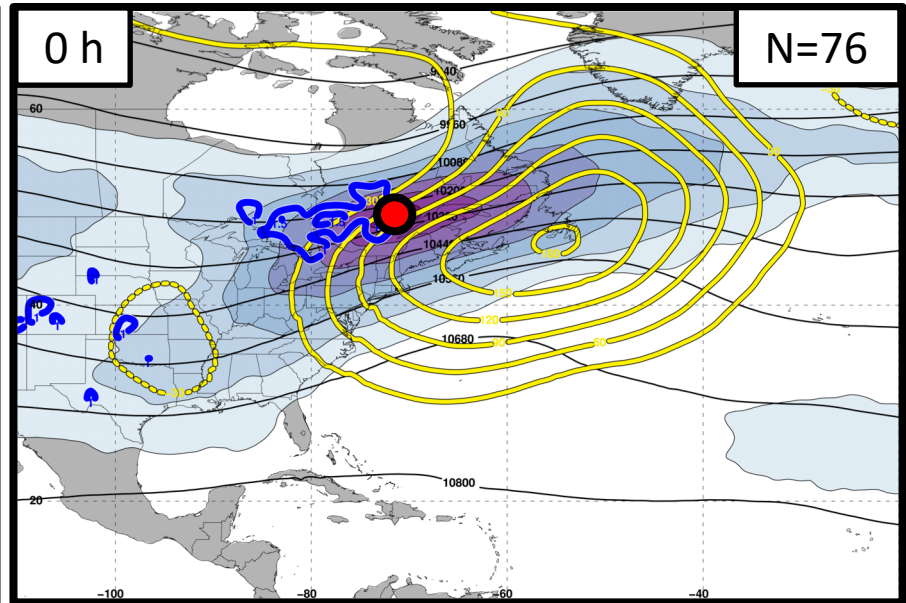
East Subtropical Dominant

Jet Superposition Event Composites

Polar Dominant Events

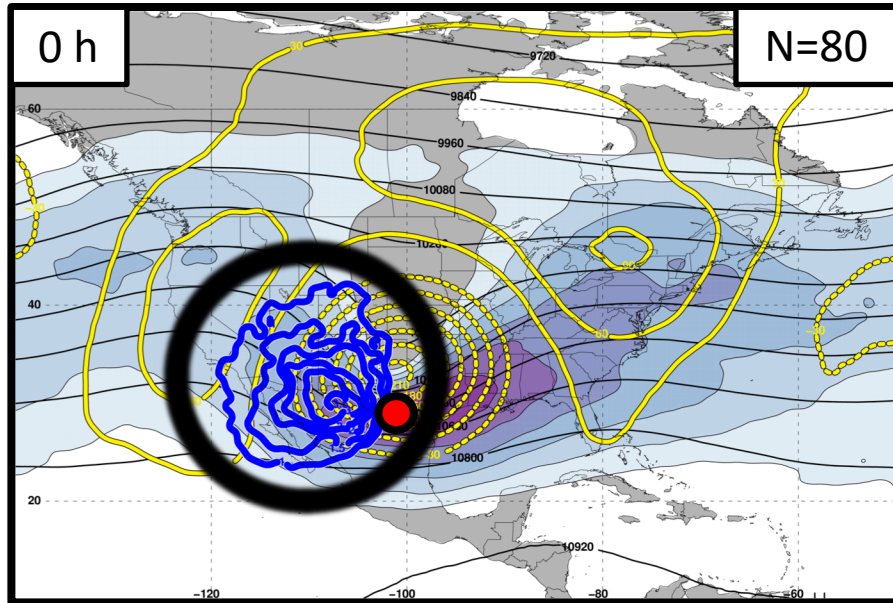


East Subtropical Dominant Events

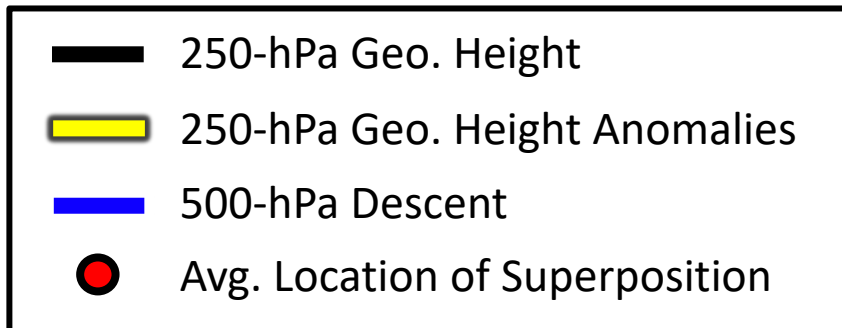
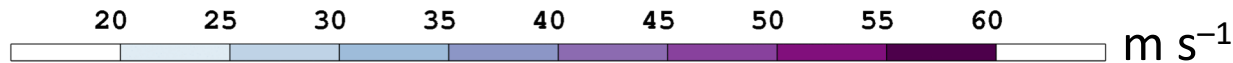
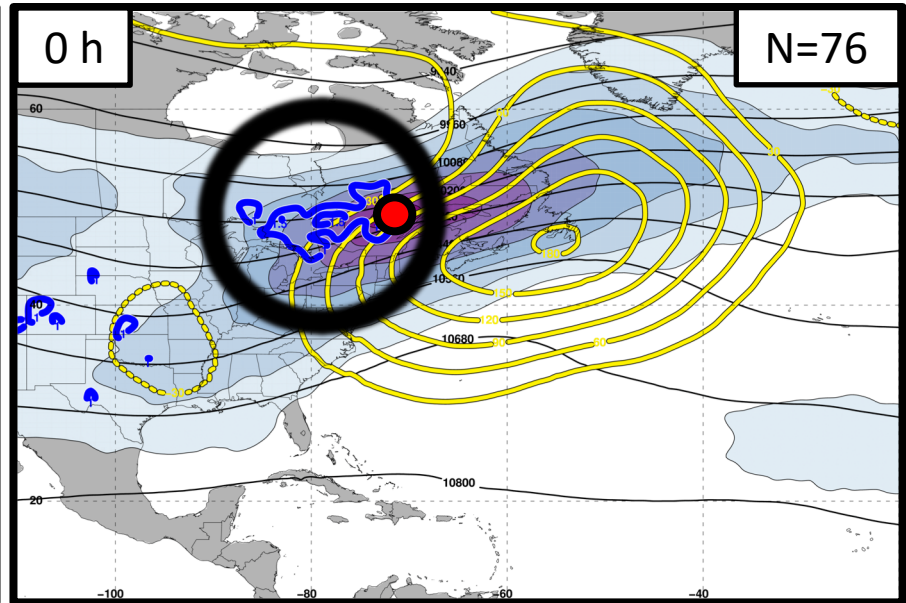


Jet Superposition Event Composites

Polar Dominant Events



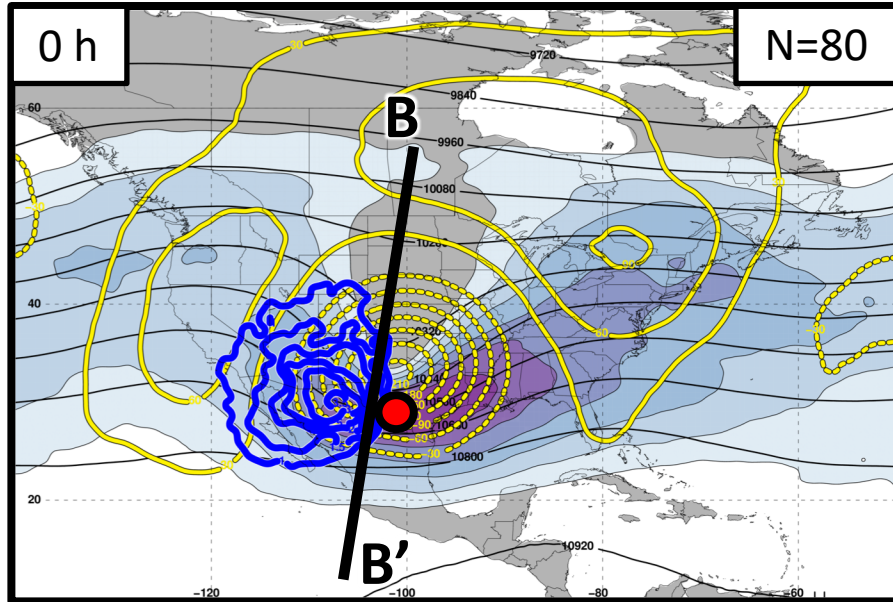
East Subtropical Dominant Events



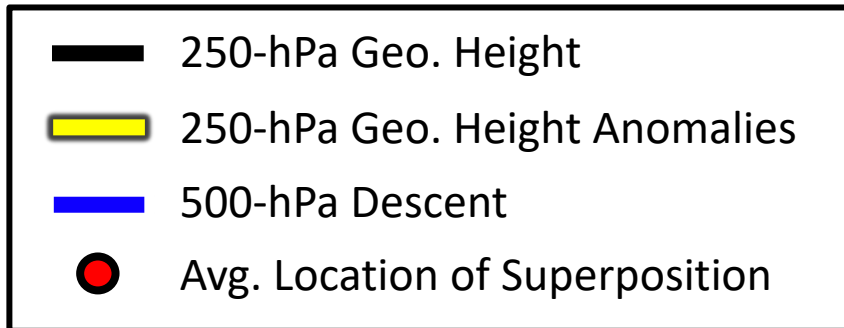
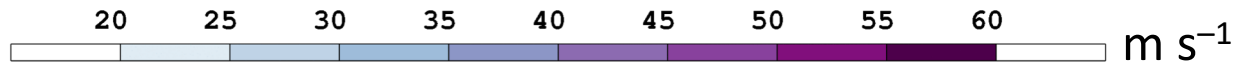
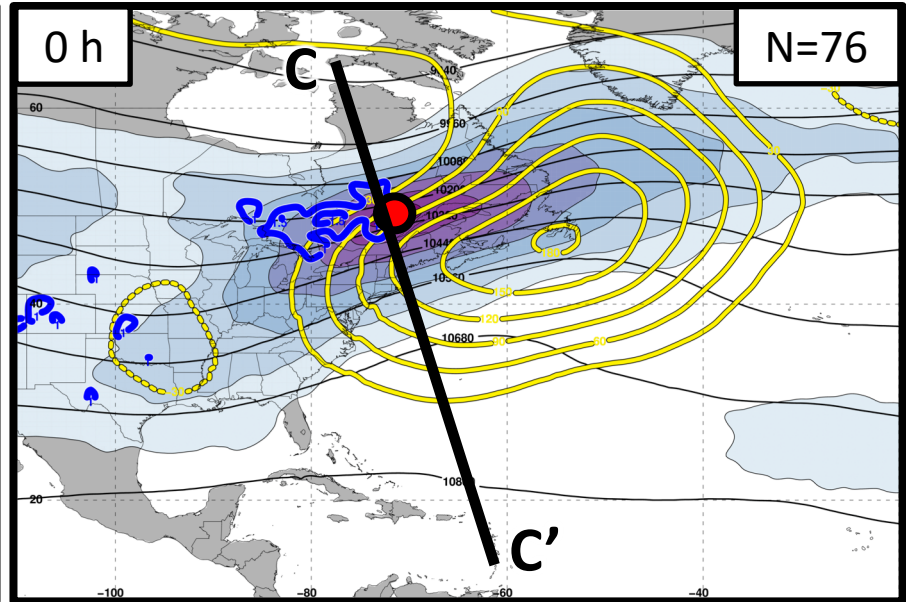
Descent within the jet-entrance region is a common element among the jet superposition event composites.

Jet Superposition Event Composites

Polar Dominant Events



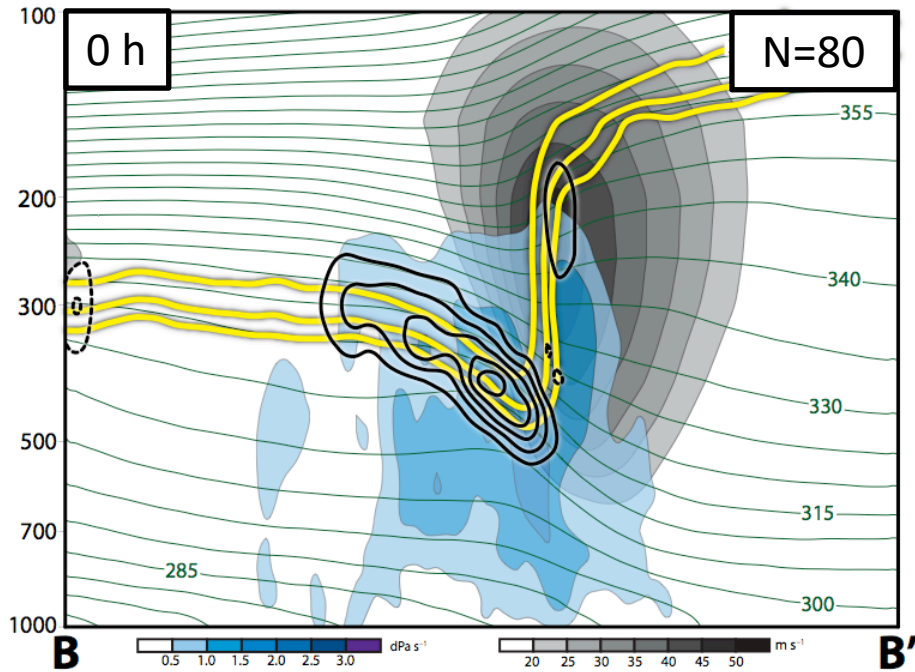
East Subtropical Dominant Events



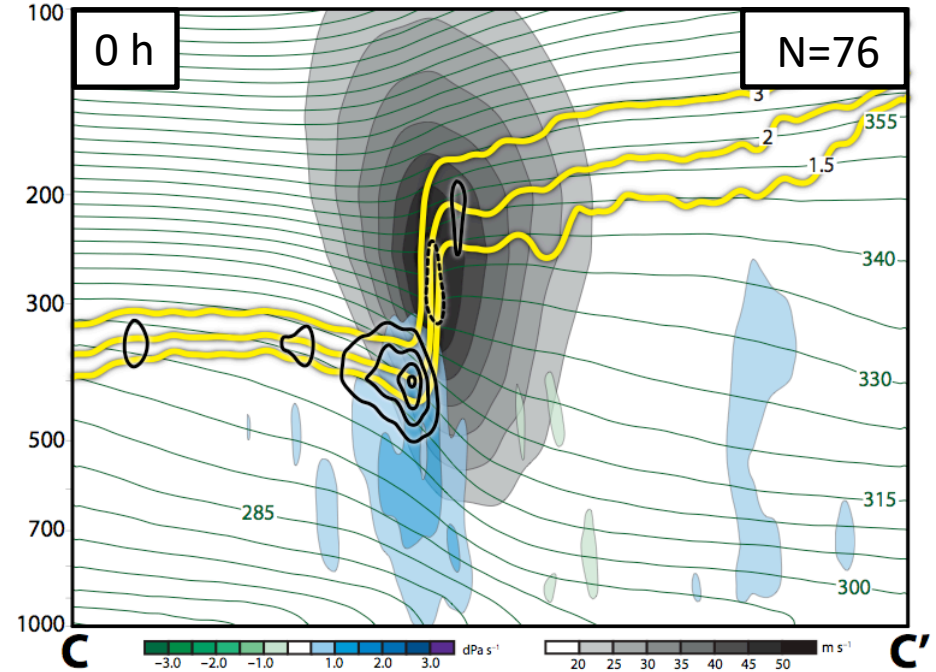
Descent within the jet-entrance region is a common element among the jet superposition event composites.

The Consistent Role of Descent

Polar Dominant Events



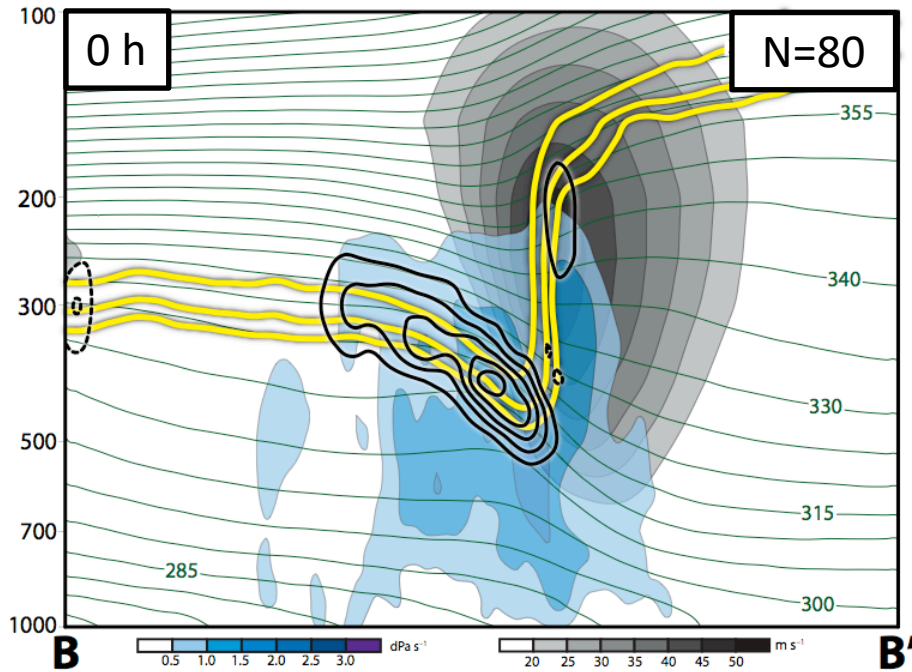
East Subtropical Dominant Events



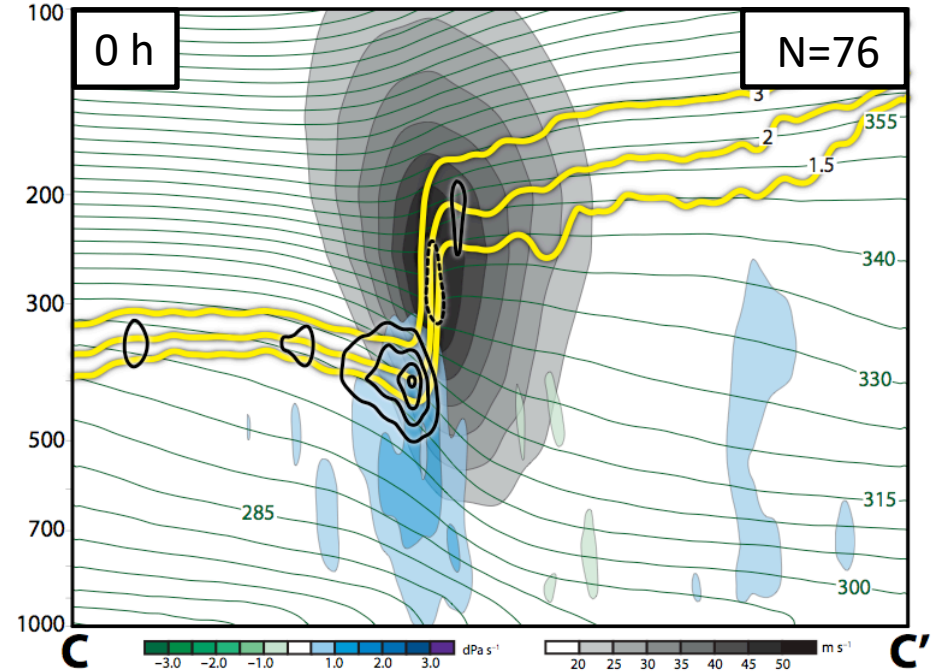
- 1.5-, 2-, 3-PVU contours
- Potential Temperature
- Positive PV advection
- Negative PV advection

The Consistent Role of Descent

Polar Dominant Events



East Subtropical Dominant Events

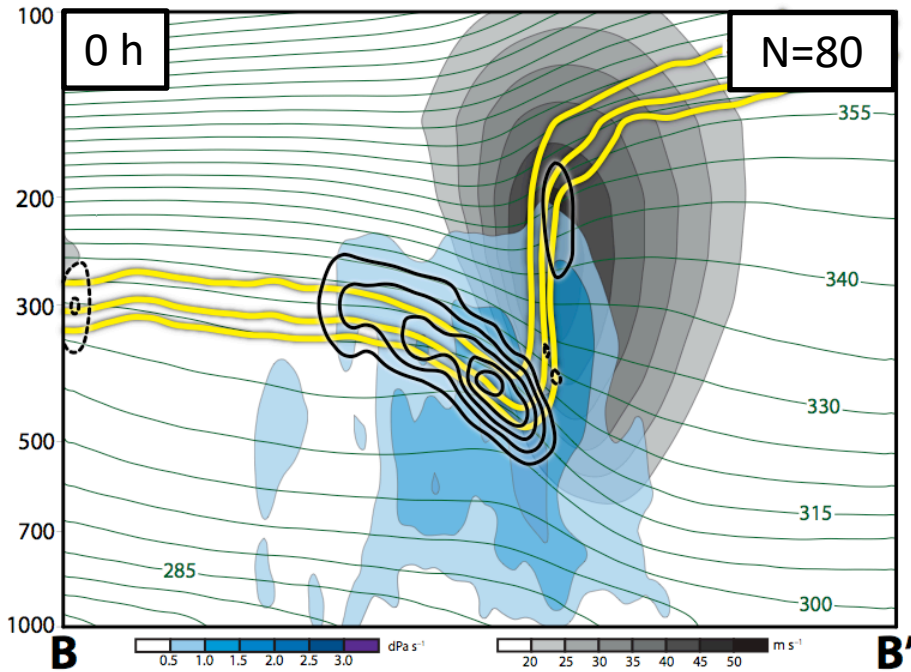


- 1.5-, 2-, 3-PVU contours
- Potential Temperature
- Positive PV advection
- Negative PV advection

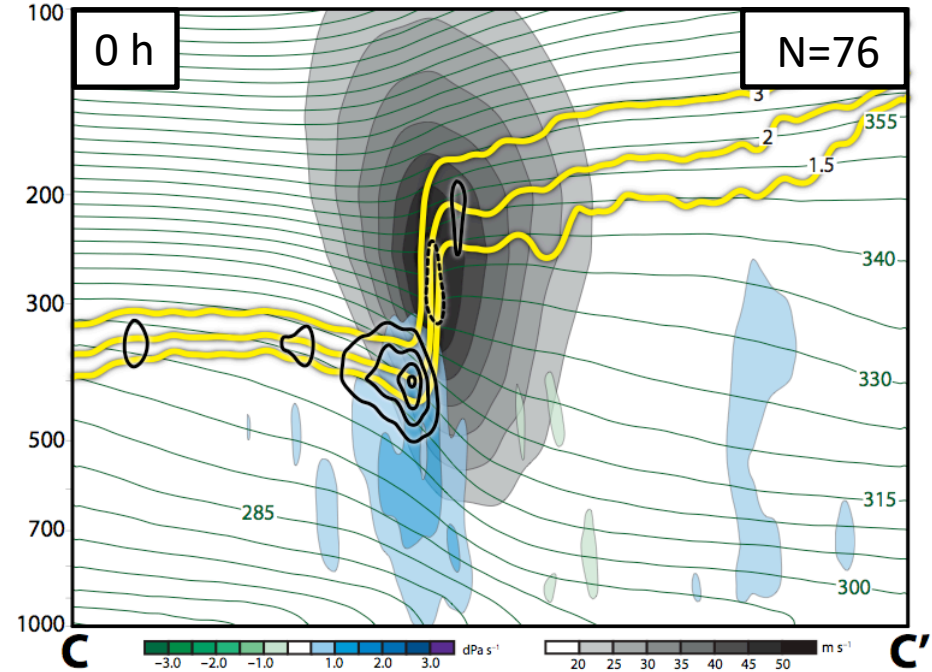
Descent results in downward PV advection within the developing tropopause fold, which acts to steepen the tropopause.

The Consistent Role of Descent

Polar Dominant Events



East Subtropical Dominant Events

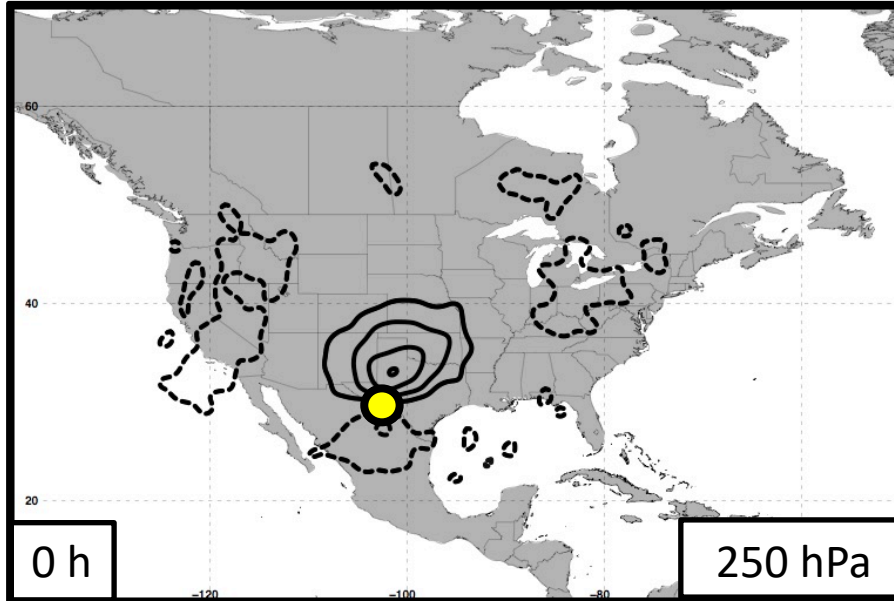


- 1.5-, 2-, 3-PVU contours
- Potential Temperature
- Positive PV advection
- Negative PV advection

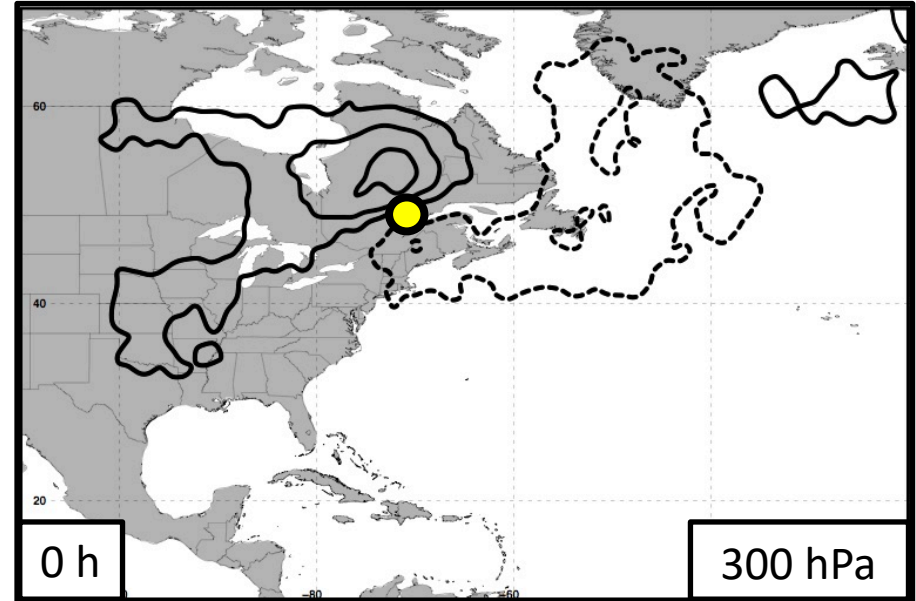
The consistent role of descent motivates further investigation of the dynamical mechanisms responsible for the observed descent.

QGPV Inversions

Polar Dominant Events



East Subtropical Dominant Events

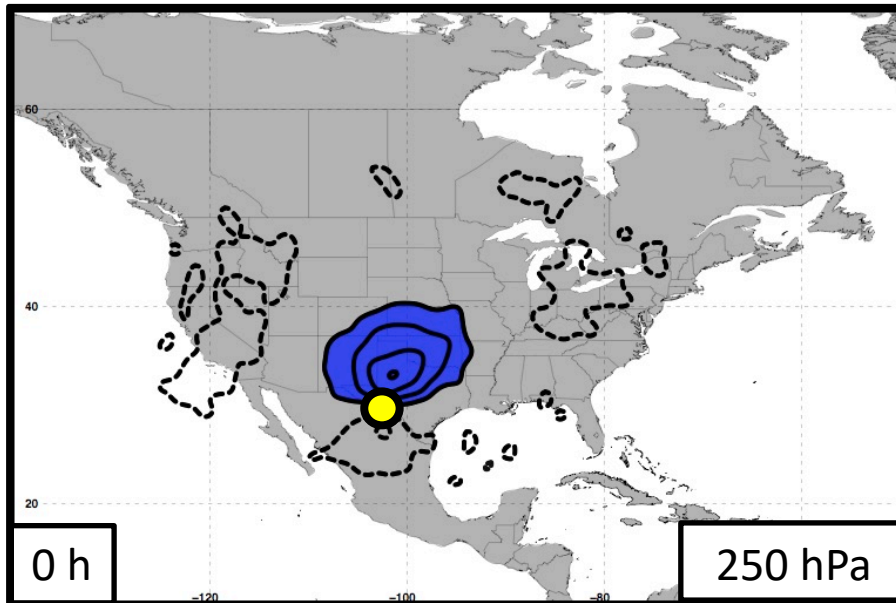


— + QGPV Anomalies - - - - - QGPV Anomalies ● Avg. Location of Jet Superposition

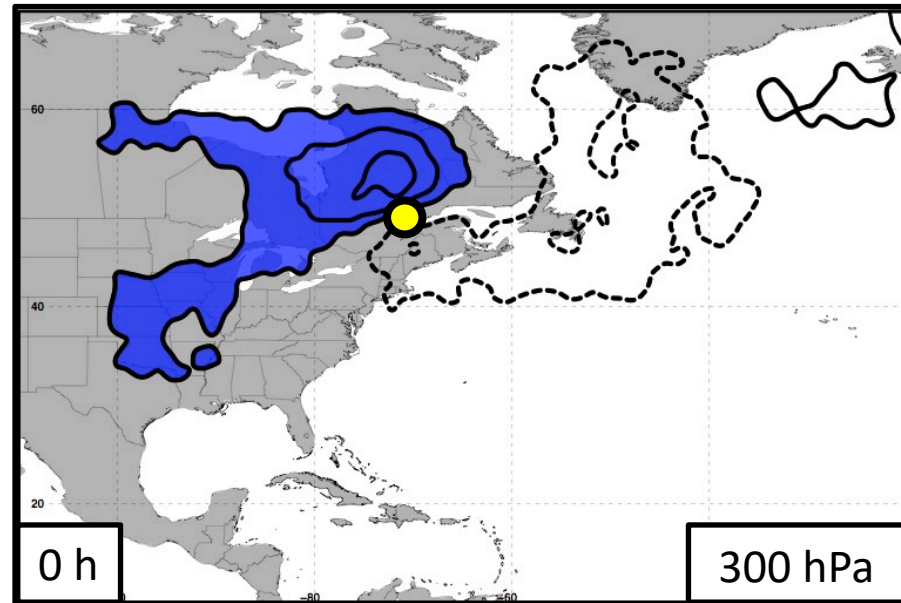
The descent characterizing each jet superposition event composite is examined further by isolating quasi-geostrophic (QG) PV anomalies in the vicinity of the jet superposition.

QGPV Inversions


Polar Dominant Events



East Subtropical Dominant Events

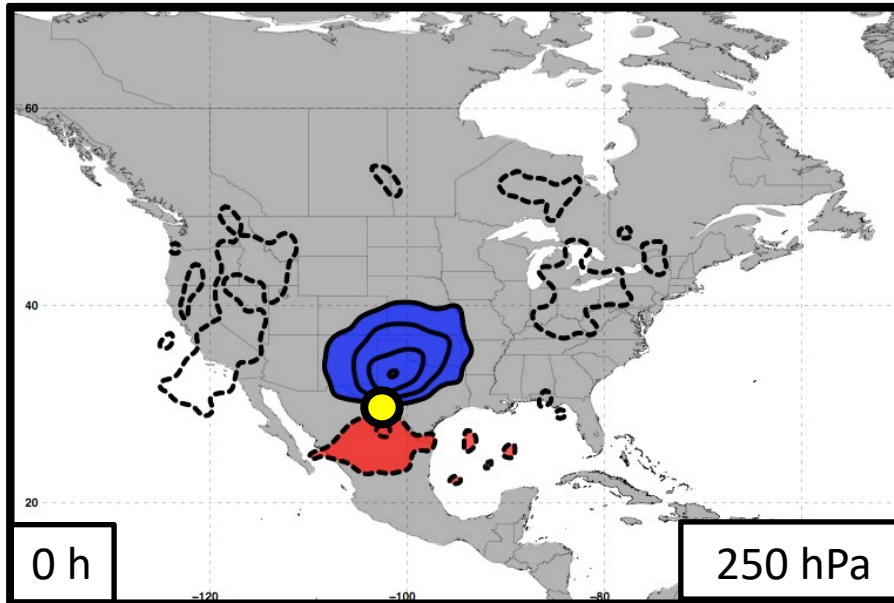


 Polar Cyclonic QGPV Anomalies

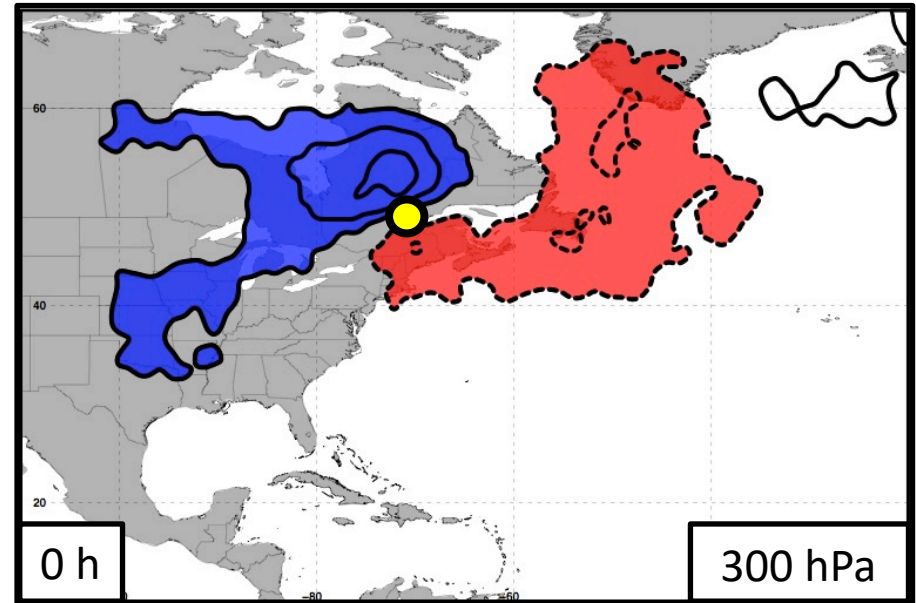
 Avg. Location of Jet Superposition

QGPV Inversions

Polar Dominant Events



East Subtropical Dominant Events

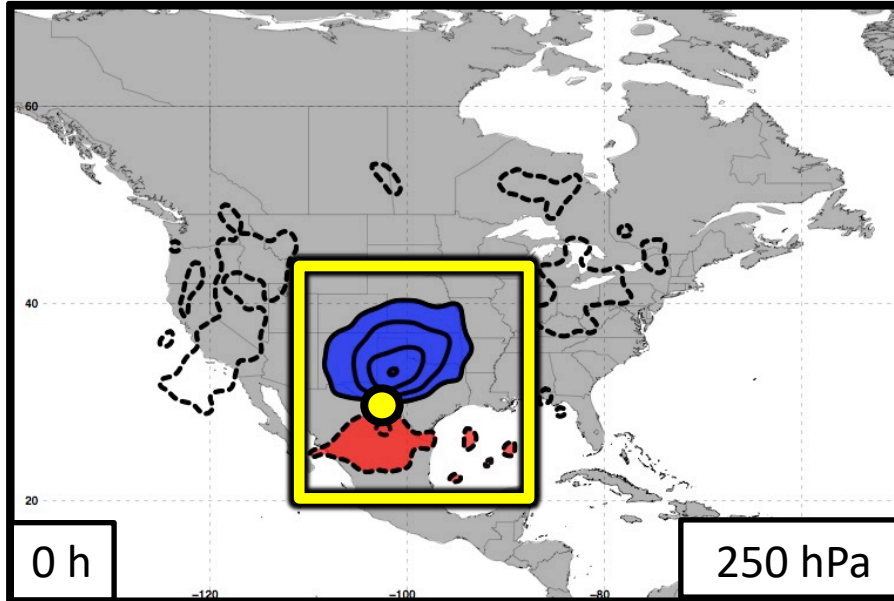


- Blue square: Polar Cyclonic QGPV Anomalies
- Red square: Tropical Anticyclonic QGPV Anomalies

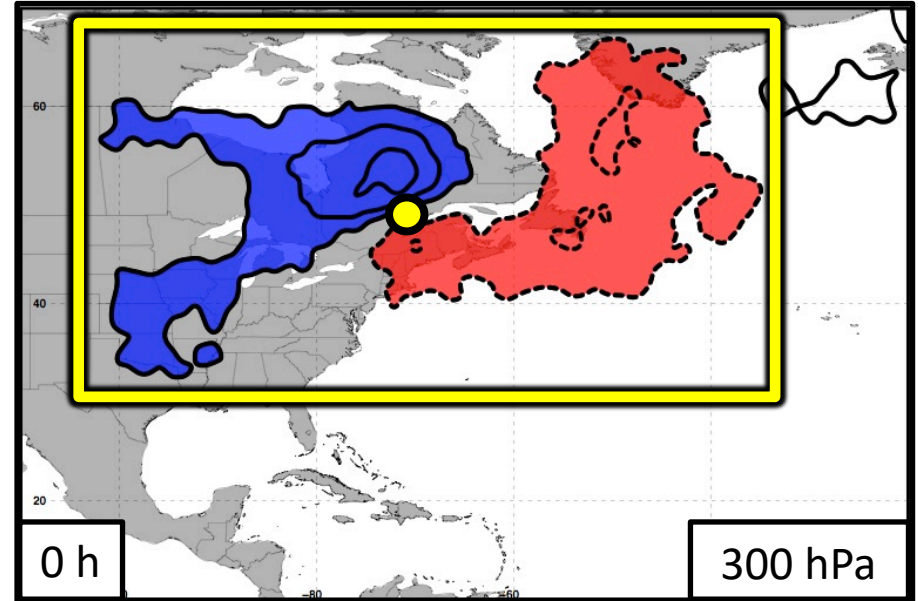
Yellow circle: Avg. Location of Jet Superposition

QGPV Inversions

Polar Dominant Events

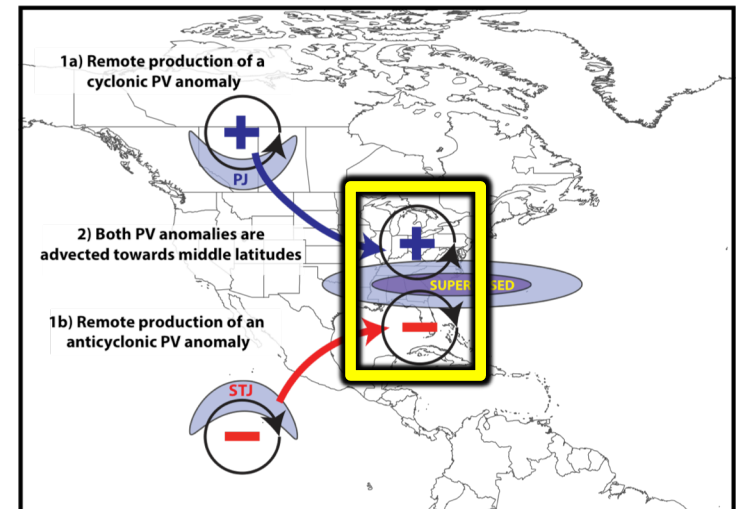


East Subtropical Dominant Events



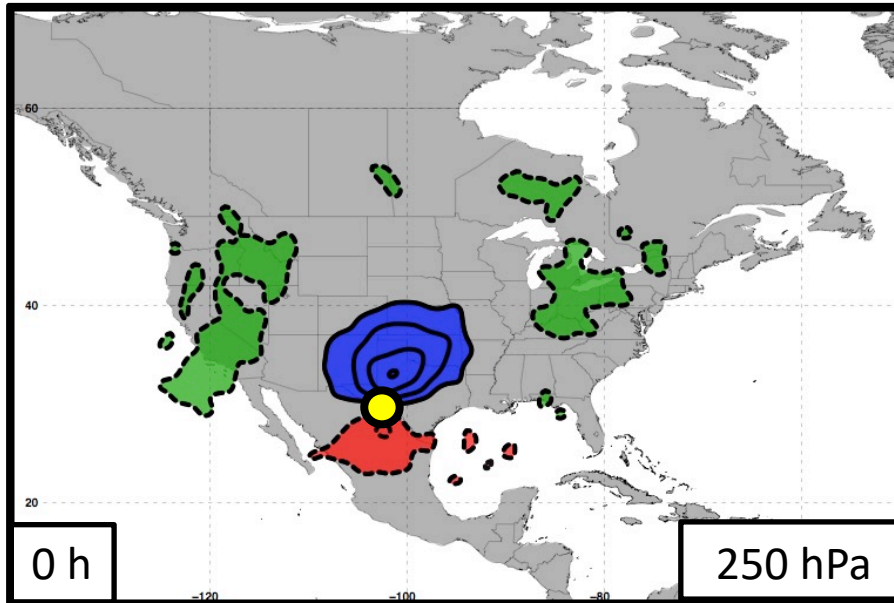
Blue Polar Cyclonic QGPV Anomalies
Red Tropical Anticyclonic QGPV Anomalies

Yellow Dot Avg. Location of Jet Superposition

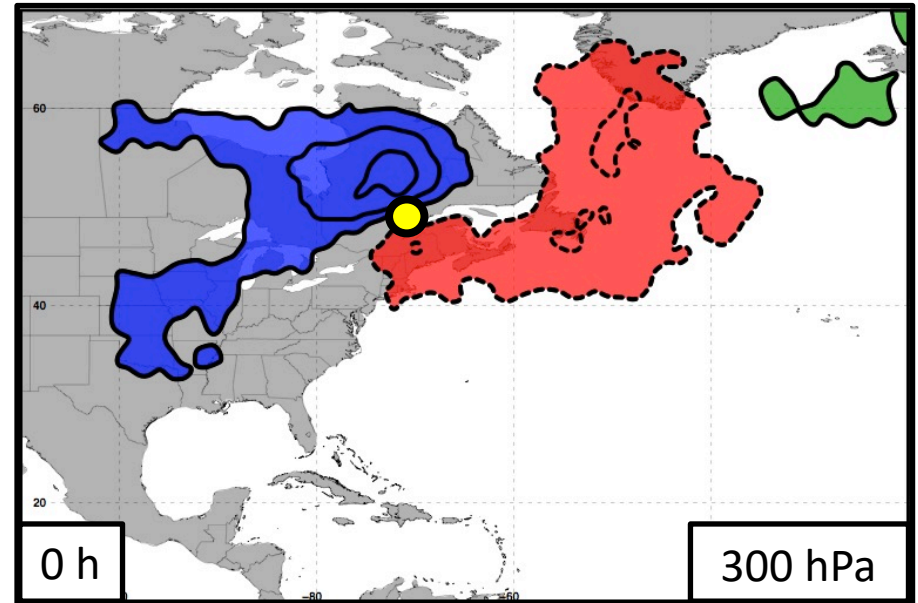


QGPV Inversions

Polar Dominant Events



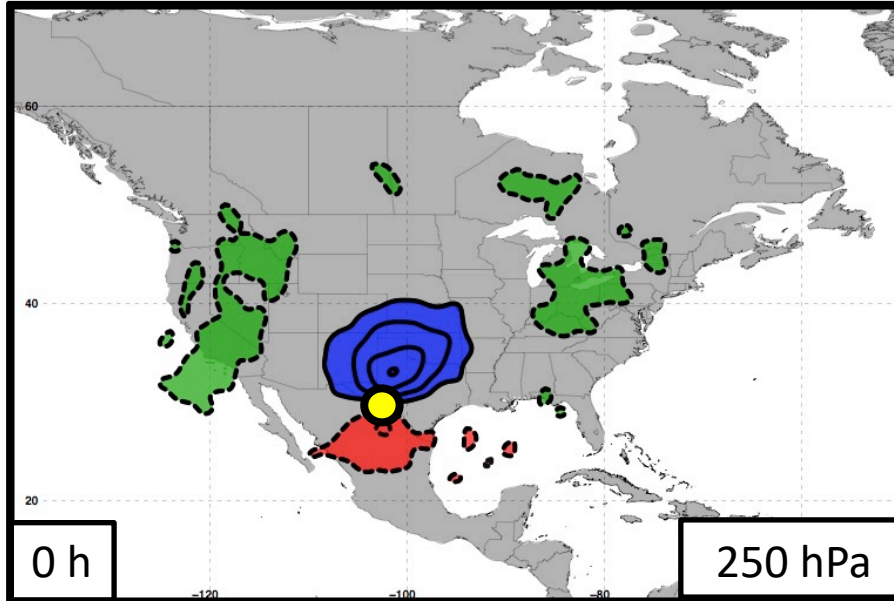
East Subtropical Dominant Events



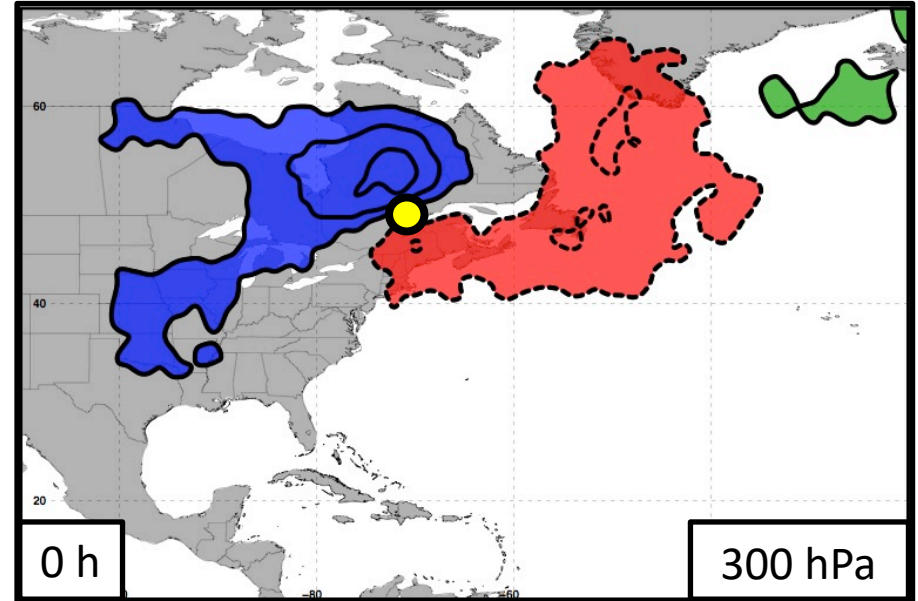
- Blue square: Polar Cyclonic QGPV Anomalies
- Red square: Tropical Anticyclonic QGPV Anomalies
- Green square: Residual Upper-Tropospheric QGPV Anomalies
- Yellow circle: Avg. Location of Jet Superposition

QGPV Inversions

Polar Dominant Events



East Subtropical Dominant Events



- Blue square: Polar Cyclonic QGPV Anomalies
- Red square: Tropical Anticyclonic QGPV Anomalies
- Green square: Residual Upper-Tropospheric QGPV Anomalies
- Pink square: Lower-Tropospheric QGPV Anomalies
- Yellow circle: Avg. Location of Jet Superposition

QGPV Inversions

Each category of QGPV anomalies (q') is inverted to determine its associated geopotential (ϕ') field:

$$q' = \frac{1}{f_0} \nabla^2 \phi' + f_0 \frac{\partial}{\partial p} \left(\frac{1}{\sigma_r} \frac{\partial \phi'}{\partial p} \right) \quad \textit{where} \quad \begin{array}{l} f_0 = \textit{Reference Coriolis Parameter} \\ \sigma_r = \textit{Static Stability of the U.S. Std. Atm.} \end{array}$$

QGPV Inversions

Each category of QGPV anomalies (q') is inverted to determine its associated geopotential (ϕ') field:

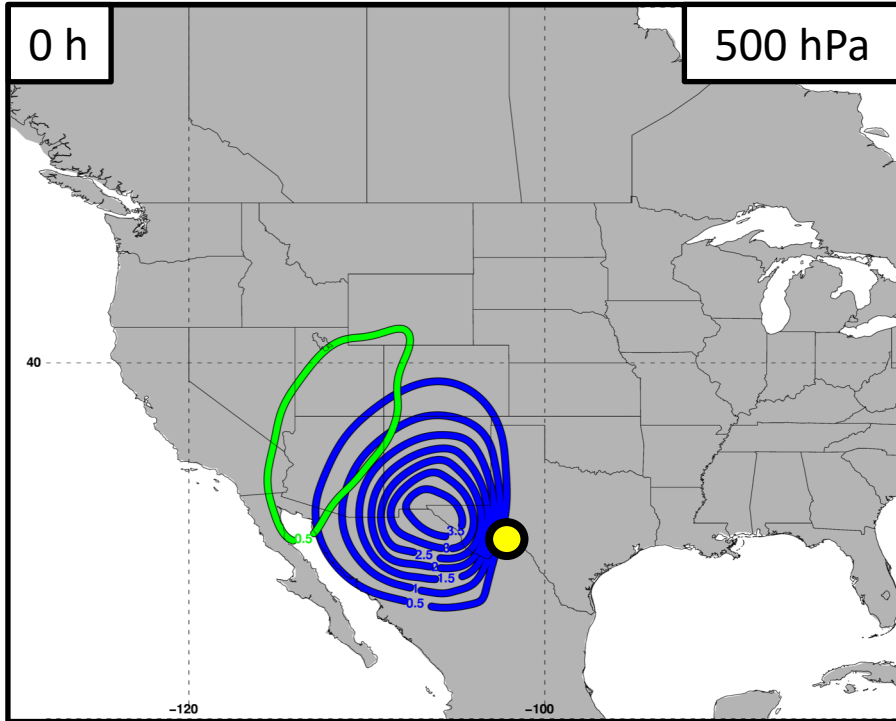
$$q' = \frac{1}{f_0} \nabla^2 \phi' + f_0 \frac{\partial}{\partial p} \left(\frac{1}{\sigma_r} \frac{\partial \phi'}{\partial p} \right) \quad \textit{where} \quad \begin{array}{l} f_0 = \textit{Reference Coriolis Parameter} \\ \sigma_r = \textit{Static Stability of the U.S. Std. Atm.} \end{array}$$

The geopotential fields and the composite temperature (T) field are used to determine the QG vertical motion (ω) associated with each category of QGPV:

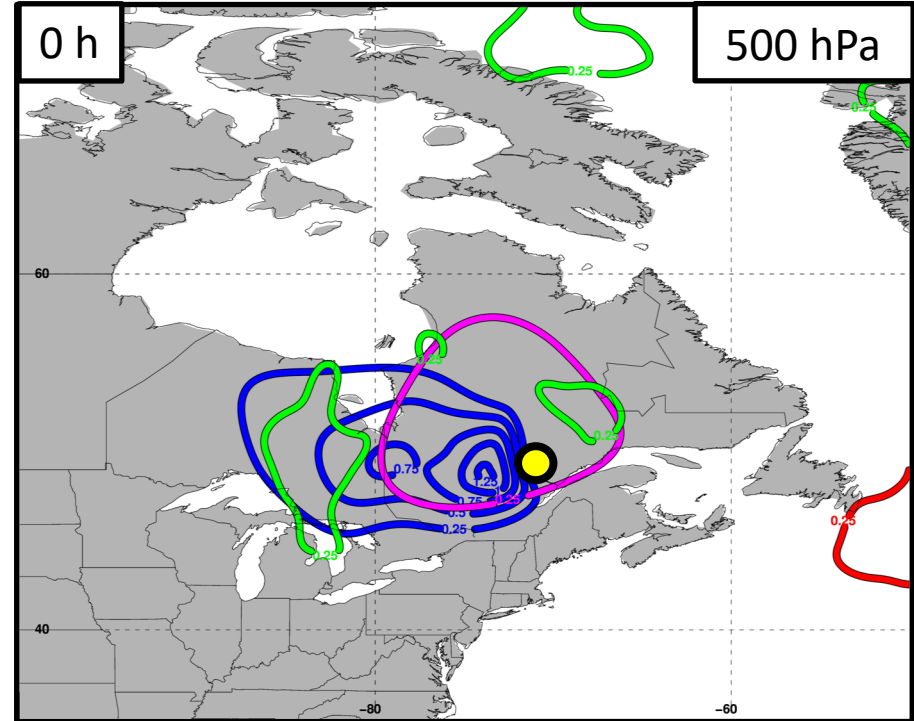
$$\sigma_r \nabla^2 \omega + f_0^2 \frac{\partial^2 \omega}{\partial p^2} = -2 \nabla \cdot \vec{Q} \quad \textit{where} \quad \begin{array}{l} \vec{V}_g' = -(1/f_0)(\hat{k} \times \nabla \phi') \\ \vec{Q} = -\frac{R}{p} \left[\left(\frac{\partial \vec{V}_g'}{\partial x} \cdot \nabla T \right), \left(\frac{\partial \vec{V}_g'}{\partial y} \cdot \nabla T \right) \right] \end{array}$$

QG Descent

Polar Dominant Events



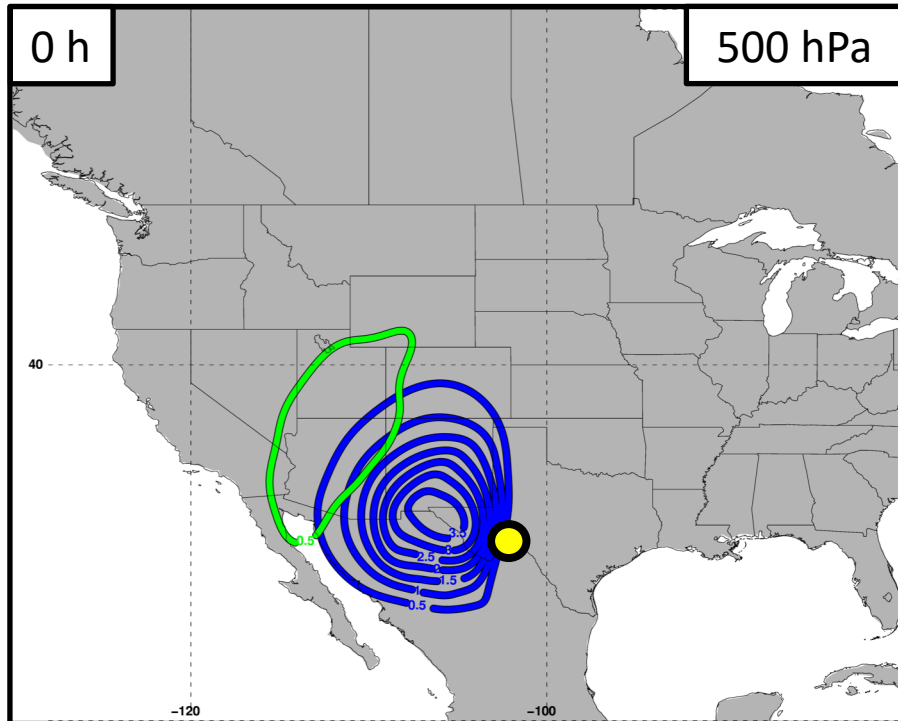
East Subtropical Dominant Events



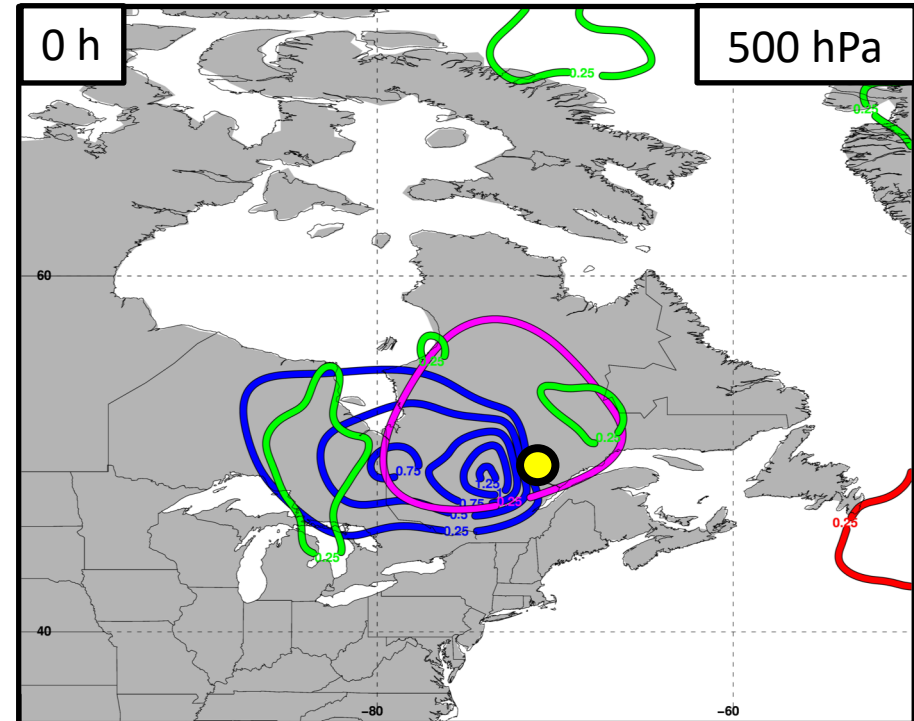
- Blue: Polar Cyclonic QGPV Anomalies
- Red: Tropical Anticyclonic QGPV Anomalies
- Green: Residual Upper-Tropospheric QGPV Anomalies
- Magenta: Lower-Tropospheric QGPV Anomalies
- Yellow: Avg. Location of Jet Superposition

QG Descent

Polar Dominant Events



East Subtropical Dominant Events



- Polar Cyclonic QGPV Anomalies
- Tropical Anticyclonic QGPV Anomalies
- Residual Upper-Tropospheric QGPV Anomalies
- Lower-Tropospheric QGPV Anomalies
- Avg. Location of Jet Superposition

Descent is primarily associated with polar cyclonic QGPV anomalies.

Summary

- Jet superpositions typify a dynamical and thermodynamic environment that is particularly conducive to high-impact weather.
- Descent within the jet-entrance region is a common element among jet superpositions, regardless of the event type.
- Descent is primarily associated with the geostrophic flow attributed to polar cyclonic QGPV anomalies.
- The latter result underscores the critical role that polar cyclonic QGPV anomalies play during jet superpositions.

Contact: acwinters@albany.edu

Supplementary Slides

References

Cavallo, S. M., and G. J. Hakim, 2010: Composite structure of tropopause polar cyclones. *Mon. Wea. Rev.*, **138**, 3840–3857.

Christenson, C. E., J. E. Martin, and Z. J. Handlos, 2017: A synoptic-climatology of Northern Hemisphere, cold season polar and subtropical jet superposition events. *J. Climate*, **30**, 7231-7246.

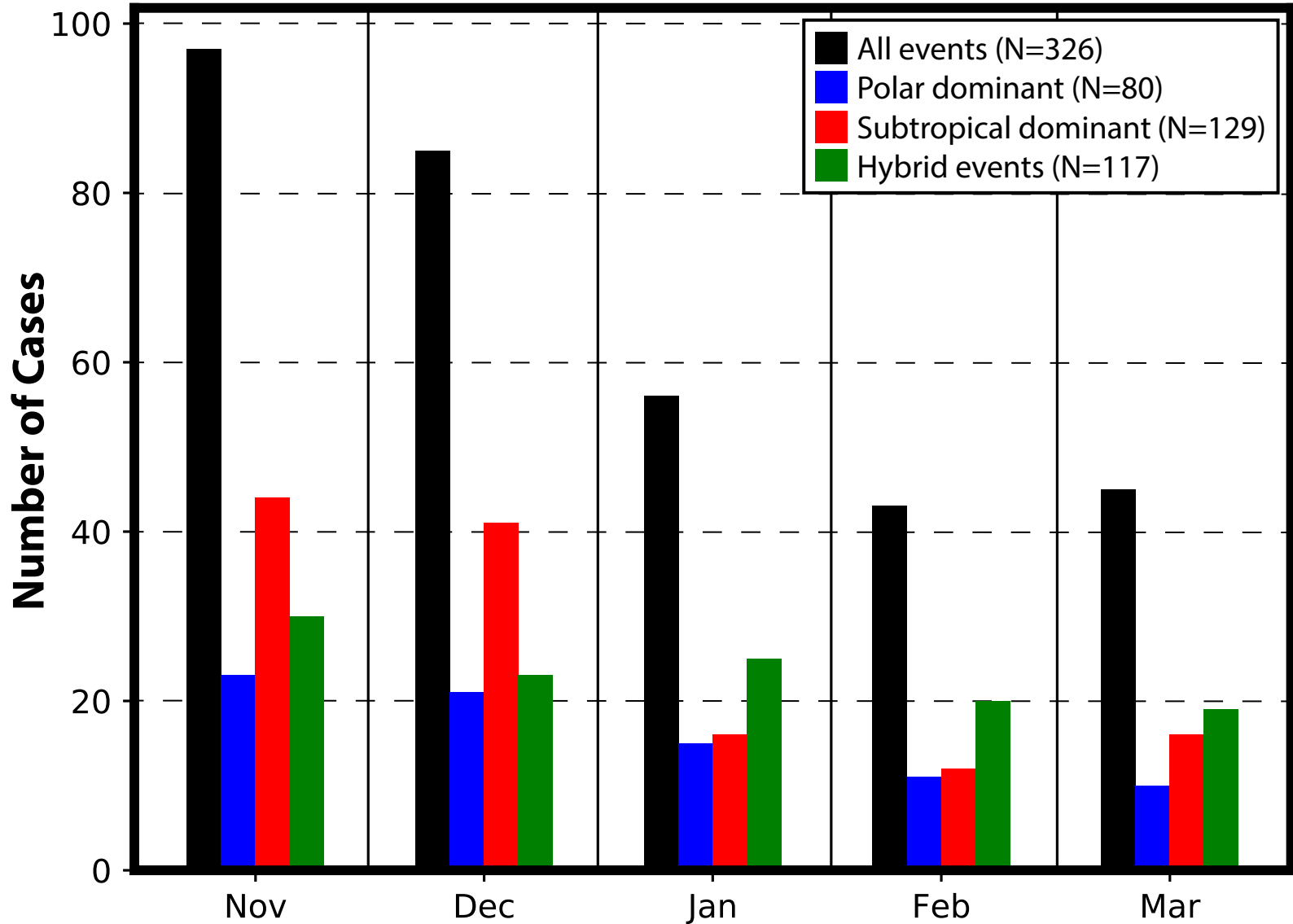
Pyle, M. E., D. Keyser, and L. F. Bosart, 2004: A diagnostic study of jet streaks: Kinematic signatures and relationship to coherent tropopause disturbances. *Mon. Wea. Rev.*, **132**, 297–319.

Saha, S. and co-authors, 2014: The NCEP Climate Forecast System Version 2. *J. Climate*, **27**, 2185–2208.

Winters, A. C., and J. E. Martin, 2017: Diagnosis of a North American polar/subtropical jet superposition employing piecewise potential vorticity inversion. *Mon. Wea. Rev.*, **145**, 1853-1873.

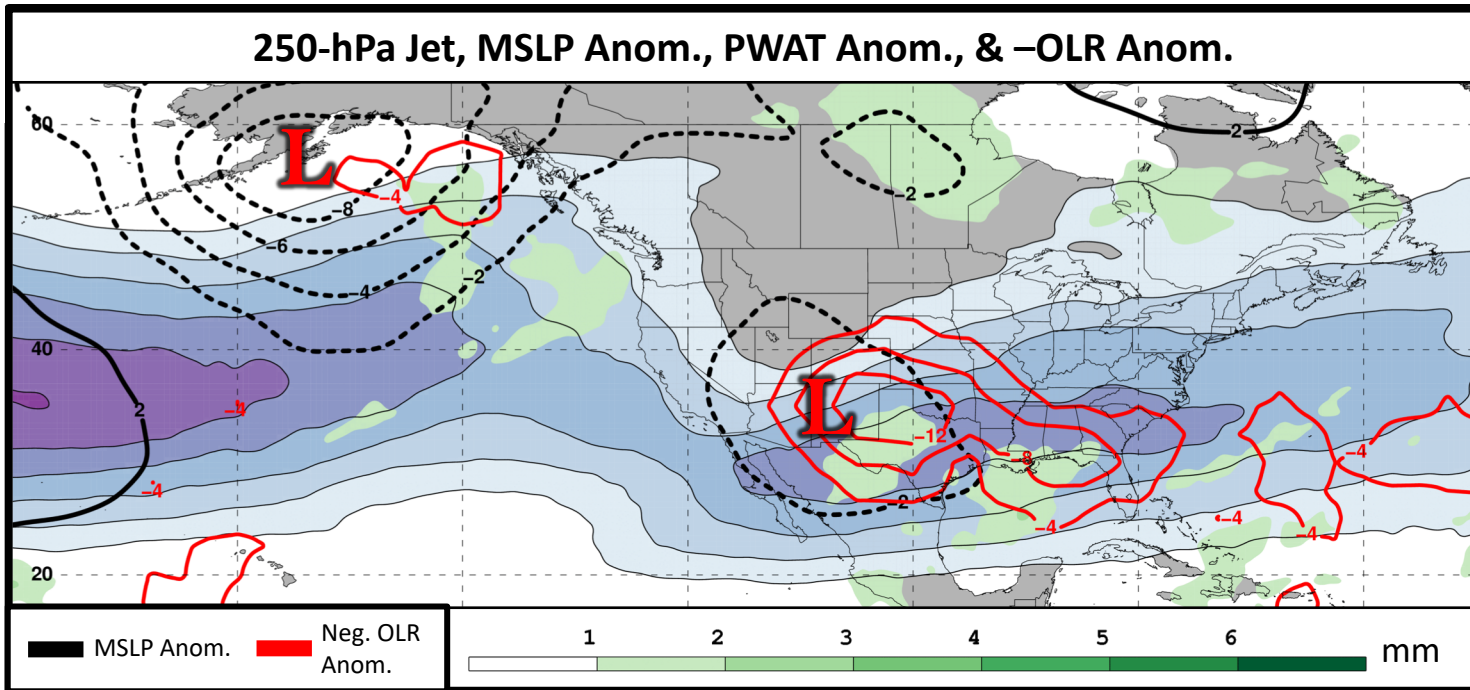
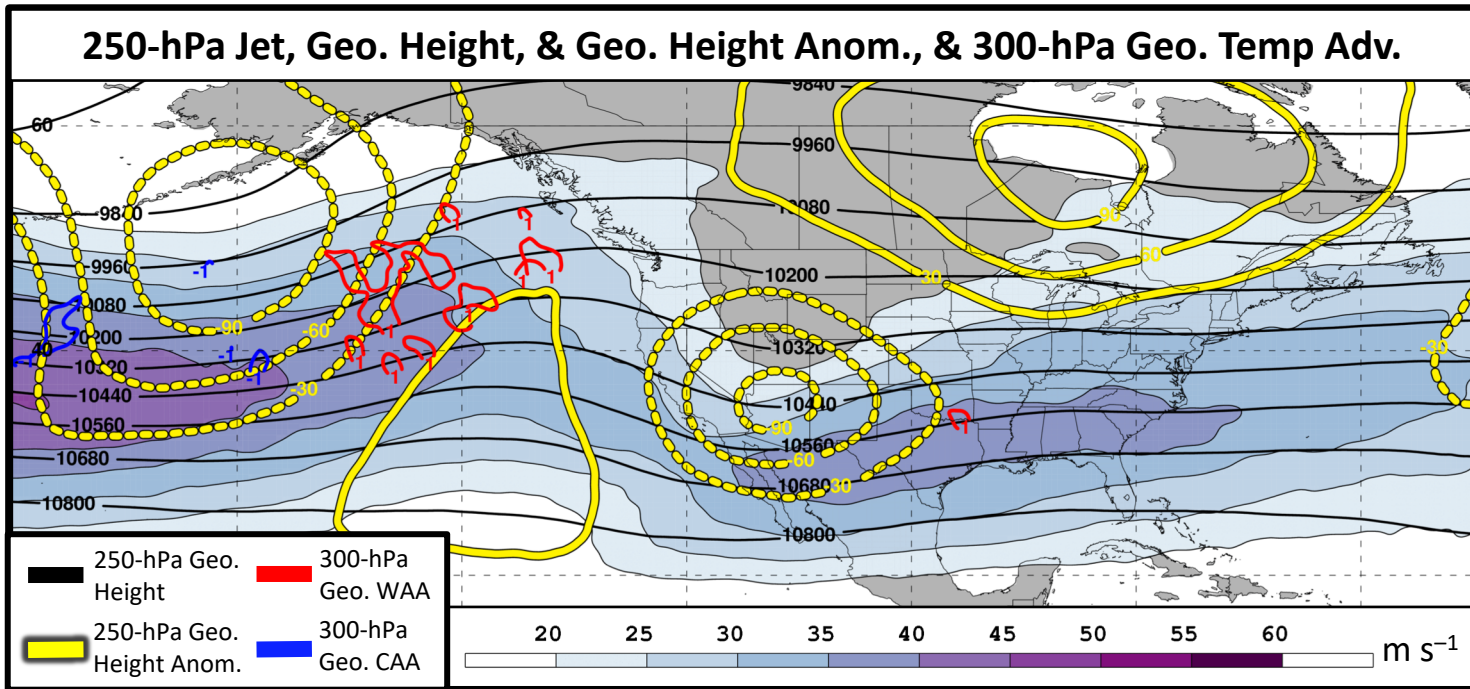
Composite Characteristics

Jet Superposition Event Characteristics



Polar Dominant Jet Superposition Events

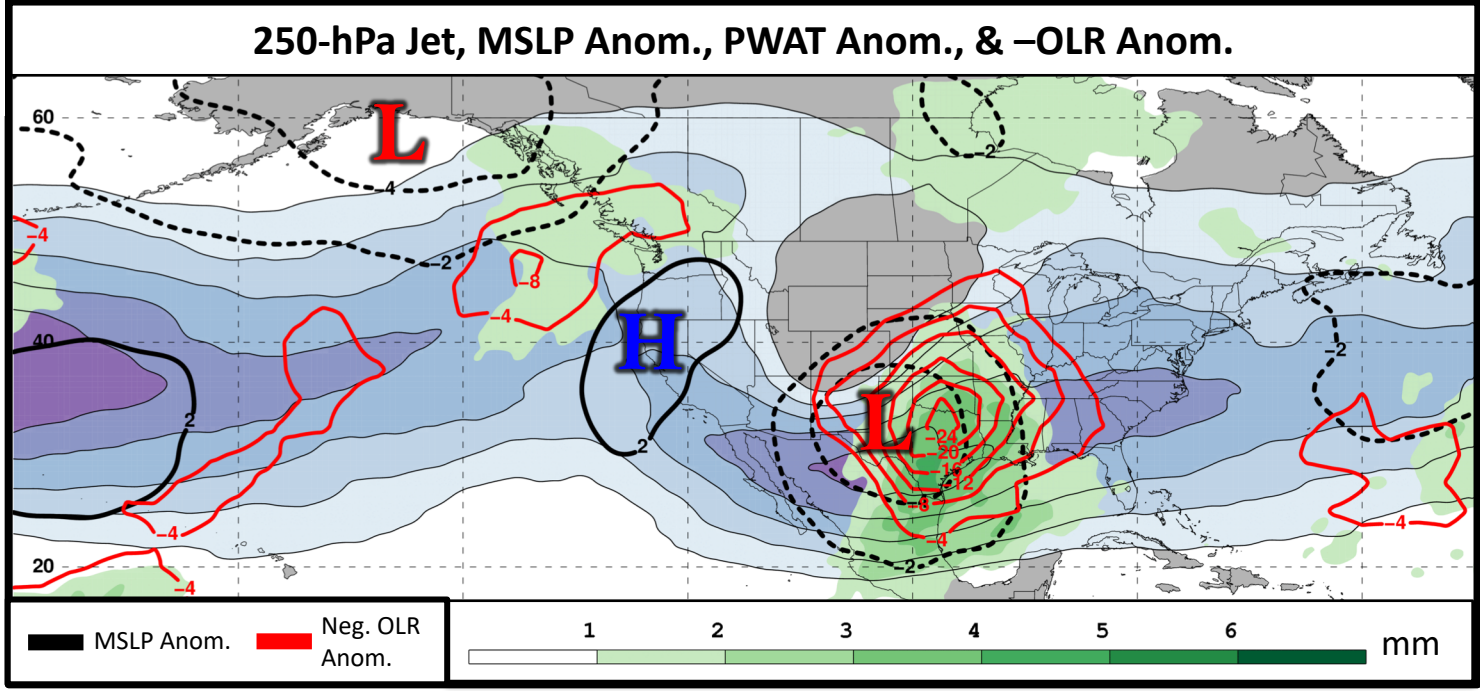
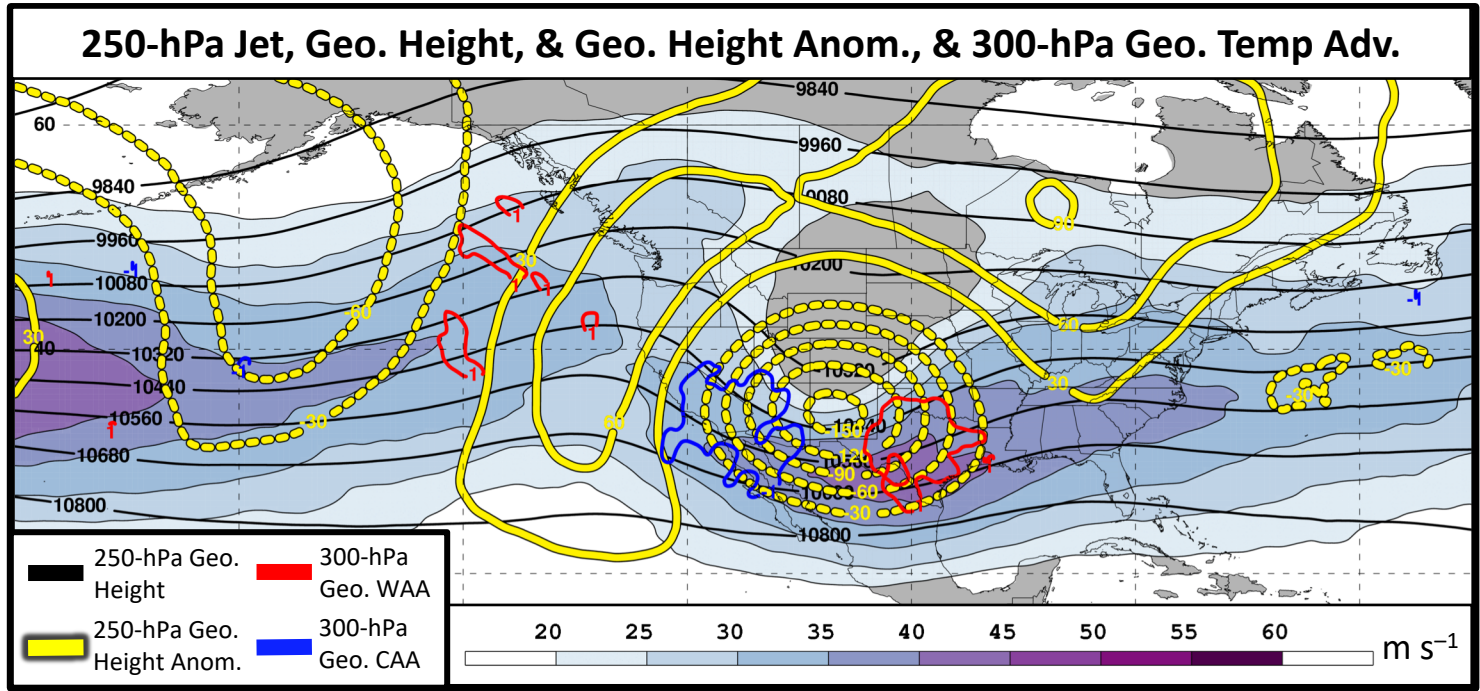
2 Days
Prior to Jet
Superposition



N=80

Polar Dominant Jet Superposition Events

1 Day
Prior to Jet
Superposition



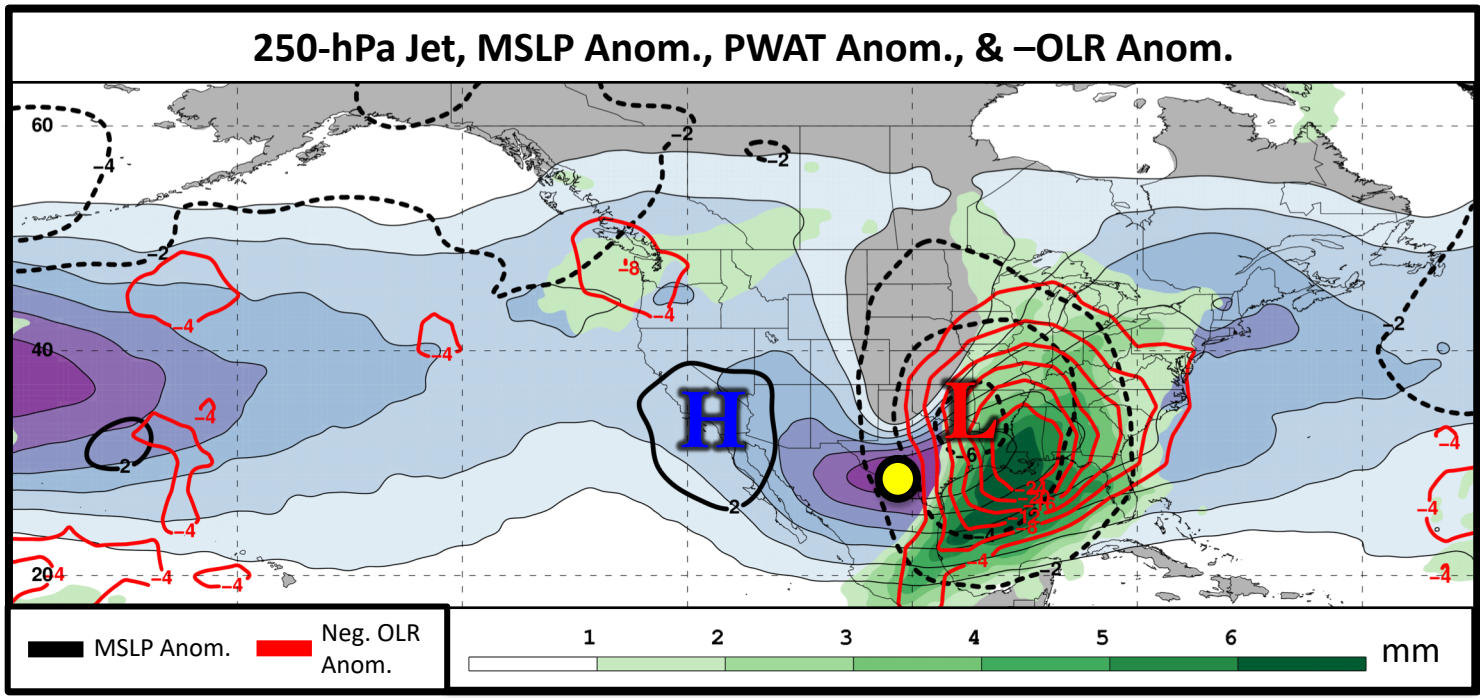
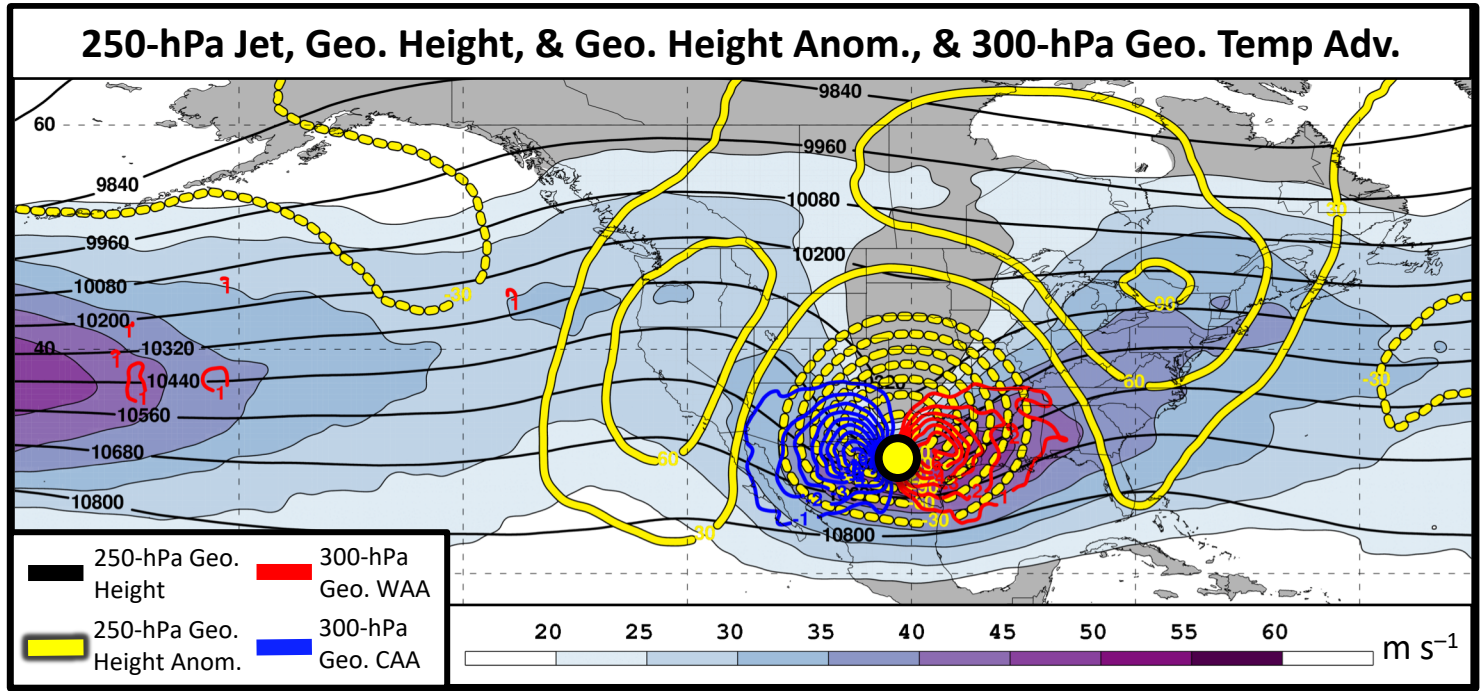
N=80

Polar Dominant Jet Superposition Events

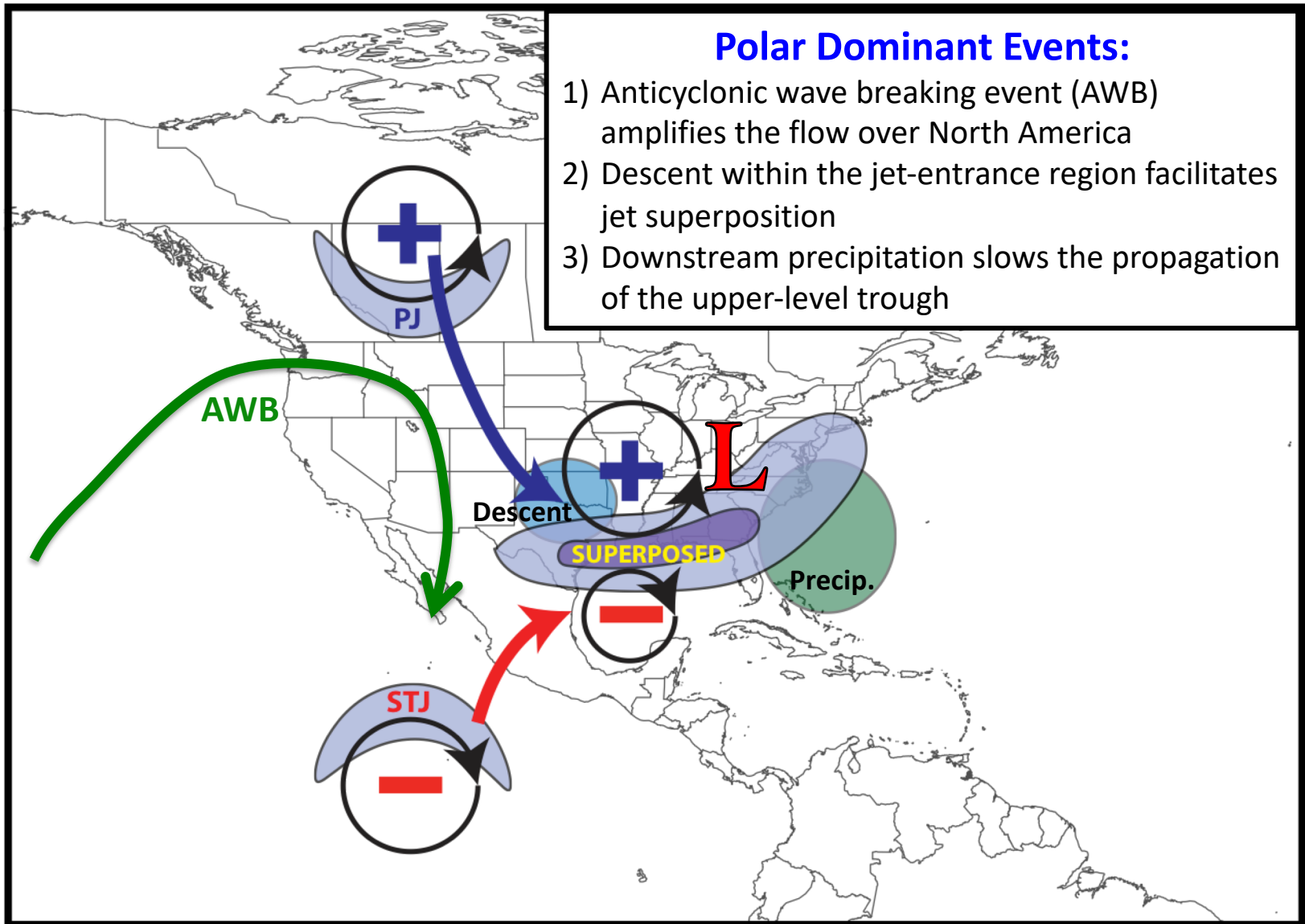
0 Days
Prior to Jet
Superposition

Jet
Superposition
Centroid

N=80

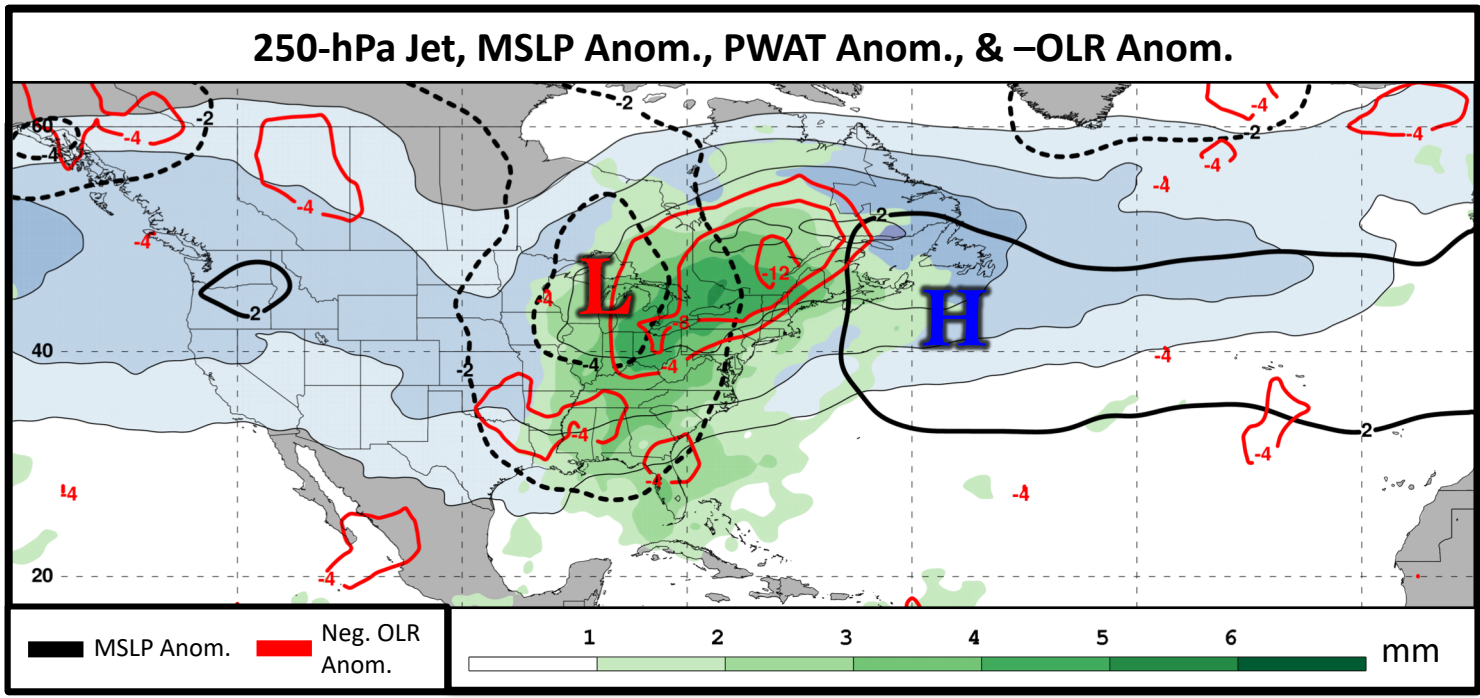
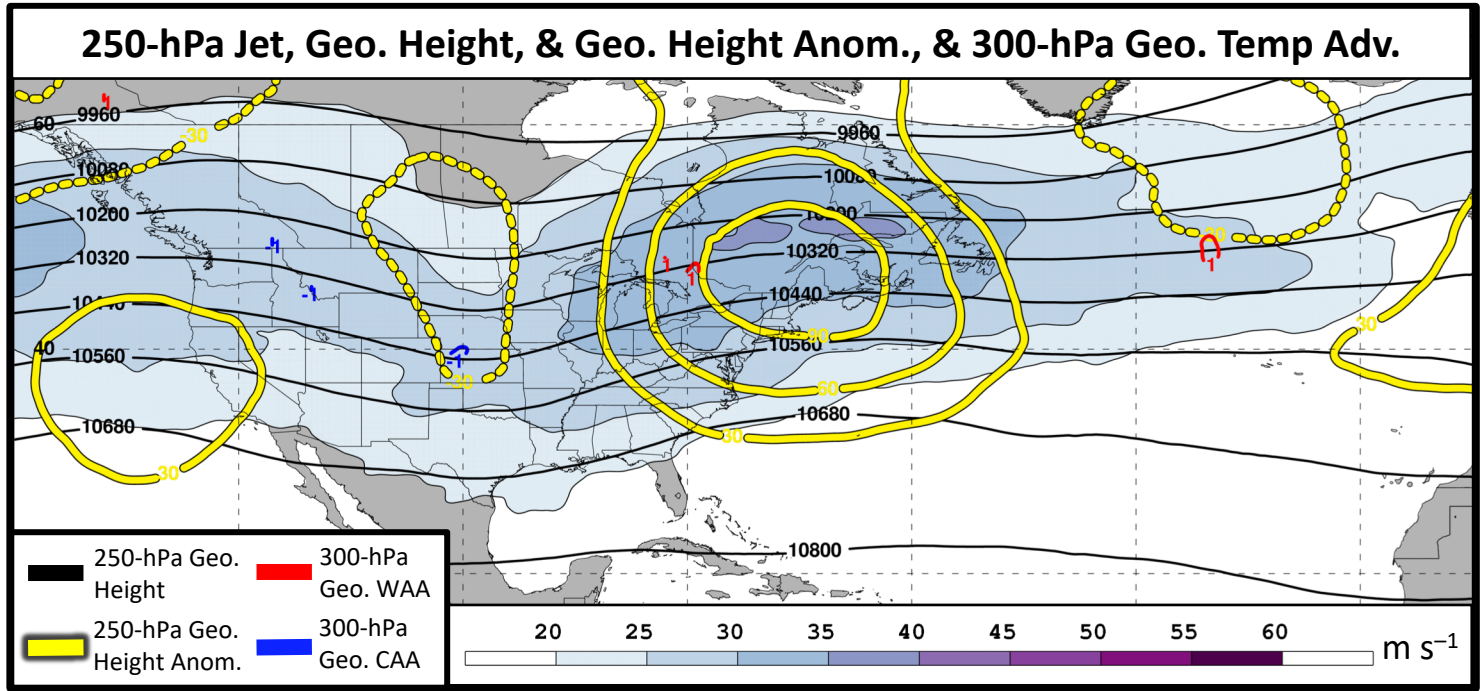


Jet Superposition Event Composites



E. Subtropical Dominant Jet Superposition Events

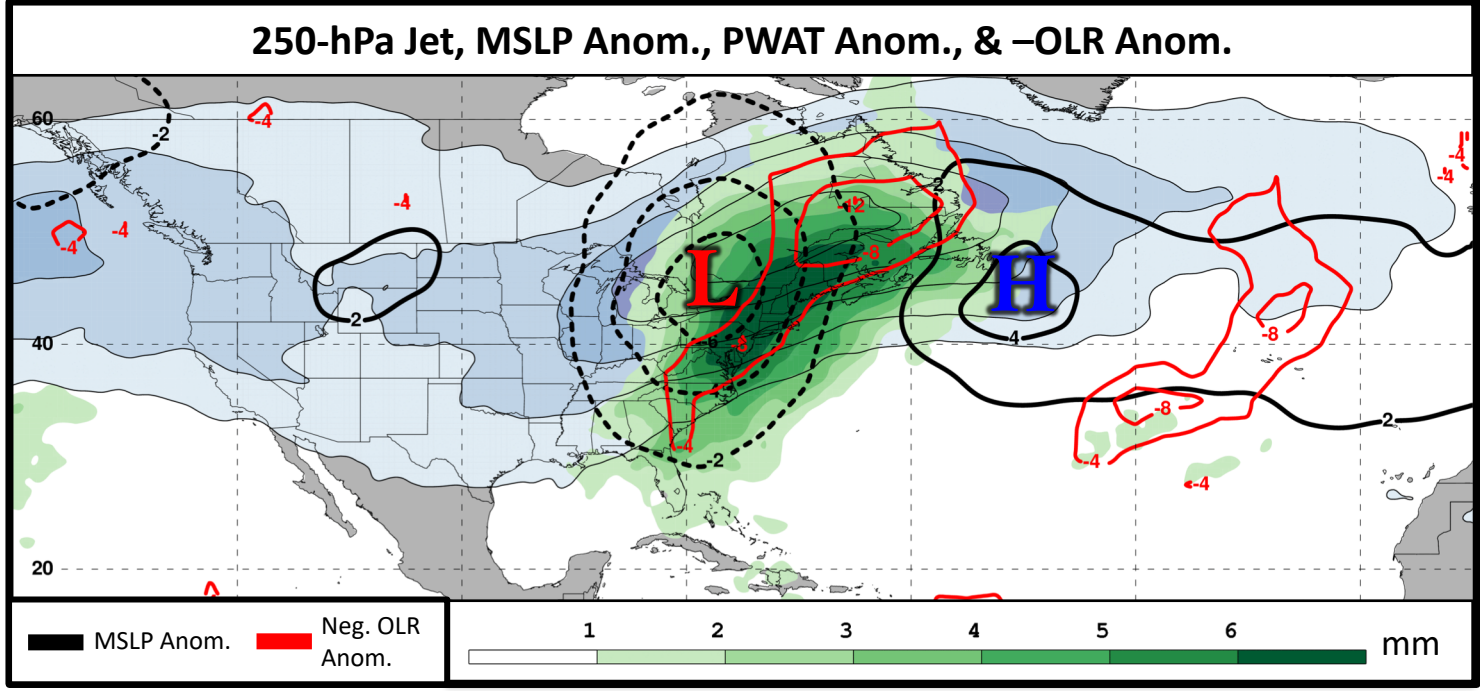
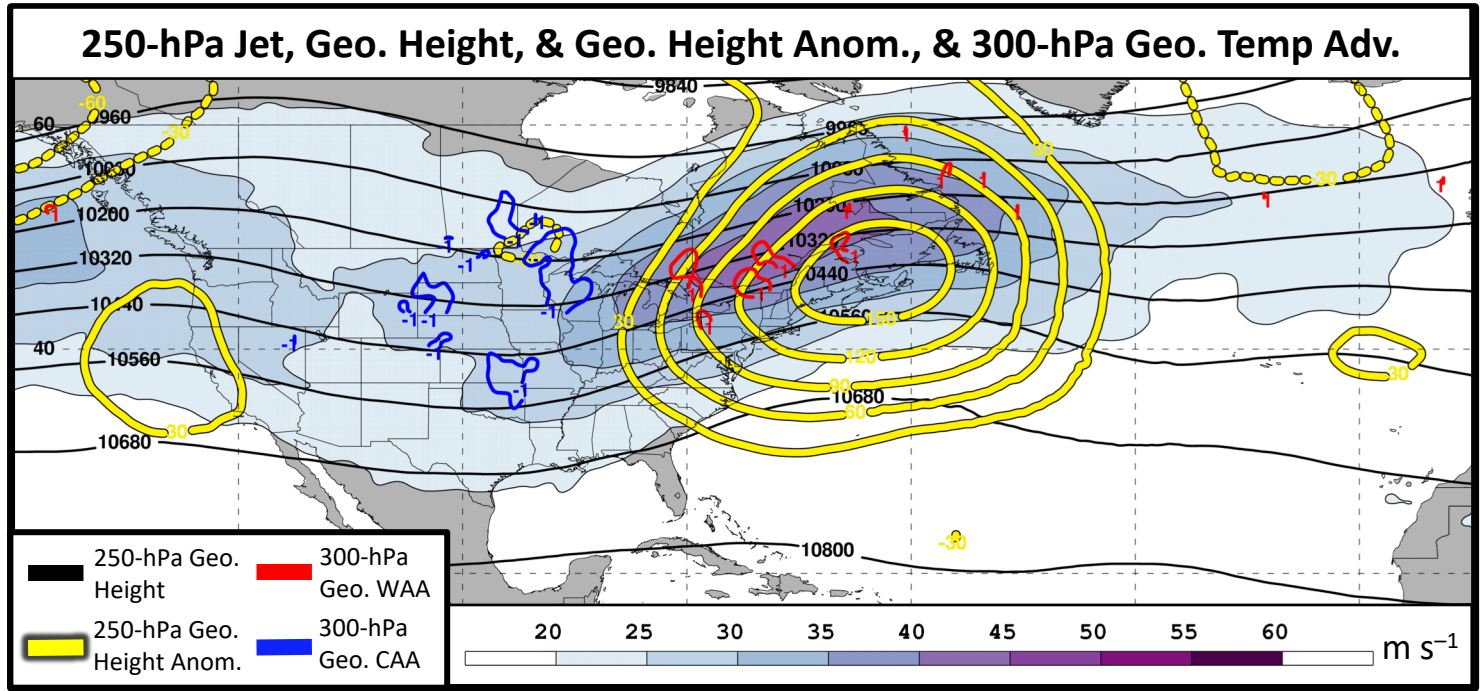
2 Days
Prior to Jet
Superposition



N=76

E. Subtropical Dominant Jet Superposition Events

1 Day Prior to Jet Superposition



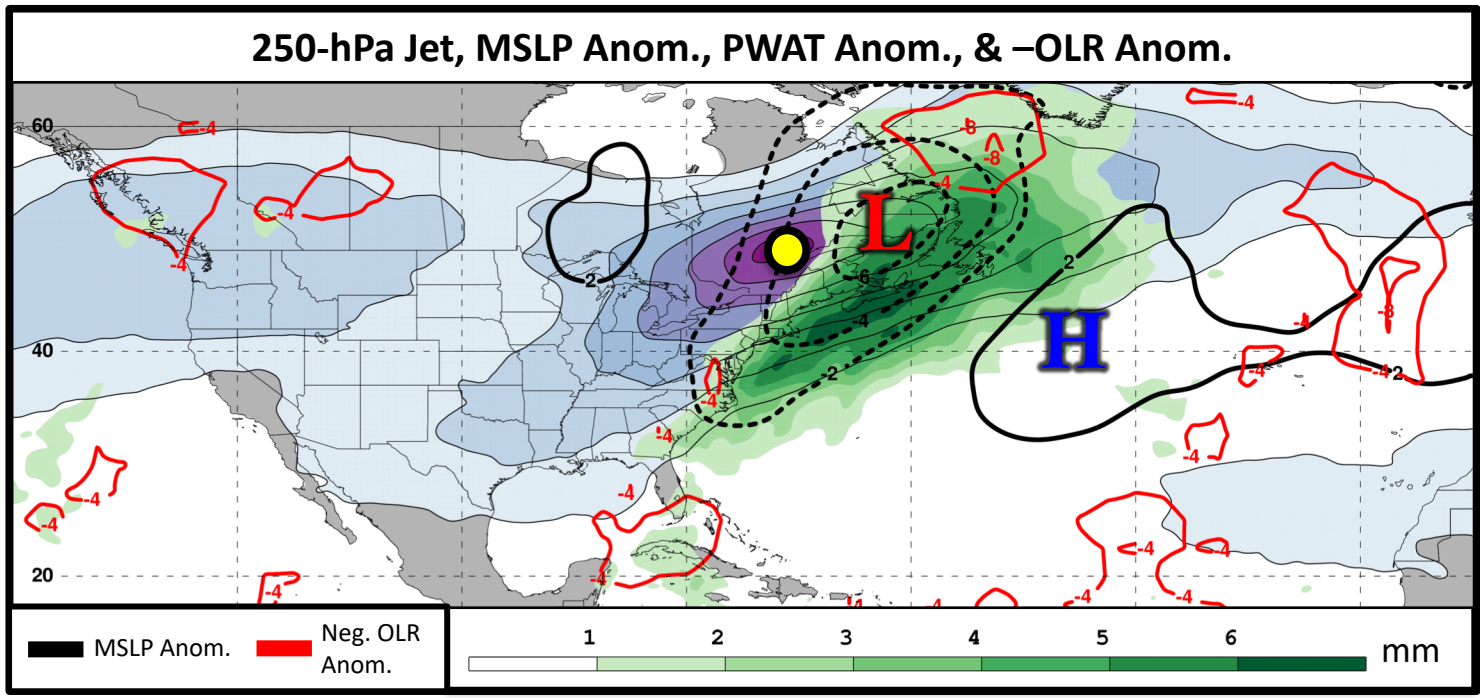
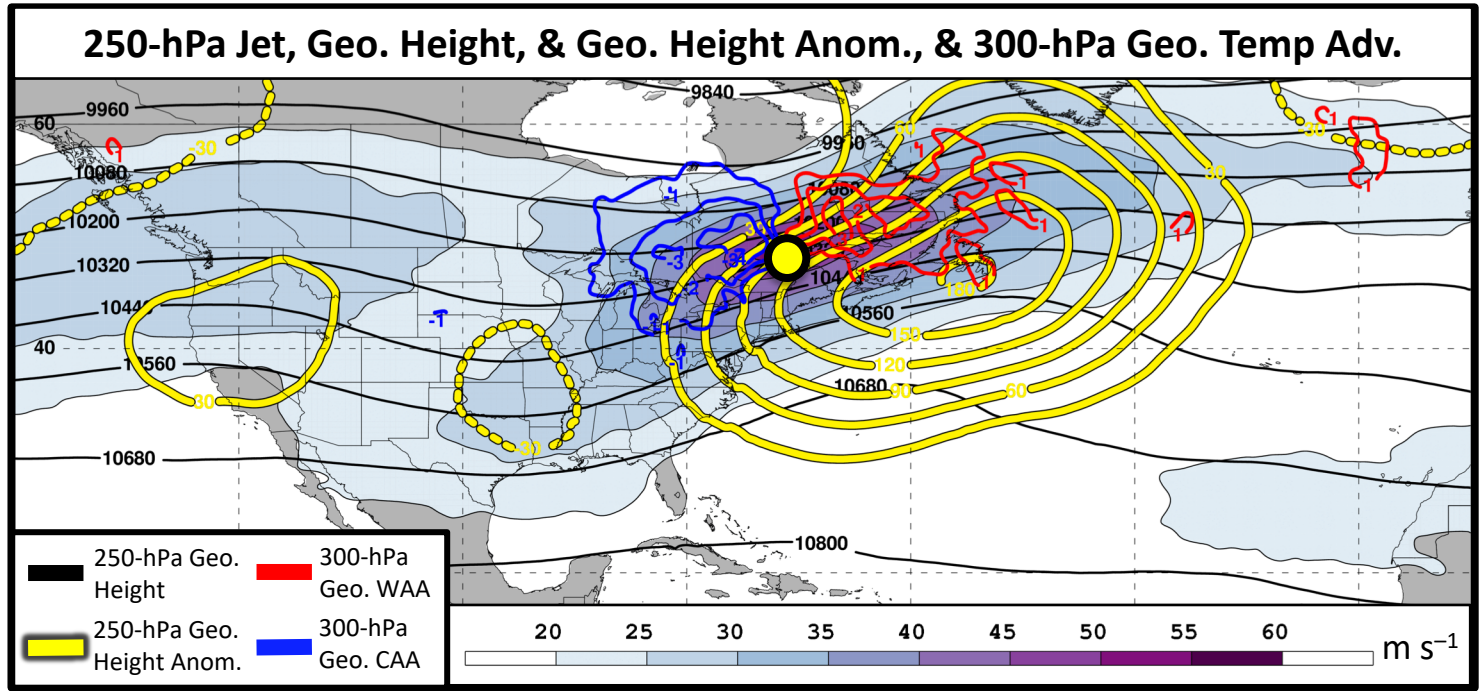
N=76

E. Subtropical Dominant Jet Superposition Events

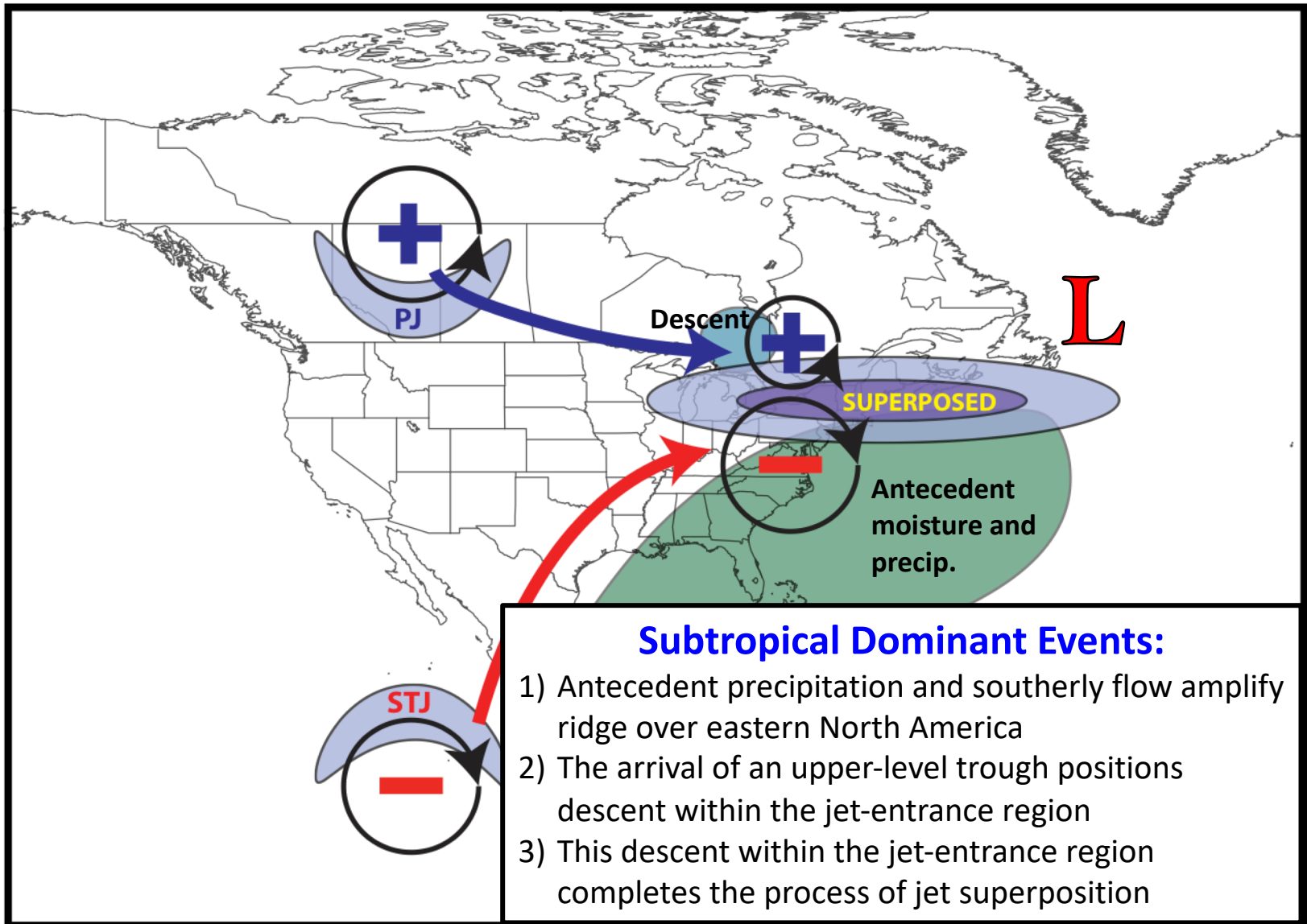
0 Days
Prior to Jet
Superposition

Jet
Superposition
Centroid

N=76

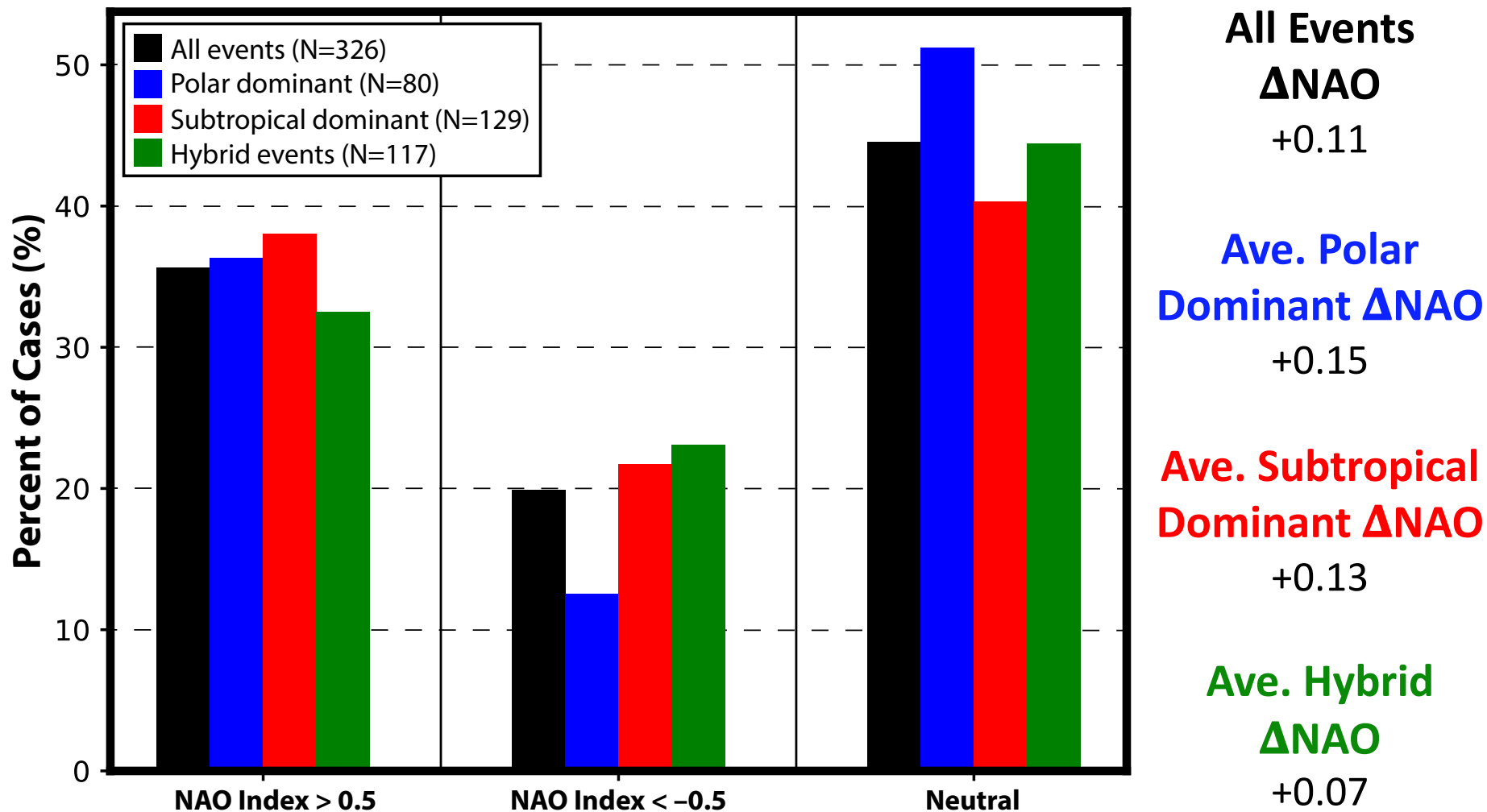


Jet Superposition Event Composites



Downstream Consequences

North Atlantic Oscillation: 5 Days After Jet Superposition



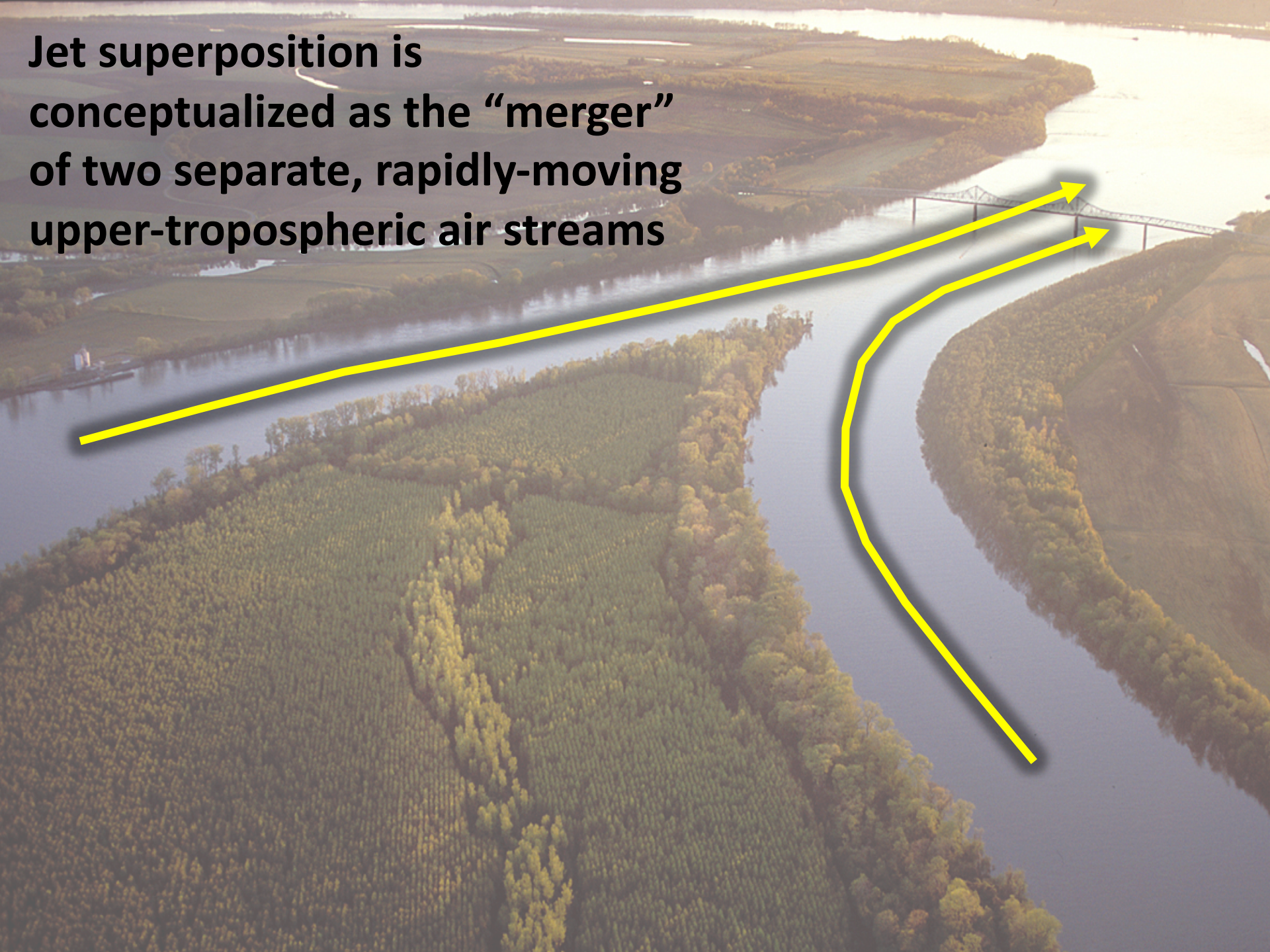
QGPV and QG Omega Inversions

QGPV Category	Physical Interpretation
Polar Cyclonic QGPV Anomalies	Circulation associated with near-jet cyclonic QGPV anomalies
Tropical Anticyclonic QGPV Anomalies	Circulation associated with near-jet anticyclonic QGPV anomalies
Residual Upper-Tropospheric QGPV Anomalies	Circulation associated with the background upper-tropospheric flow
Lower-Tropospheric QGPV Anomalies	Circulation associated with surface cyclones and anticyclones
Mean QGPV	Circulation associated with the climatological mean flow

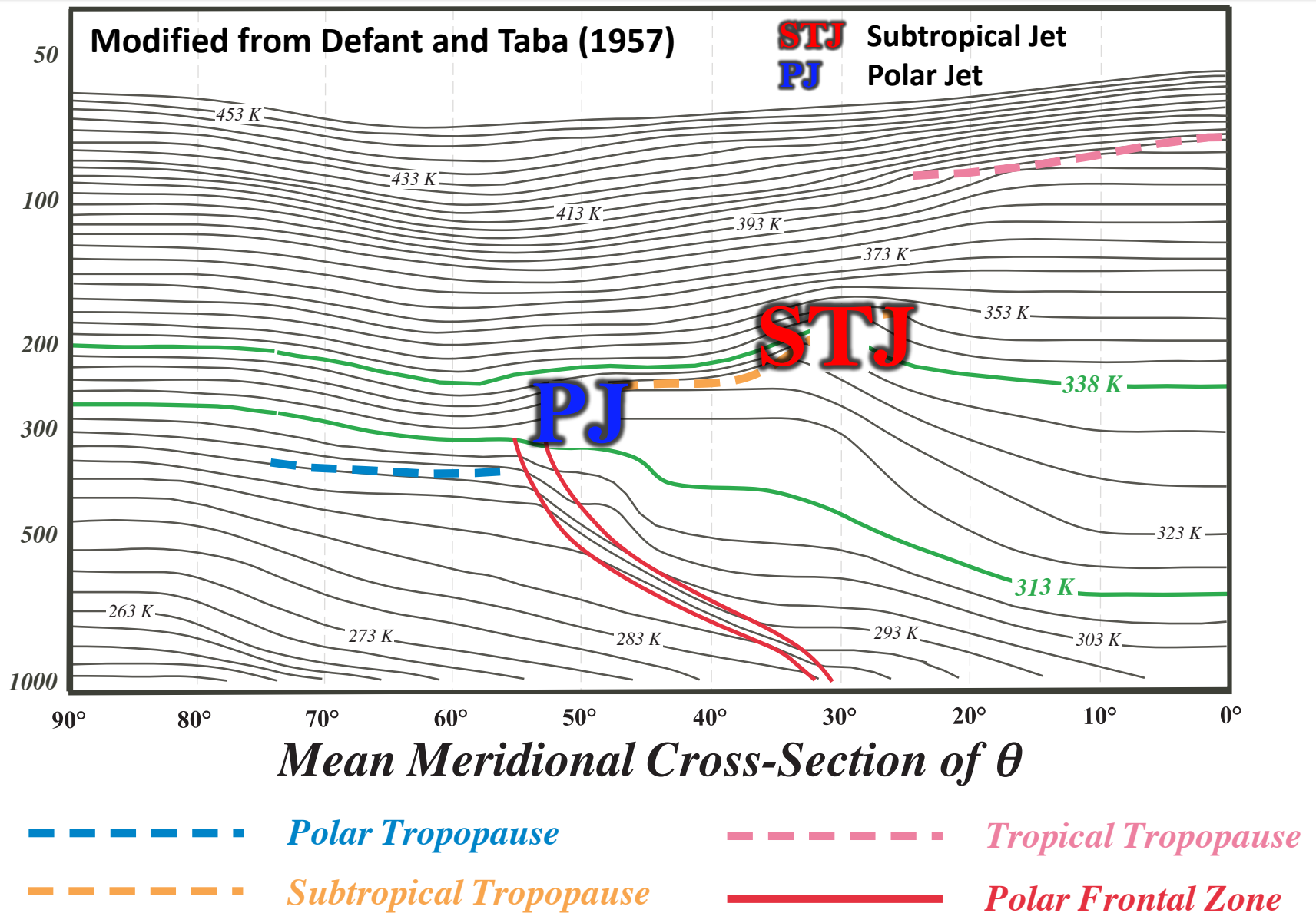
The descent characterizing each jet superposition event composite is examined further by isolating quasi-geostrophic (QG) PV anomalies in the vicinity of the jet superposition.

Background Material

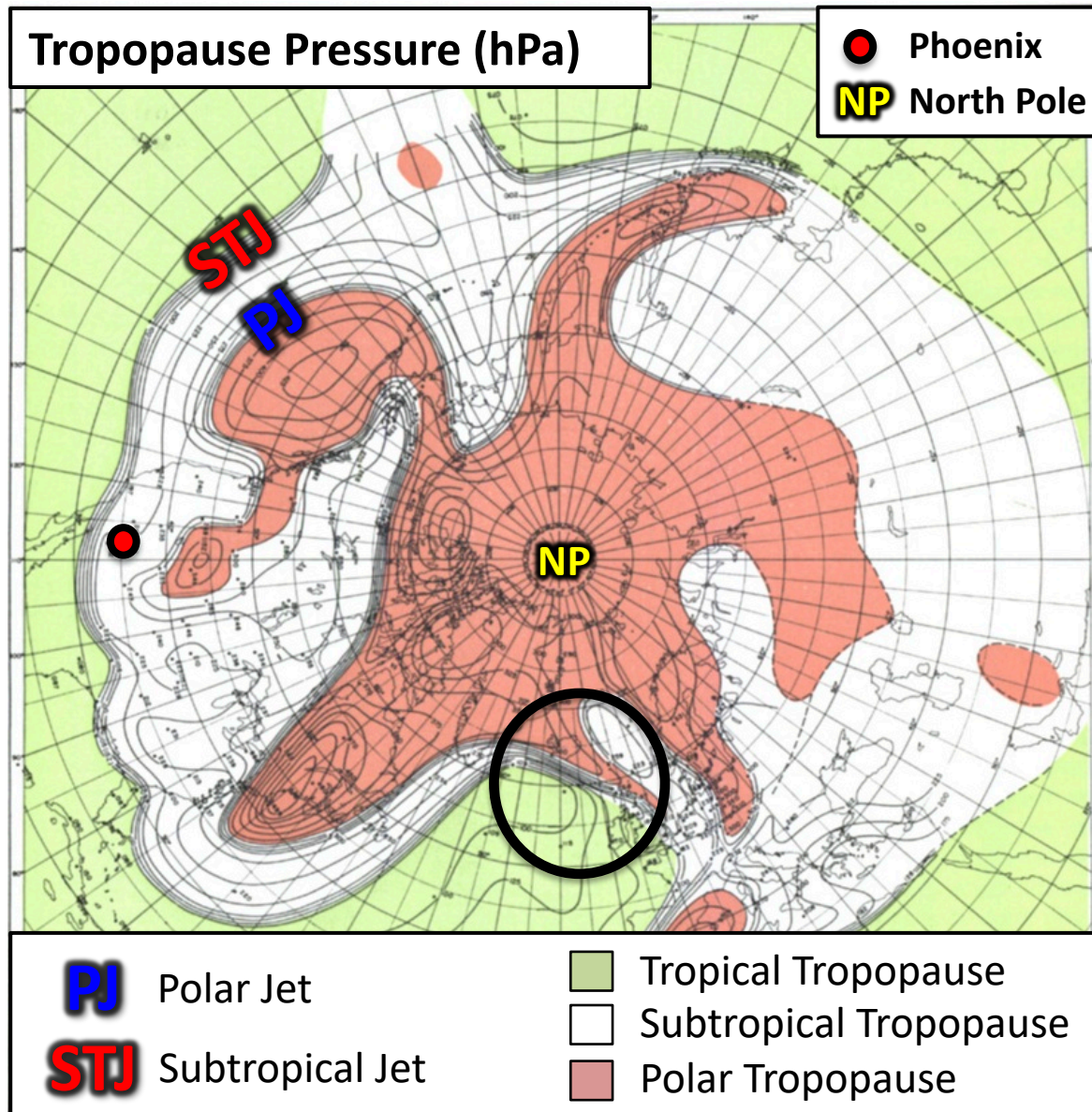
Jet superposition is conceptualized as the “merger” of two separate, rapidly-moving upper-tropospheric air streams



Background



Background



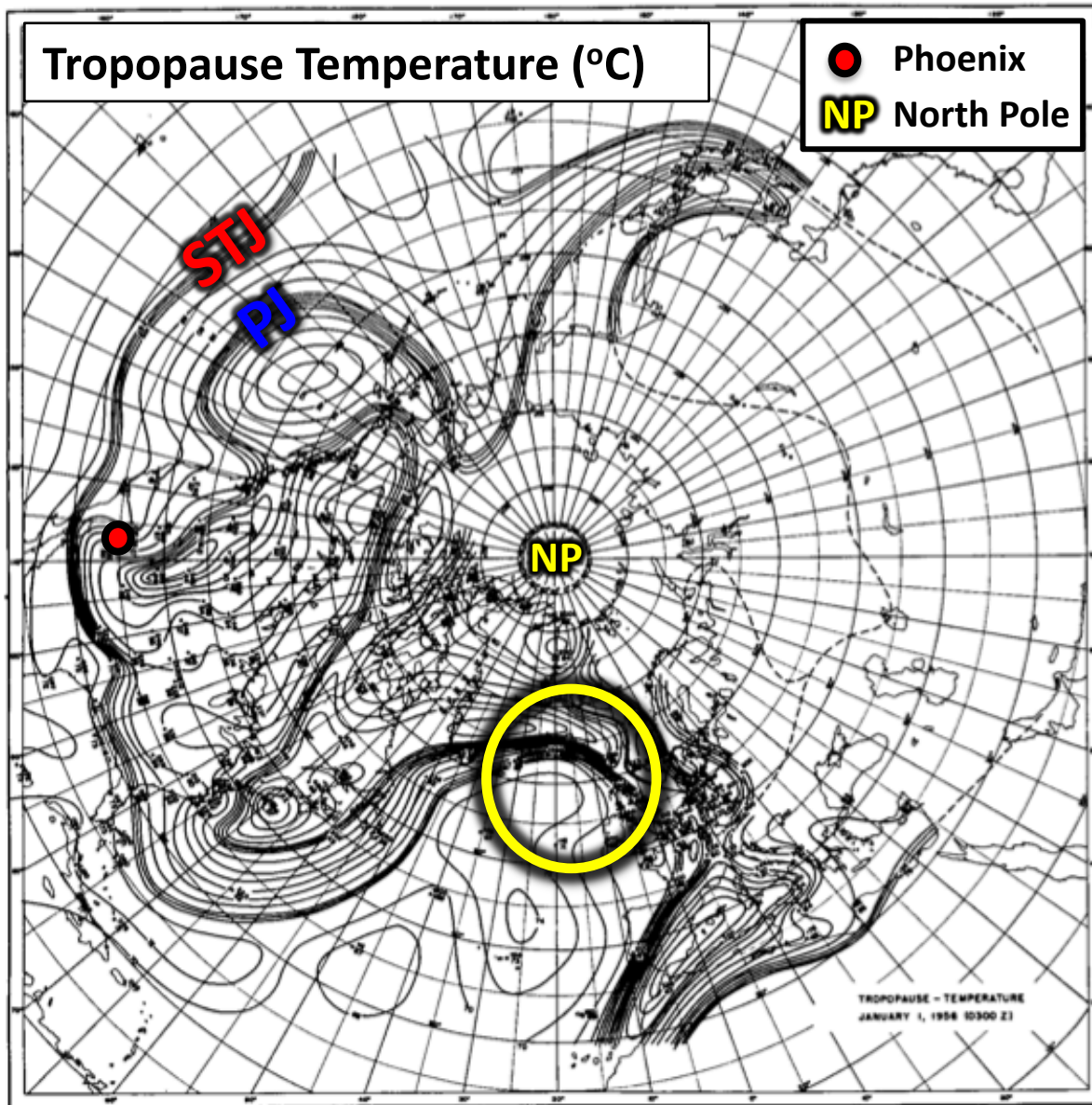
Maps of tropopause pressure help to identify the location of the jets.

While each jet occupies its own climatological latitude band, substantial meanders are common.

Occasionally, the latitudinal separation between the jets can vanish resulting in a vertical **jet superposition**.

Modified from Defant and Taba (1957)

Background



The pole-to-equator baroclinicity is combined into a much narrower zone of contrast in the vicinity of a jet superposition.

Intensified frontal structure is often attended by a strengthening of the superposed jet's transverse circulation.

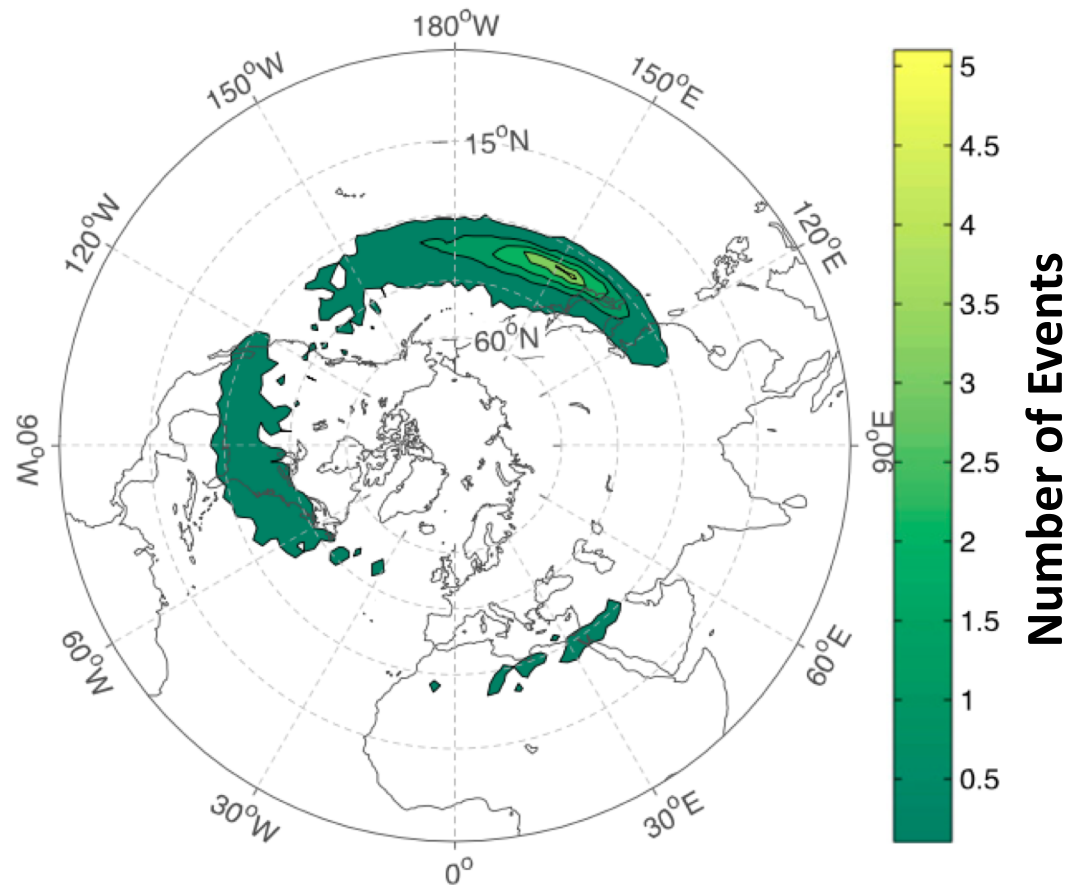
Modified from Defant and Taba (1957)

Background

Christenson et al. (2017) highlight three locations that experience the greatest frequency of jet superpositions:

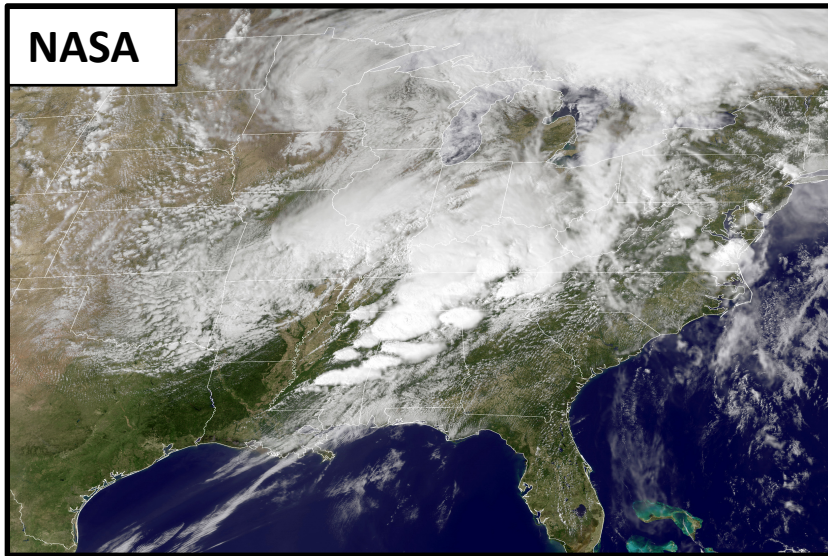
- 1) Western Pacific
- 2) North America
- 3) Northern Africa

Climatological frequency of Northern Hemisphere jet superposition events per cold season (Nov–Mar) 1960–2010



Christenson et al. (2017)

Jet Superpositions and High-Impact Weather



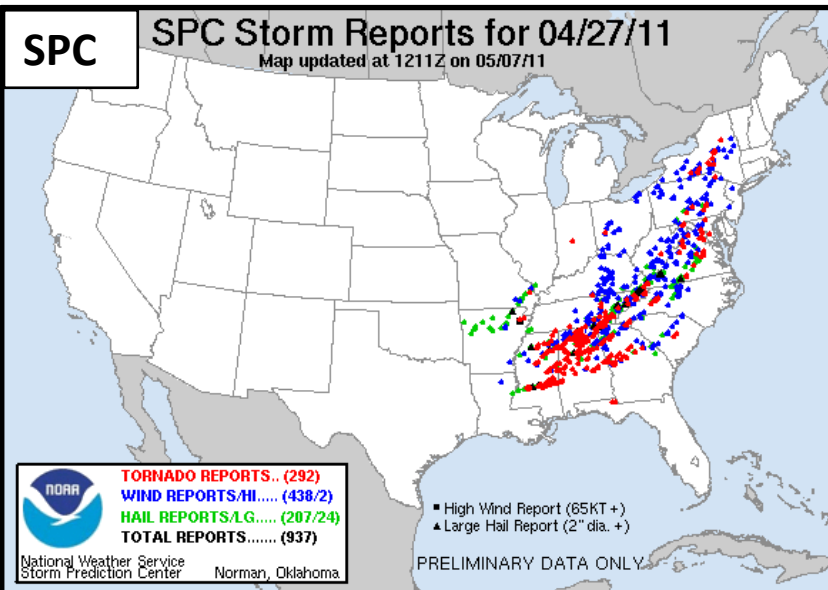
Jet superpositions can be an element of high-impact weather events

1–3 May 2010 Nashville Flood

- Jet superposition enhanced the poleward moisture transport via its ageostrophic circulation (Winters and Martin 2014; 2016).

18–20 December 2009 Mid-Atlantic Blizzard

- Jet superposition was associated with a rapidly deepening East Coast cyclone (Winters and Martin 2016; 2017).



26 October 2010: Explosive Cyclogenesis Event

- Jet superposition over the West Pacific preceded the development of an intense Midwest U.S. cyclone.

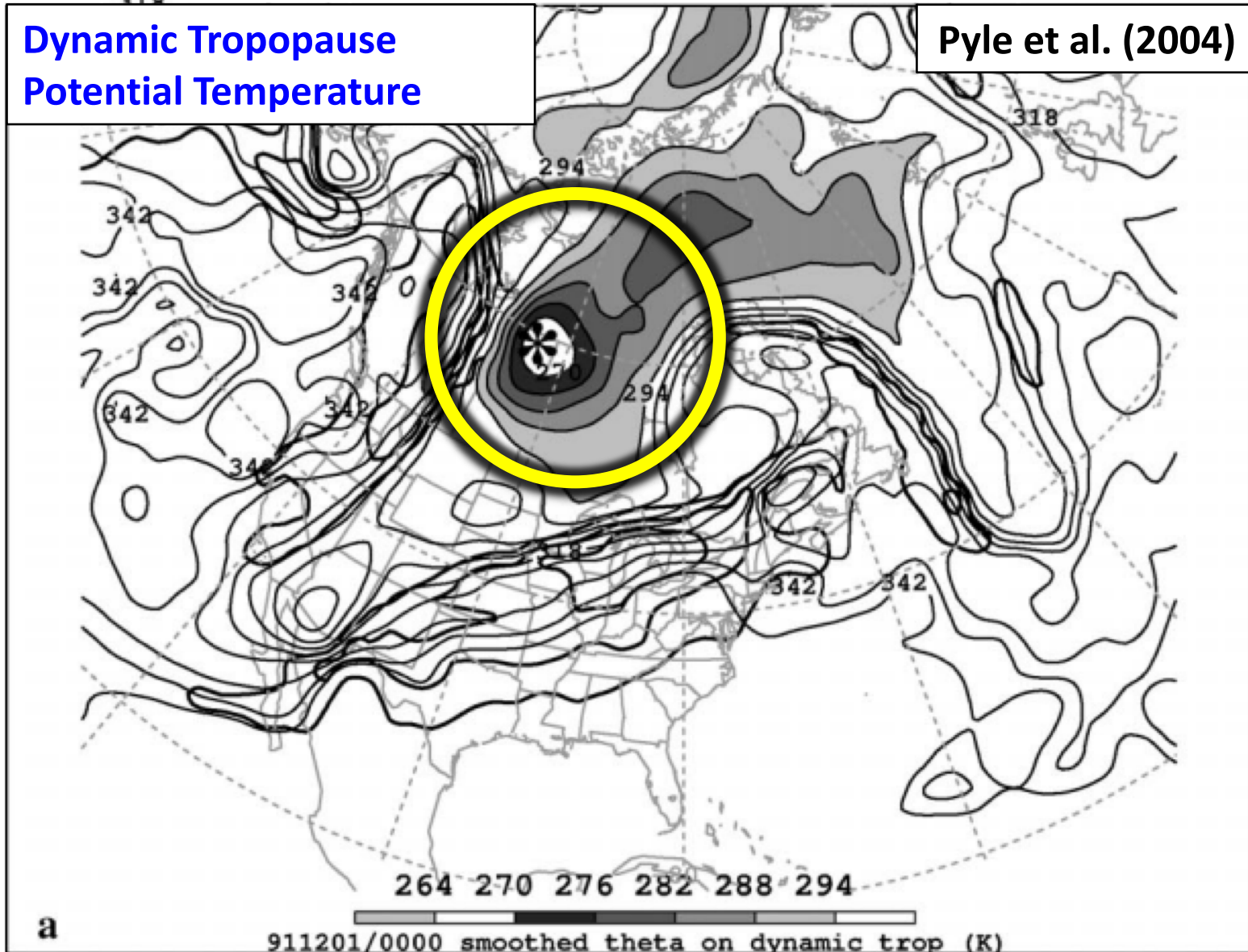
25–28 April 2011 Tornado Outbreak

- Jet superposition occurred over the West Pacific prior to the outbreak (Knupp et al. 2014; Christenson and Martin 2012).

Jet Superposition Conceptual Model

Dynamic Tropopause
Potential Temperature

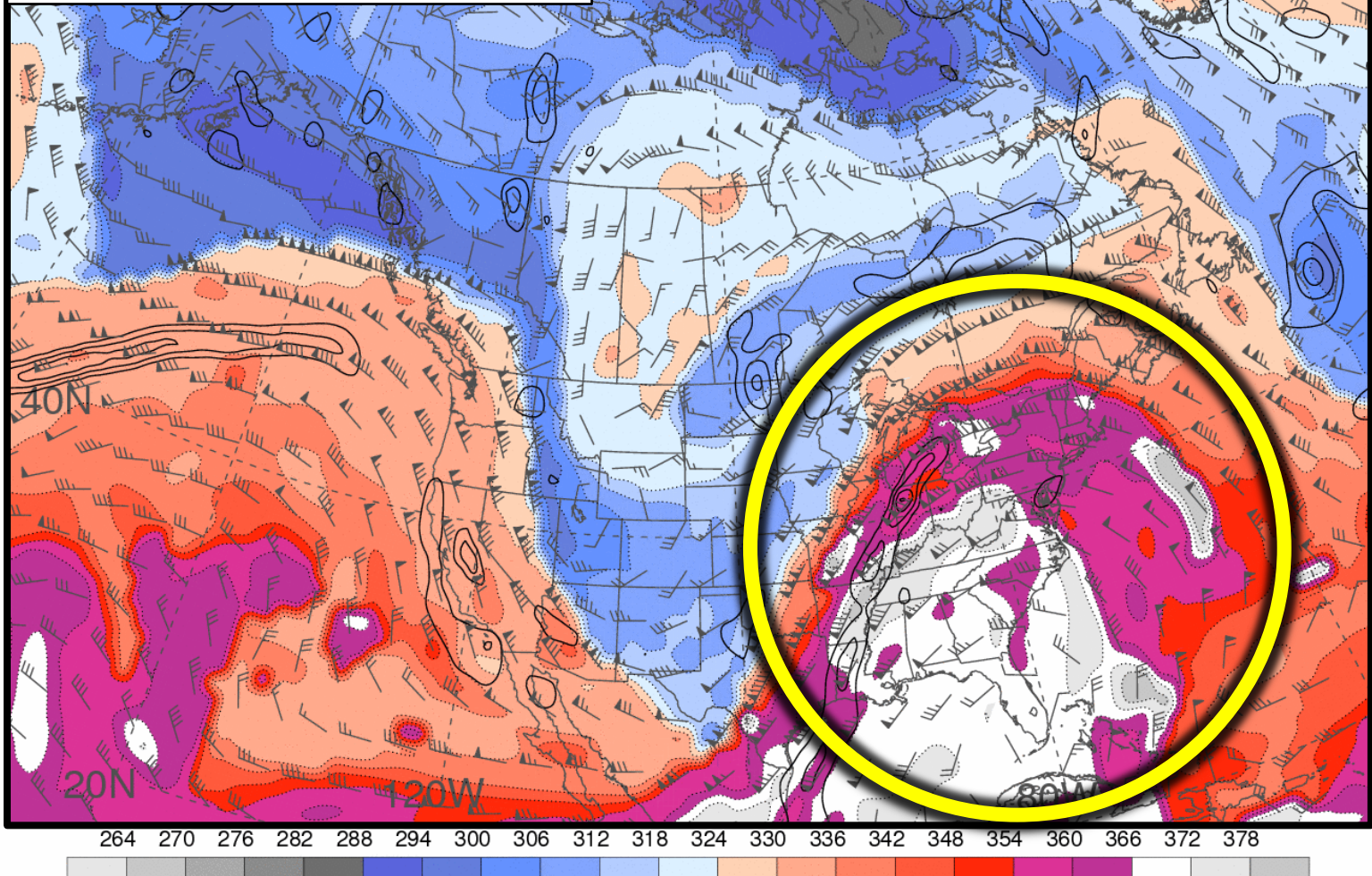
Pyle et al. (2004)



Jet Superposition Conceptual Model

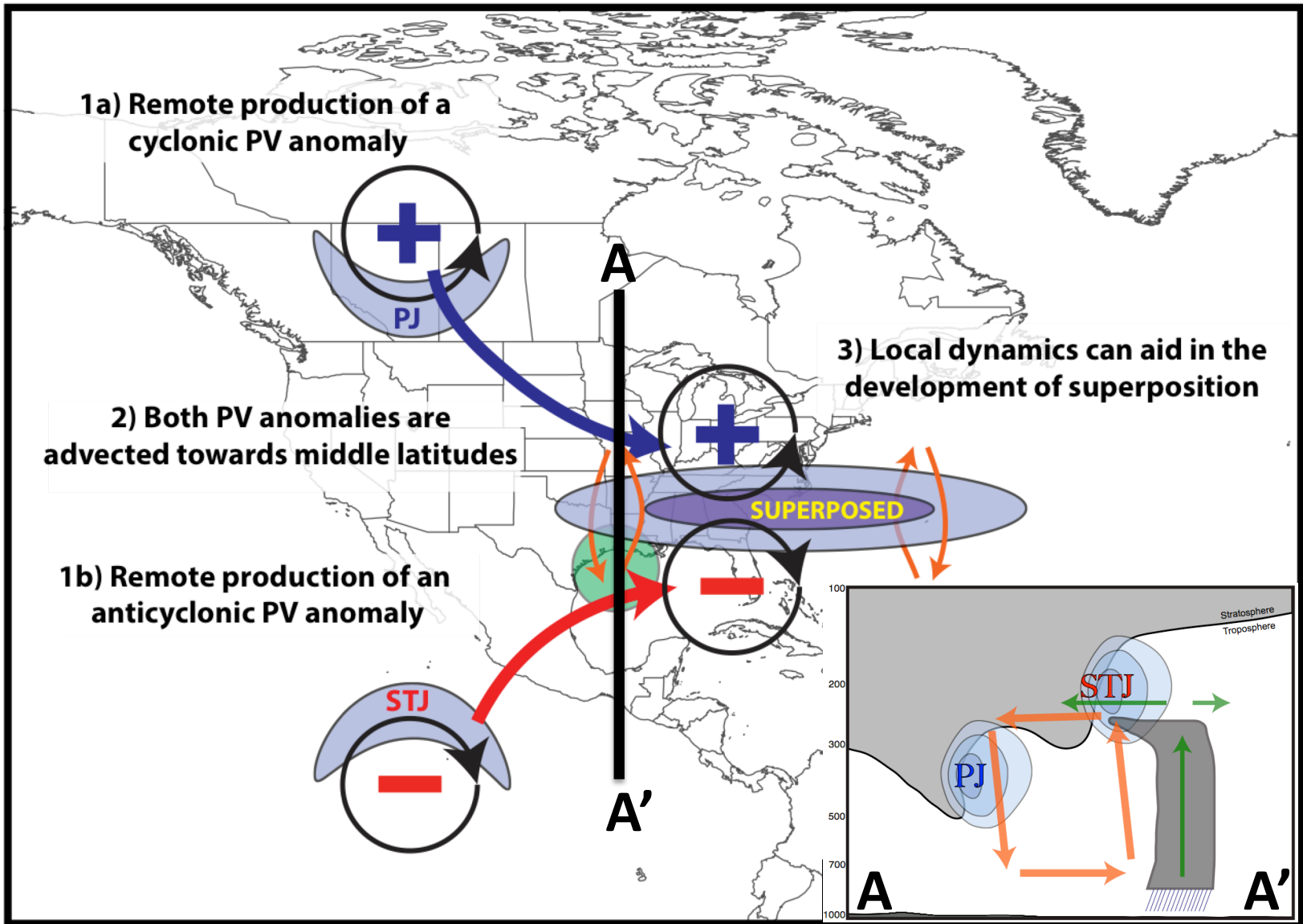
Dynamic Tropopause
Potential Temperature

Heather Archambault



DT THTA & WND; LL REL VORT 100502/1200

Jet Superposition Conceptual Model



Ageostrophic Transverse Jet Circulations

Traditional four-quadrant model

Geo. cold-air advection (CAA)

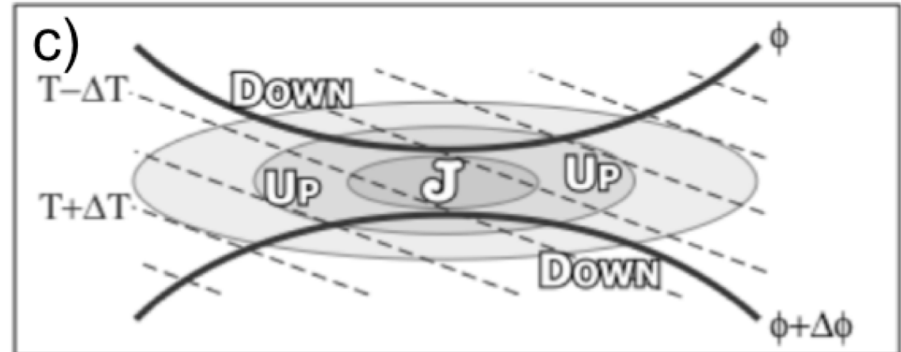
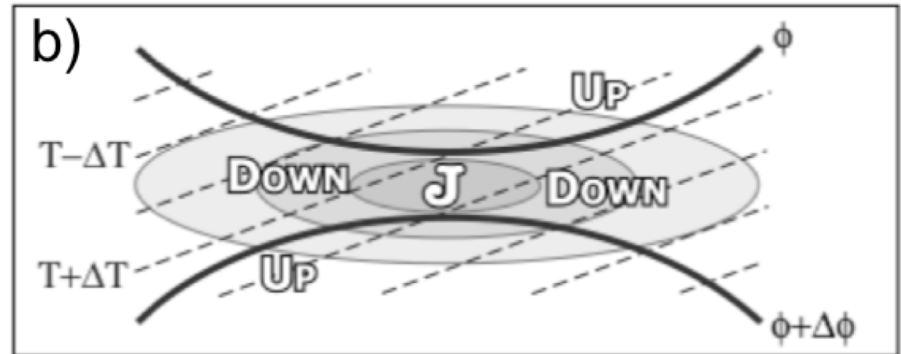
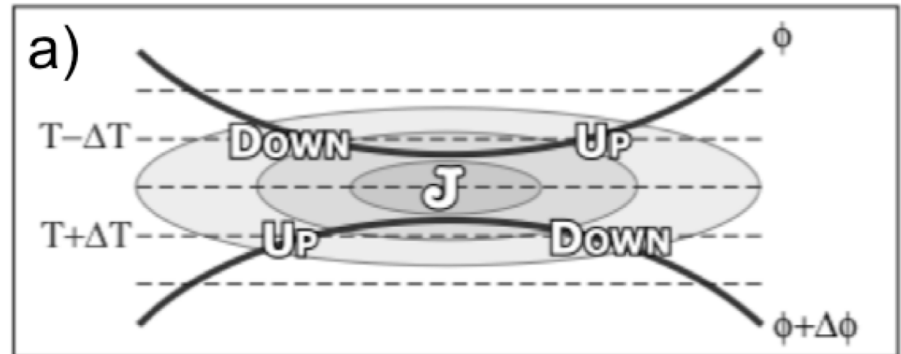
along the jet axis promotes **subsidence** through the jet core

Geo. warm-air advection (WAA)

along the jet axis promotes **ascent** through the jet core

Lang and Martin (2012)

Upper Troposphere

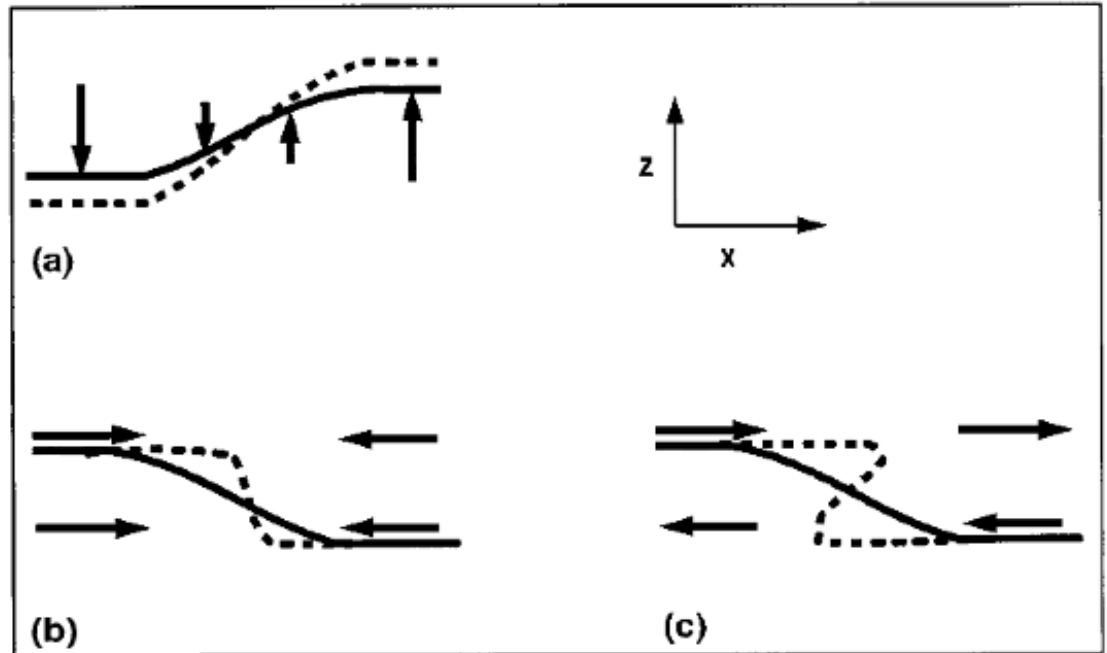


Background

Insight into how the tropopause can be restructured from a PV perspective can be found by consulting Wandishin et al. (2000)

Two processes can account for “foldogenesis”:

- 1) **Differential vertical motions** can vertically steepen the tropopause.
- 2) **Convergence or a vertical shear** can produce a differential horizontal advection of the tropopause surface.



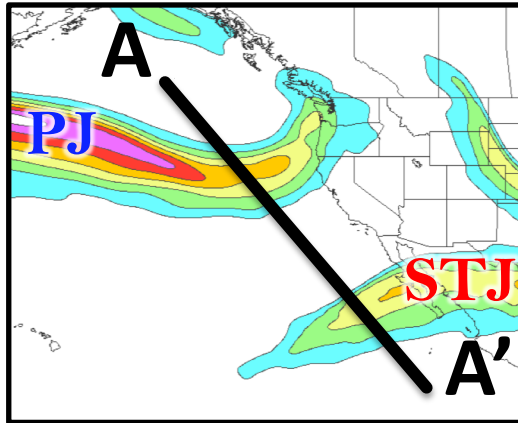
Wandishin et al. 2000

These same mechanisms are also likely to play an important role in superpositions.

Jet Identification

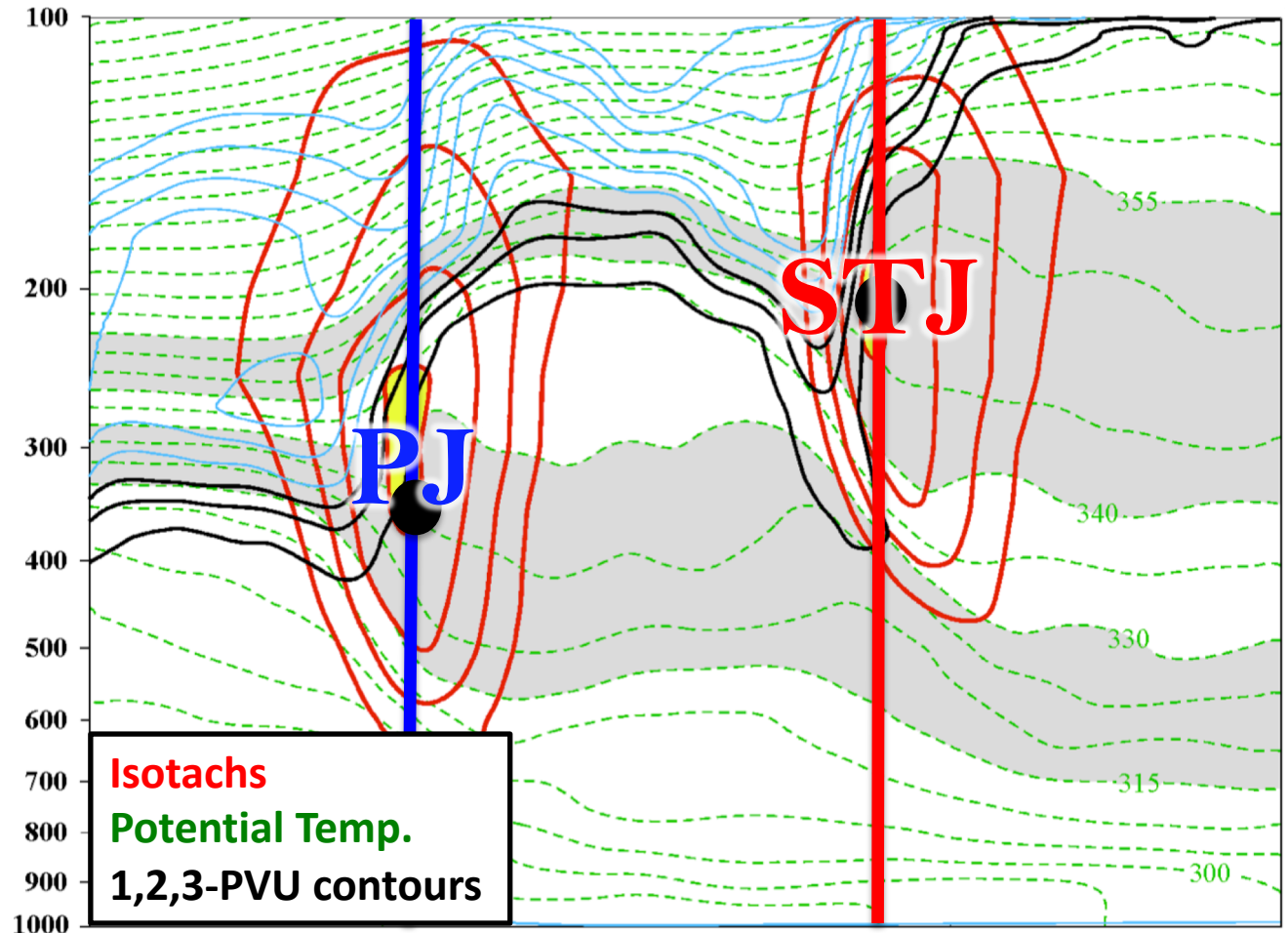
Jet Superposition Event Identification

0000 UTC 27 April 2010



250-hPa wind speed

Isolated grid points over North America in the CFSR (Saha et al. 2014) characterized by polar and subtropical jets during Nov–Mar 1979–2010.

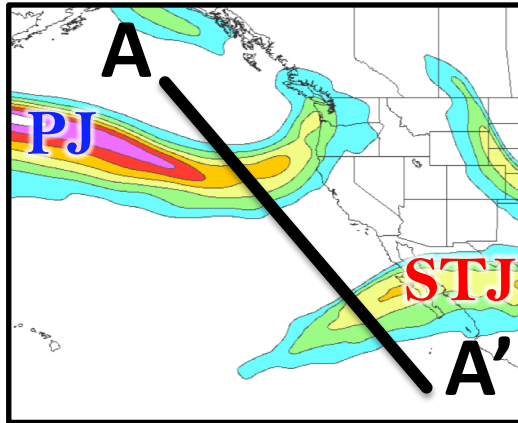


Isotachs
Potential Temp.
1,2,3-PVU contours

A Winters and Martin (2014, 2016, 2017); Christenson et al. (2017); Handlos and Martin (2016) **A'**

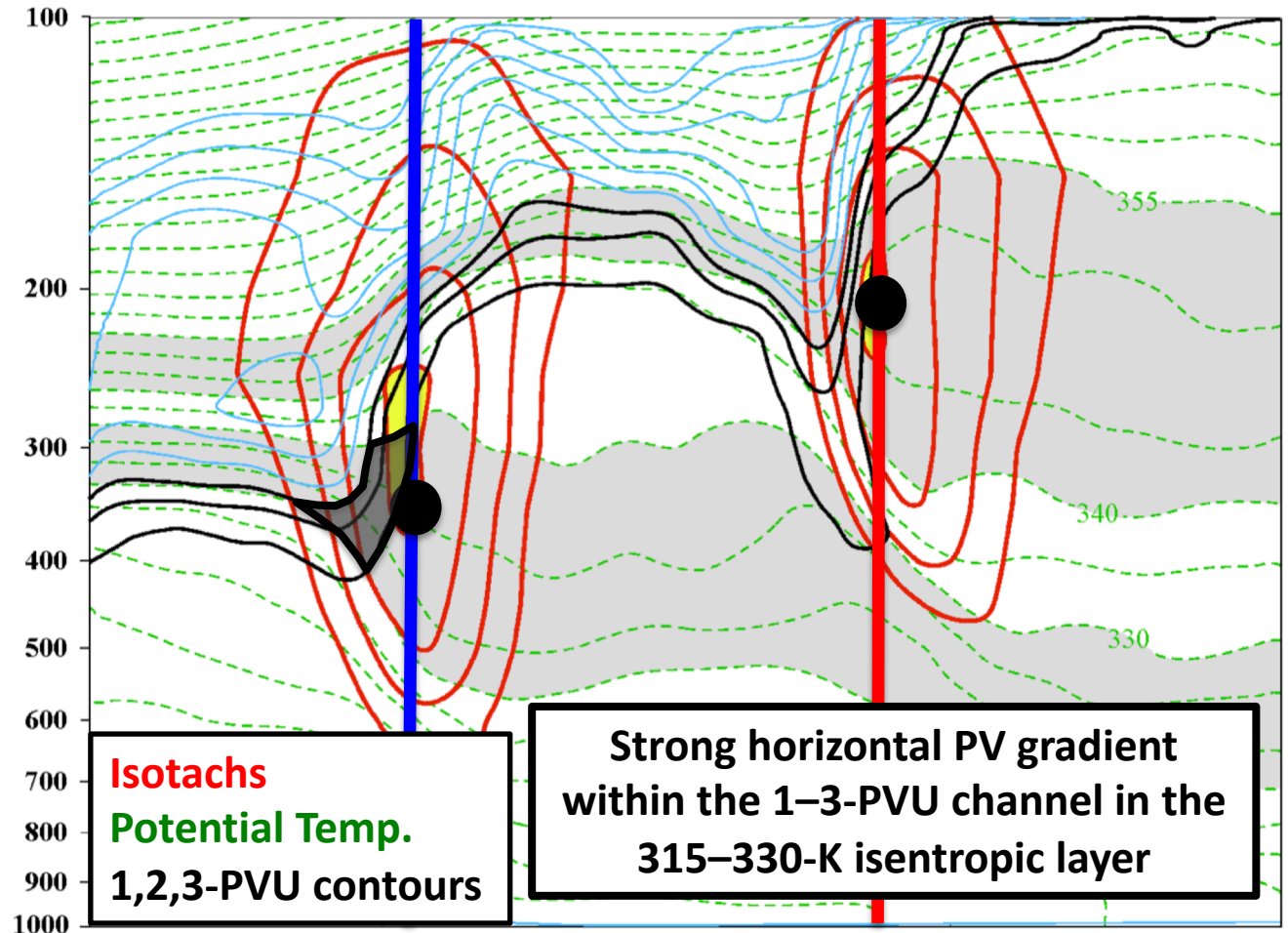
Jet Superposition Event Identification

0000 UTC 27 April 2010



250-hPa wind speed

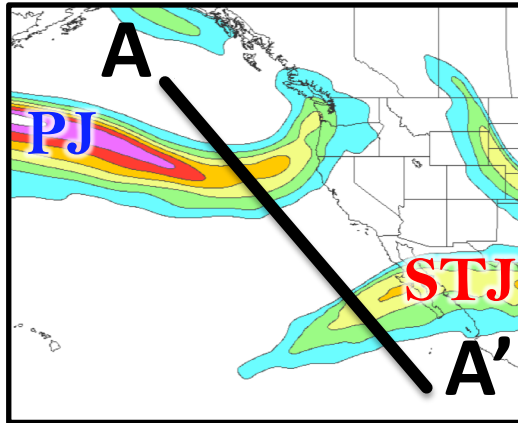
Isolated grid points over North America in the CFSR (Saha et al. 2014) characterized by polar and subtropical jets during Nov–Mar 1979–2010.



A Winters and Martin (2014, 2016, 2017); Christenson et al. (2017); Handlos and Martin (2016) **A'**

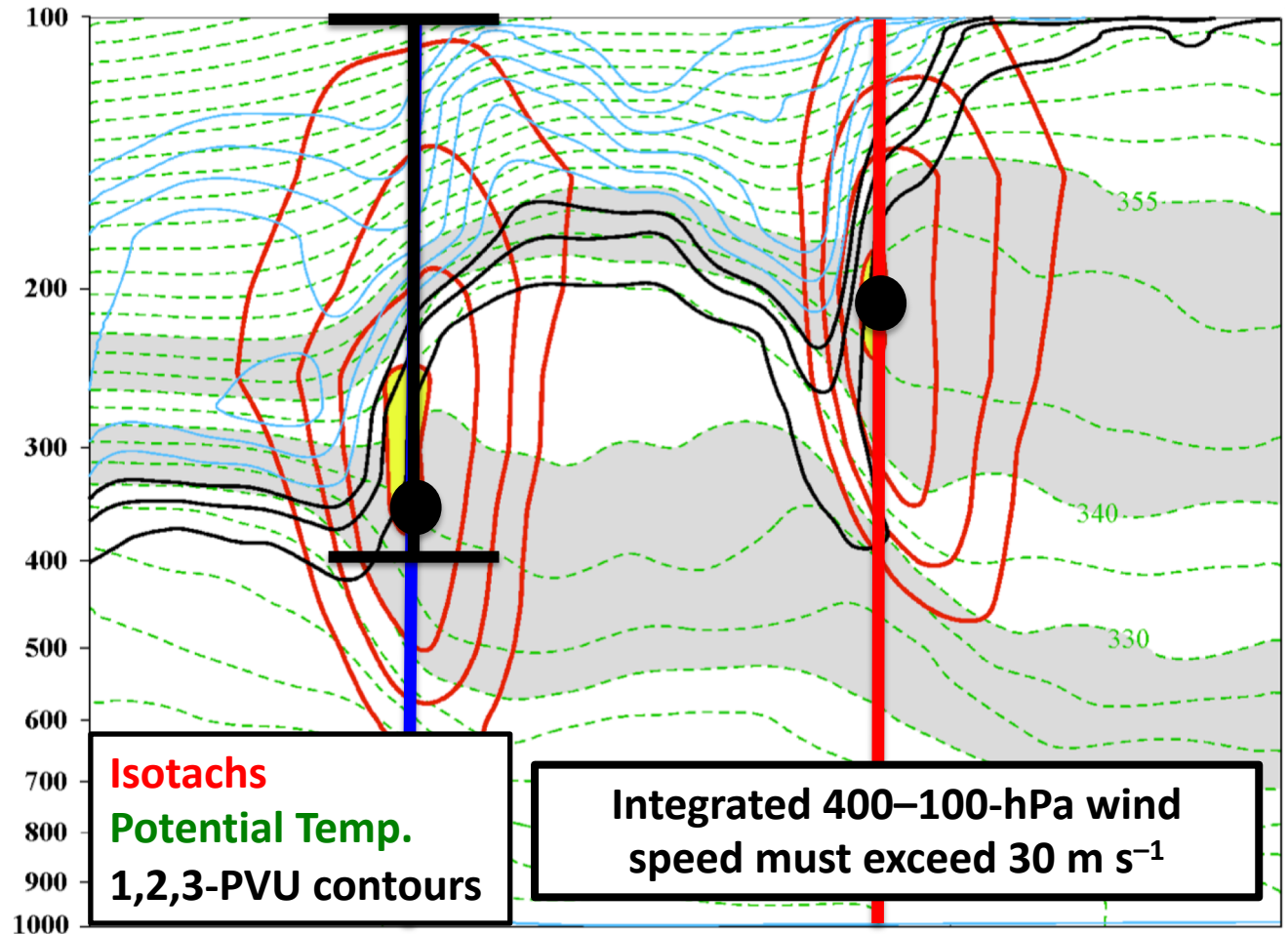
Jet Superposition Event Identification

0000 UTC 27 April 2010



250-hPa wind speed

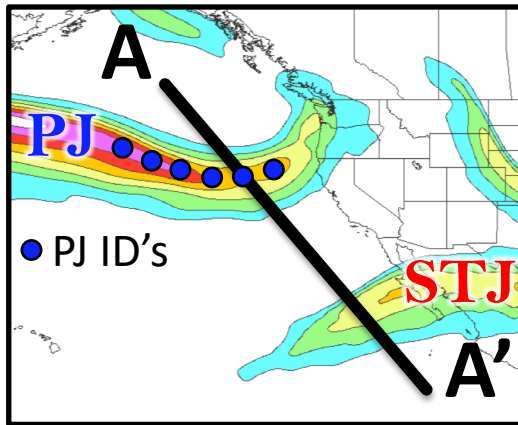
Isolated grid points over North America in the CFSR (Saha et al. 2014) characterized by polar and subtropical jets during Nov–Mar 1979–2010.



A Winters and Martin (2014, 2016, 2017); Christenson et al. (2017); Handlos and Martin (2016) **A'**

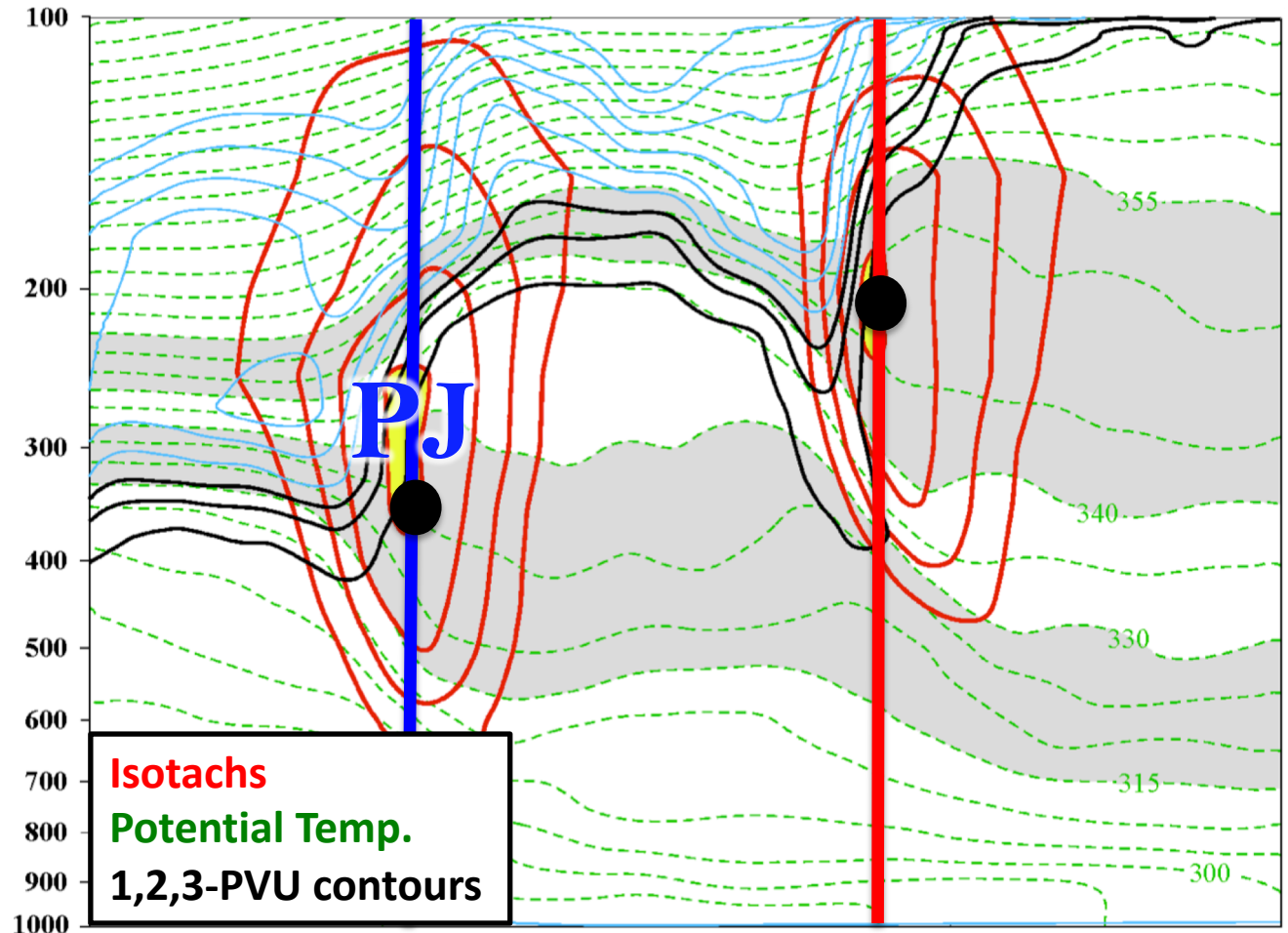
Jet Superposition Event Identification

0000 UTC 27 April 2010



250-hPa wind speed

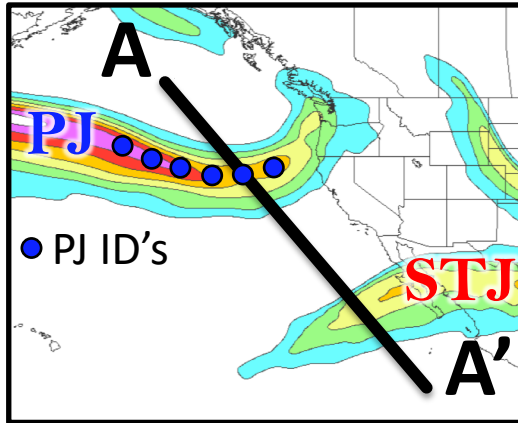
Isolated grid points over North America in the CFSR (Saha et al. 2014) characterized by polar and subtropical jets during Nov–Mar 1979–2010.



A Winters and Martin (2014, 2016, 2017); Christenson et al. (2017); Handlos and Martin (2016) **A'**

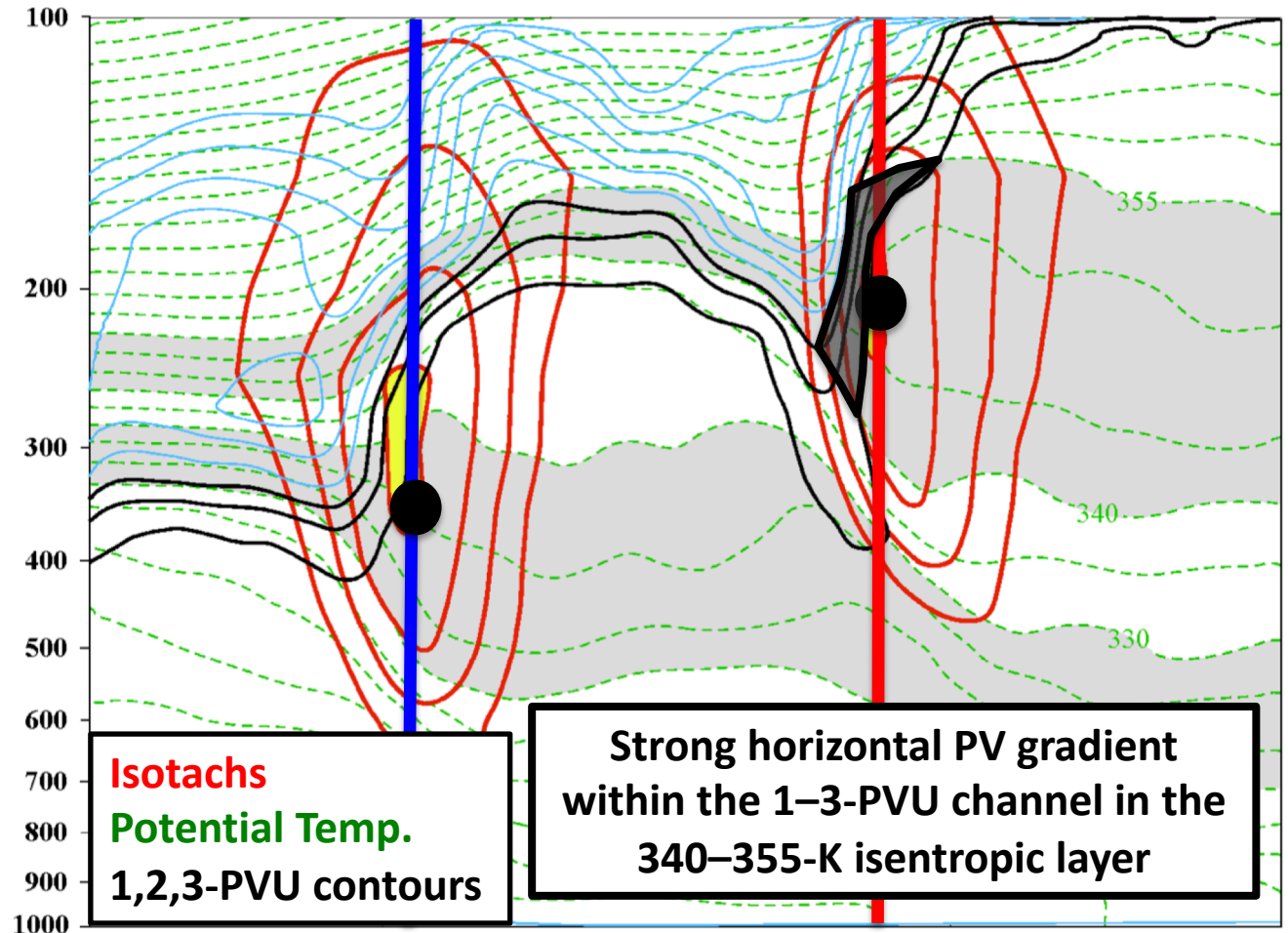
Jet Superposition Event Identification

0000 UTC 27 April 2010



250-hPa wind speed

Isolated grid points over North America in the CFSR (Saha et al. 2014) characterized by polar and subtropical jets during Nov–Mar 1979–2010.



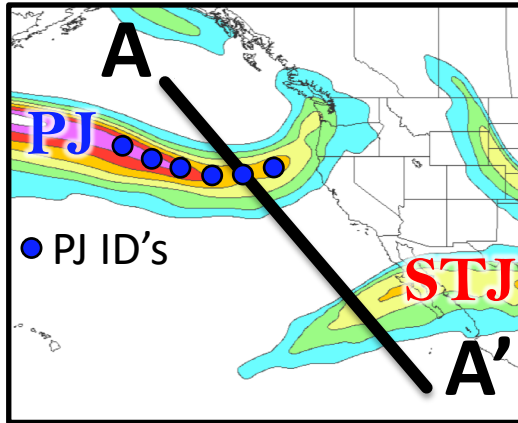
Isotachs
Potential Temp.
1,2,3-PVU contours

Strong horizontal PV gradient
within the 1–3-PVU channel in the
340–355-K isentropic layer

A Winters and Martin (2014, 2016, 2017); Christenson et al. (2017); Handlos and Martin (2016) **A'**

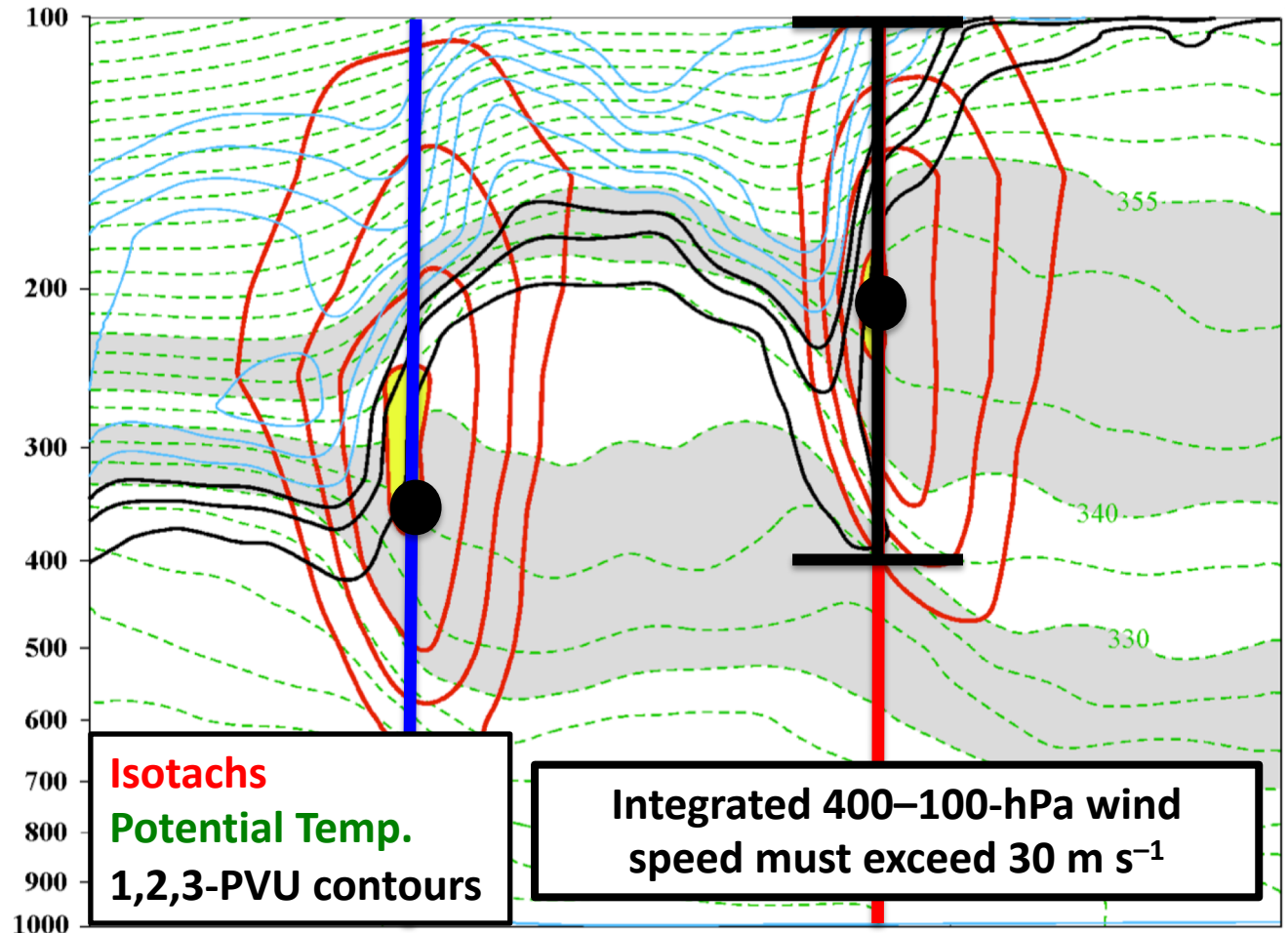
Jet Superposition Event Identification

0000 UTC 27 April 2010



250-hPa wind speed

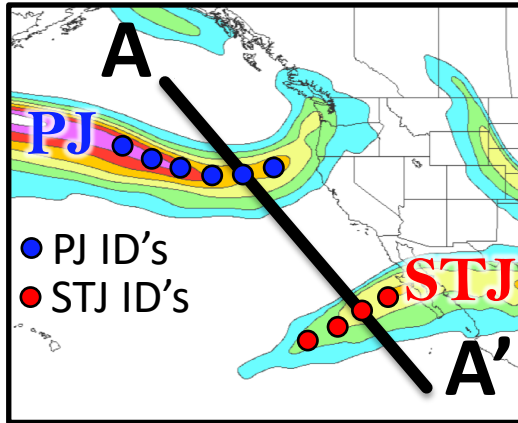
Isolated grid points over North America in the CFSR (Saha et al. 2014) characterized by polar and subtropical jets during Nov–Mar 1979–2010.



A Winters and Martin (2014, 2016, 2017); Christenson et al. (2017); Handlos and Martin (2016) **A'**

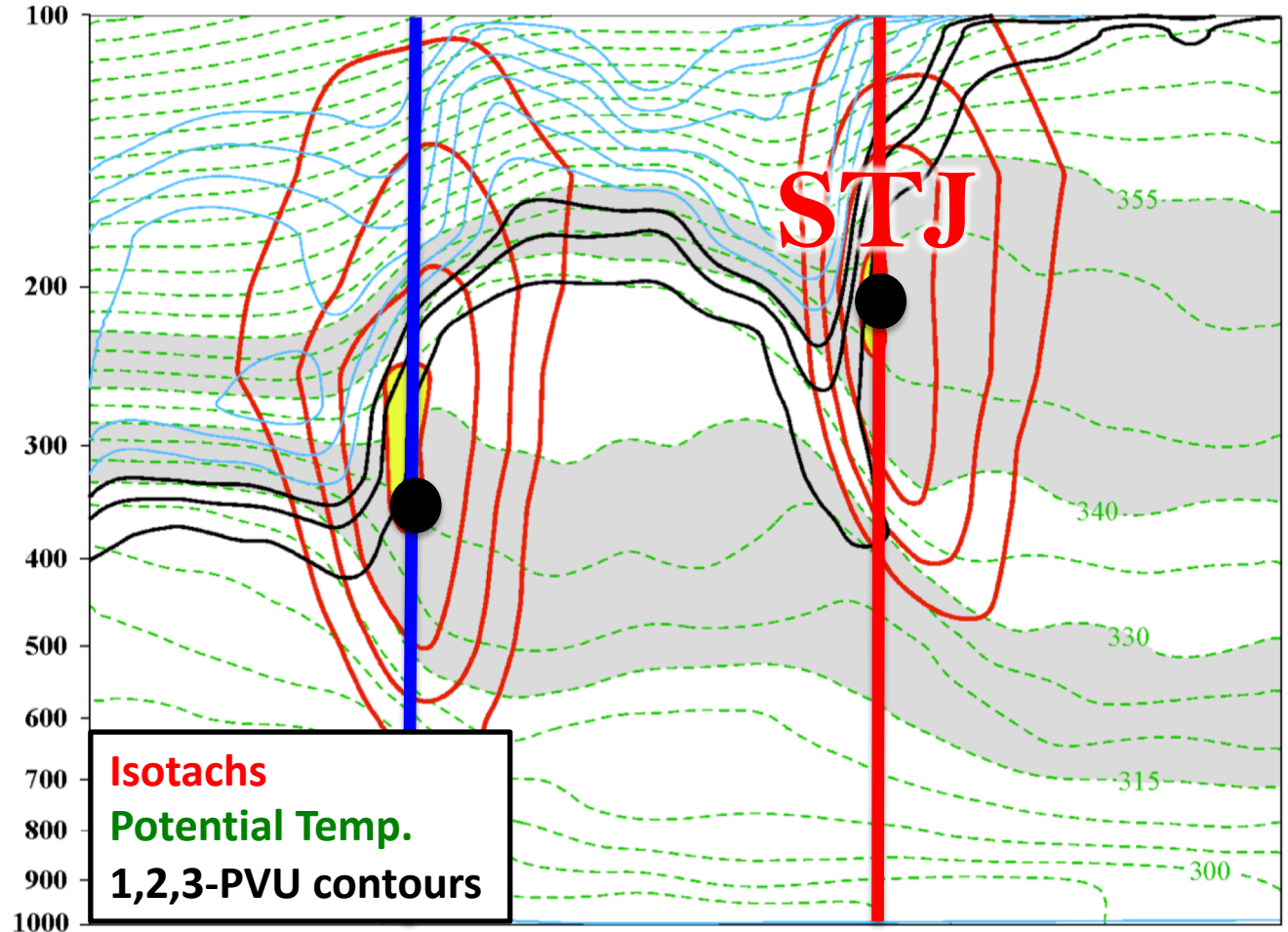
Jet Superposition Event Identification

0000 UTC 27 April 2010



250-hPa wind speed

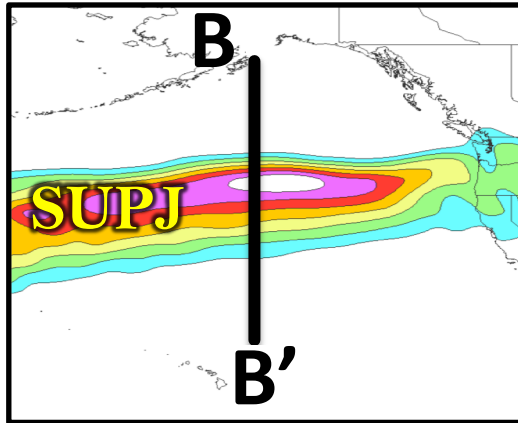
Isolated grid points over North America in the CFSR (Saha et al. 2014) characterized by polar and subtropical jets during Nov–Mar 1979–2010.



A Winters and Martin (2014, 2016, 2017); Christenson et al. (2017); Handlos and Martin (2016) **A'**

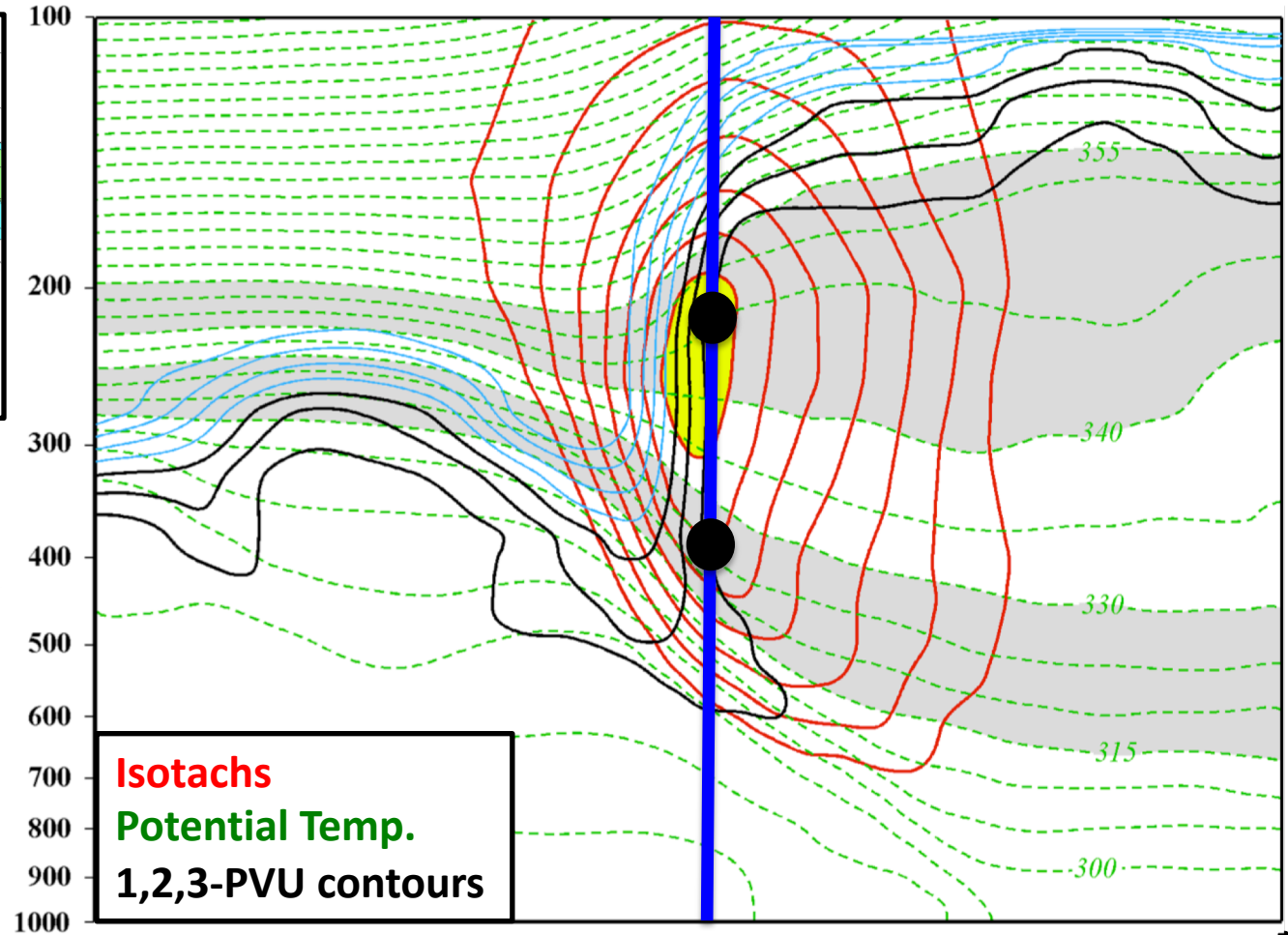
Jet Superposition Event Identification

0000 UTC 24 October 2010



250-hPa wind speed

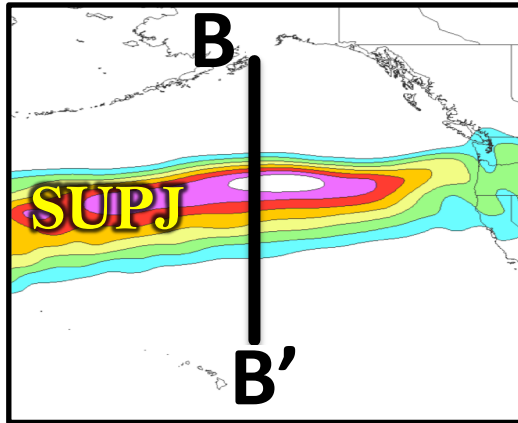
Isolated grid points over North America in the CFSR (Saha et al. 2014) characterized by a jet superposition during Nov–Mar 1979–2010.



B Winters and Martin (2014, 2016, 2017); Christenson et al. (2017); Handlos and Martin (2016) **B'**

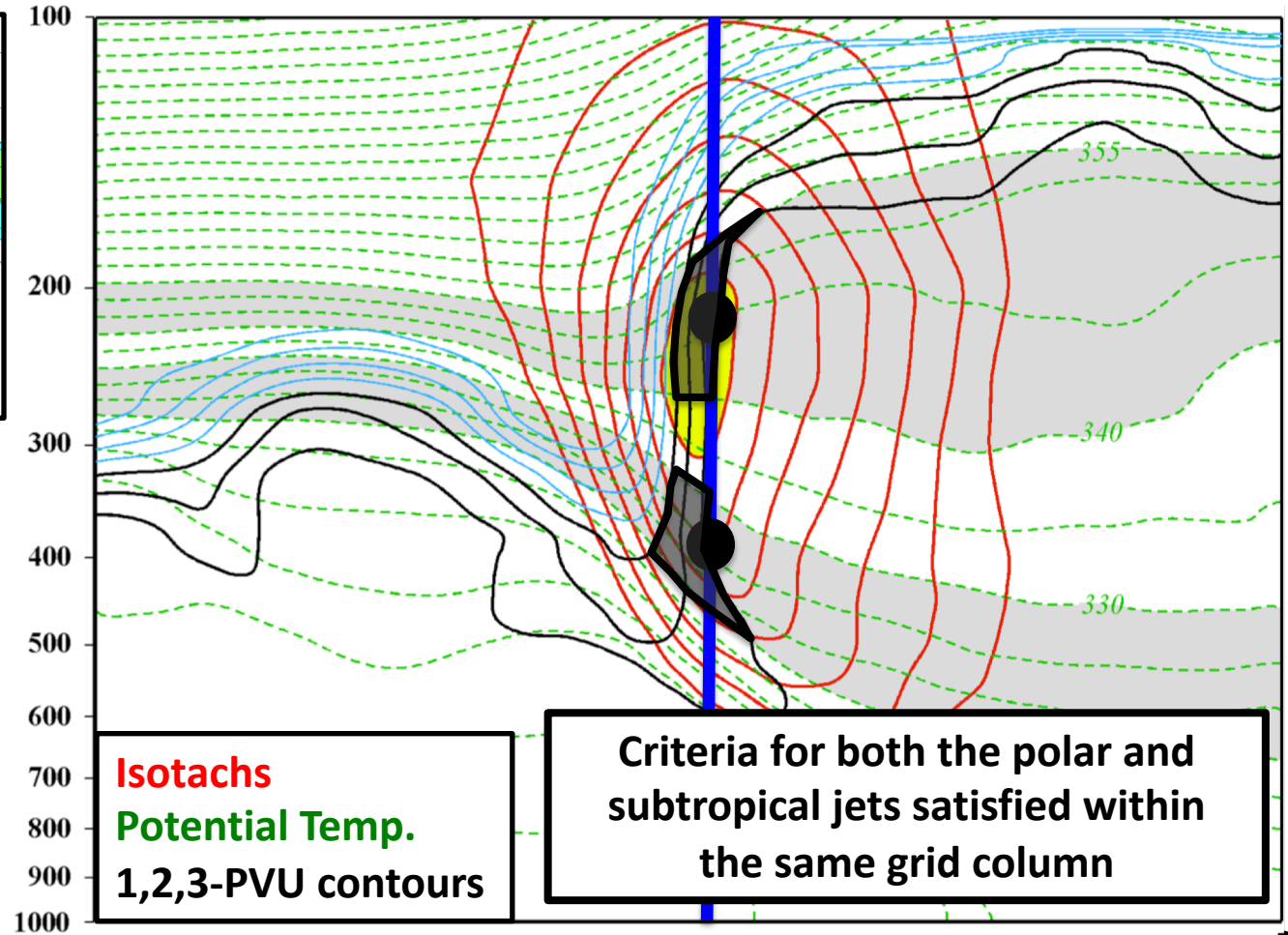
Jet Superposition Event Identification

0000 UTC 24 October 2010



250-hPa wind speed

Isolated grid points over North America in the CFSR (Saha et al. 2014) characterized by a jet superposition during Nov–Mar 1979–2010.



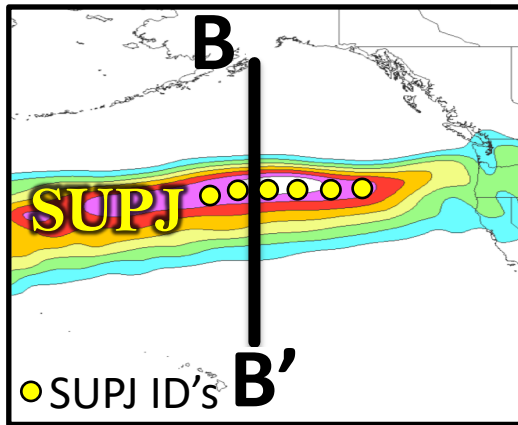
Isotachs
Potential Temp.
1,2,3-PVU contours

Criteria for both the polar and subtropical jets satisfied within the same grid column

B Winters and Martin (2014, 2016, 2017); Christenson et al. (2017); Handlos and Martin (2016) **B'**

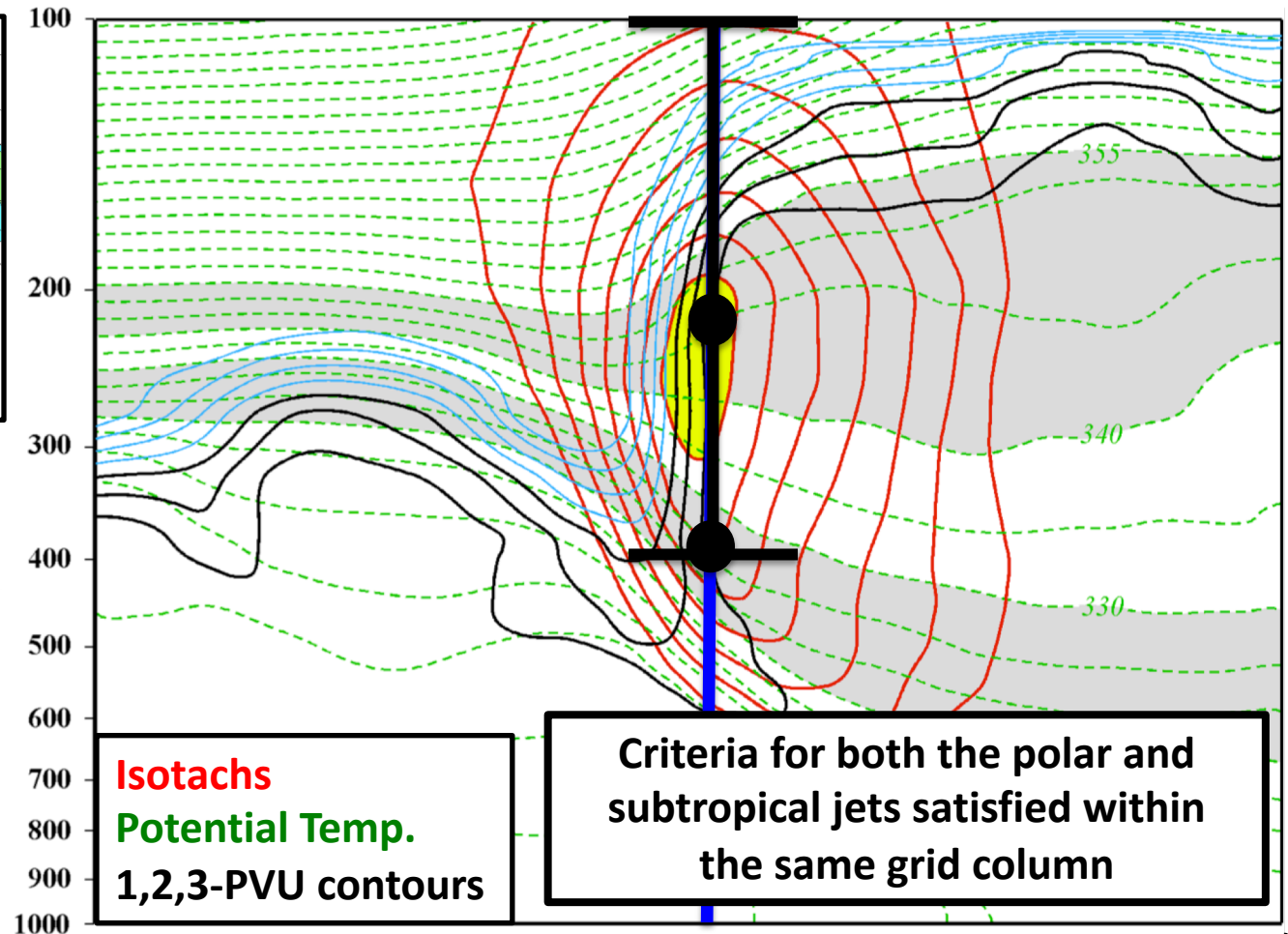
Jet Superposition Event Identification

0000 UTC 24 October 2010



250-hPa wind speed

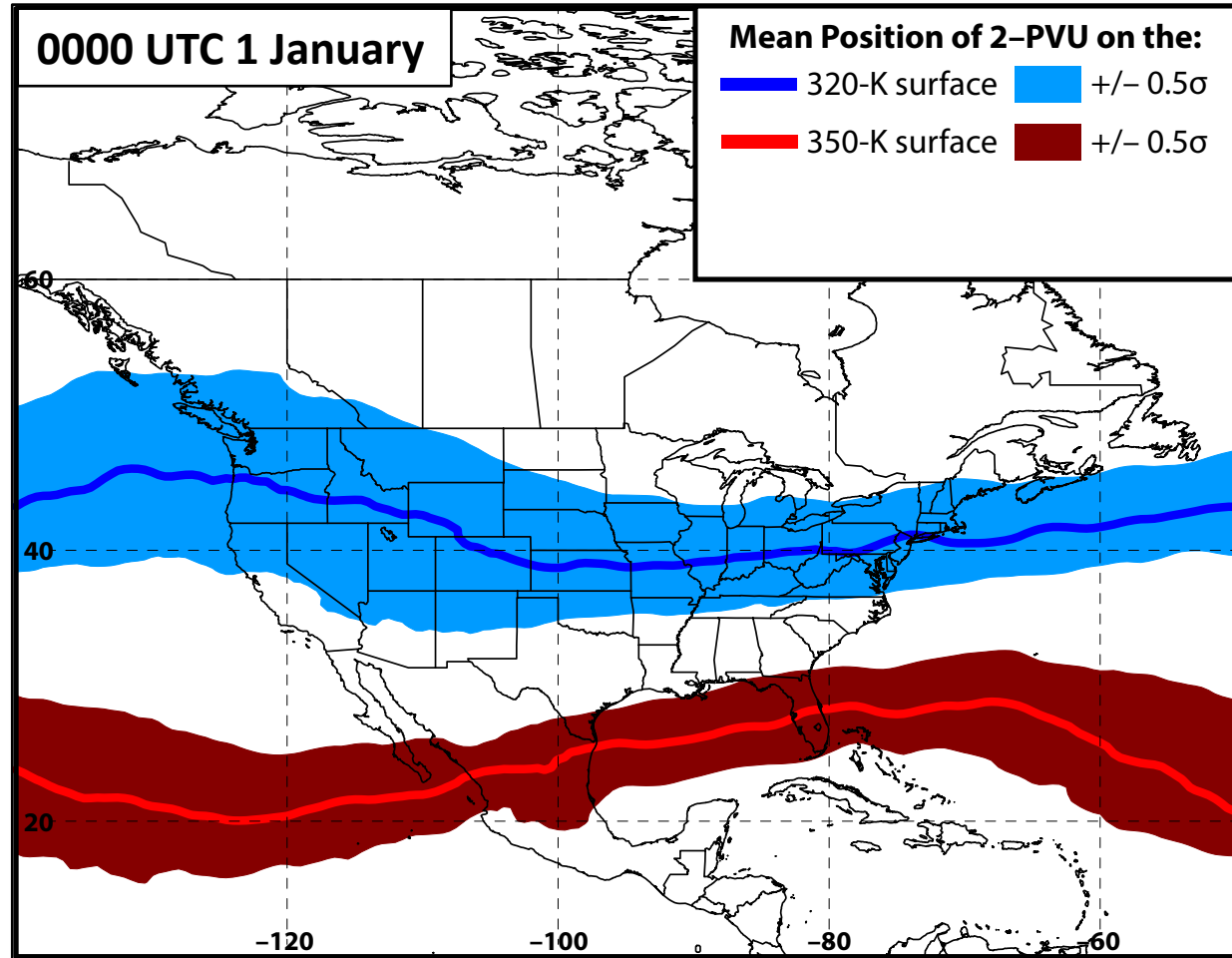
Isolated grid points over North America in the CFSR (Saha et al. 2014) characterized by a jet superposition during Nov–Mar 1979–2010.



B Winters and Martin (2014, 2016, 2017); Christenson et al. (2017); Handlos and Martin (2016) **B'**

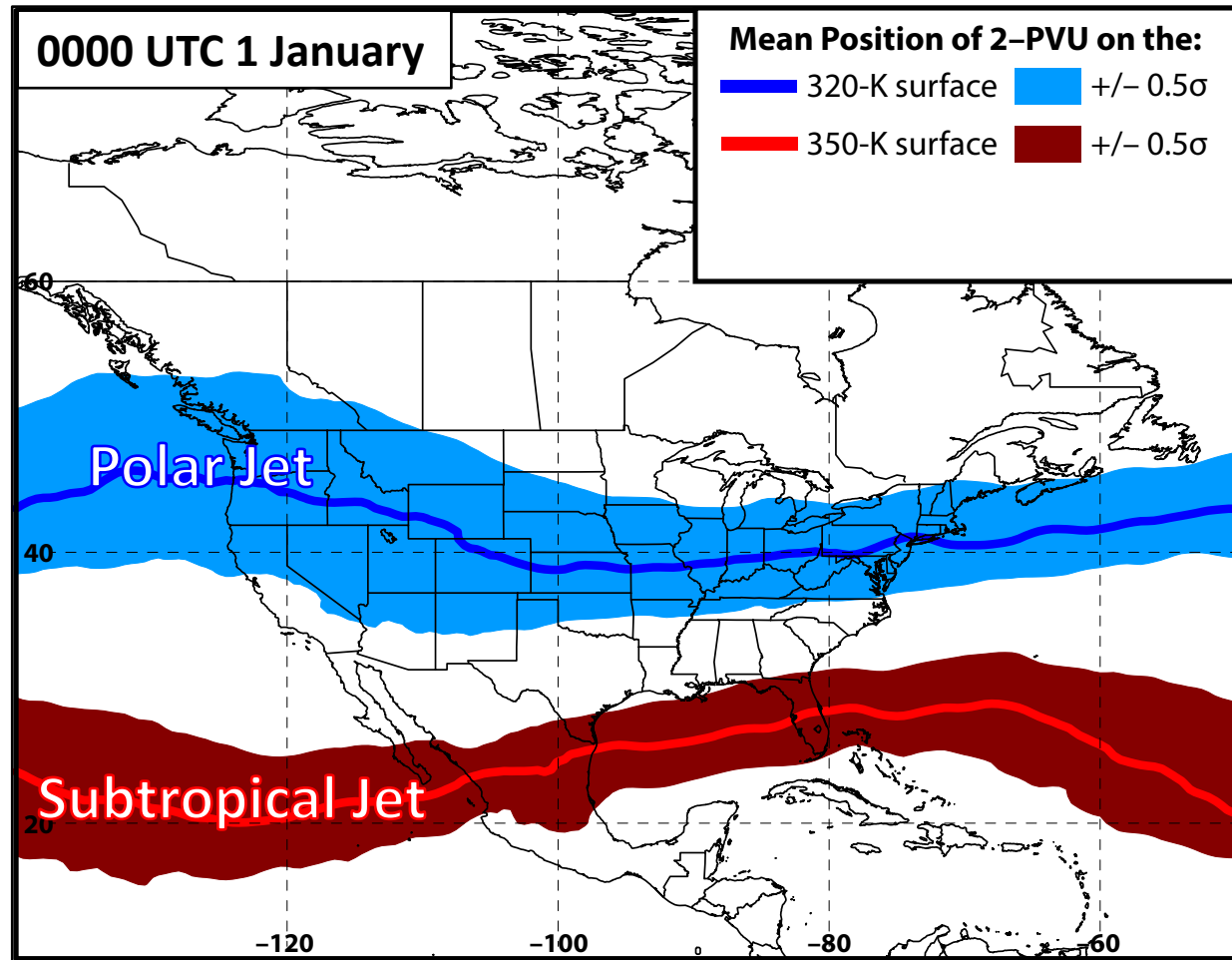
Jet Superposition Event Classification

1. Determined the mean position of the 2-PVU contour on the 320-K and 350-K surfaces at each analysis time in the CFSR.



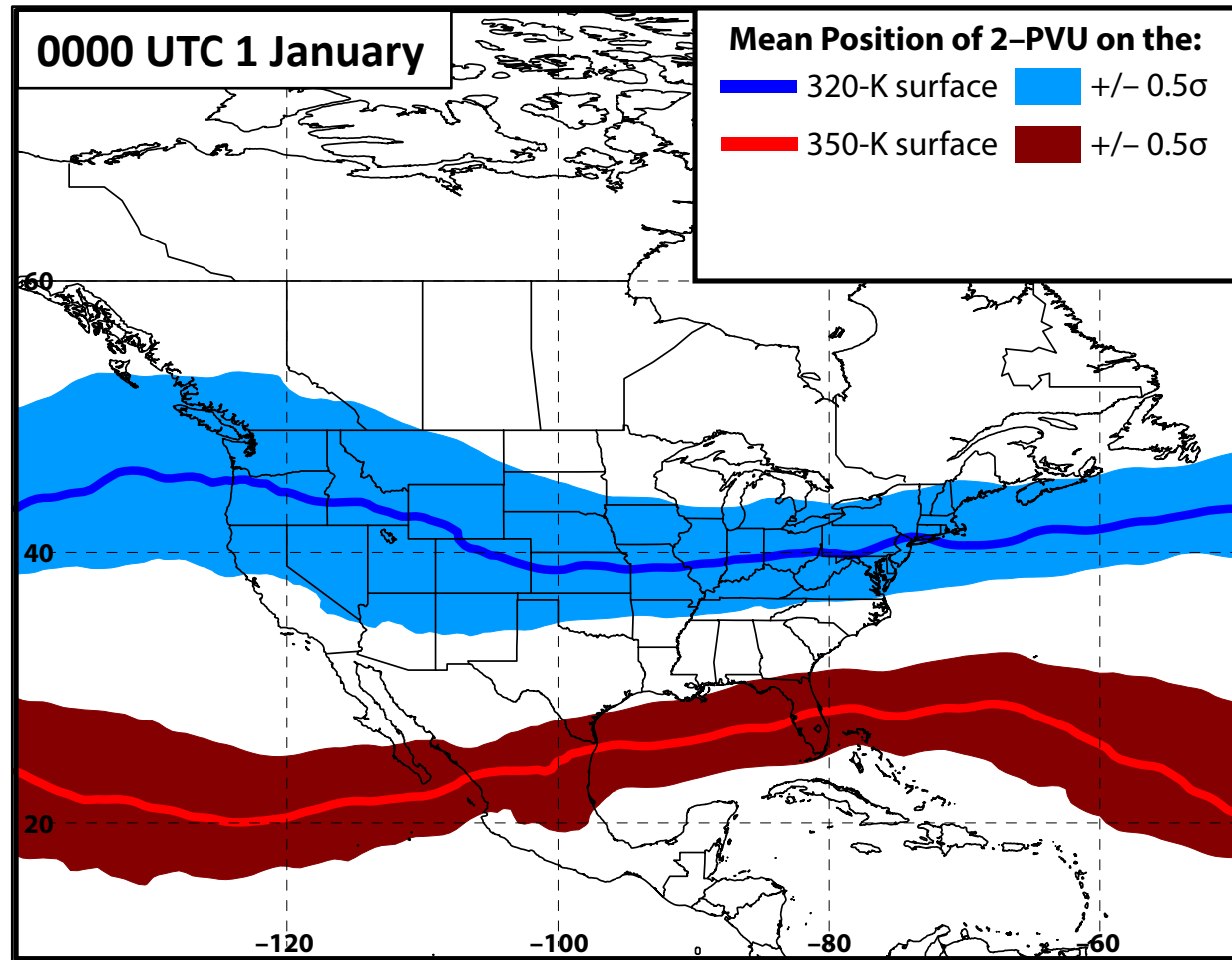
Jet Superposition Event Classification

1. Determined the mean position of the 2-PVU contour on the 320-K and 350-K surfaces at each analysis time in the CFSR.



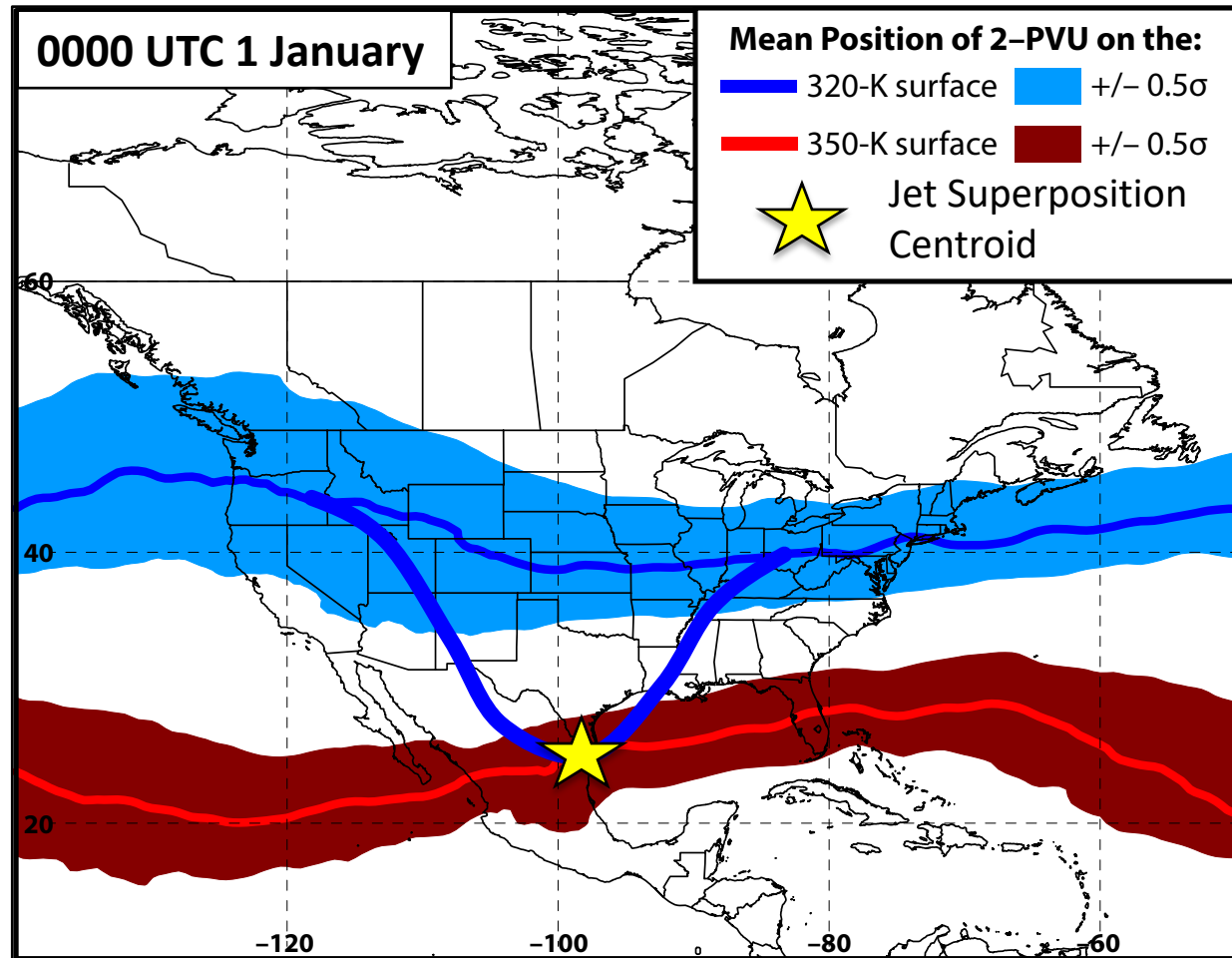
Jet Superposition Event Classification

1. Determined the mean position of the 2-PVU contour on the 320-K and 350-K surfaces at each analysis time in the CFSR.
2. Compared the position of the jet superposition centroid at the start of each event against the climatological position of the 2-PVU contour.



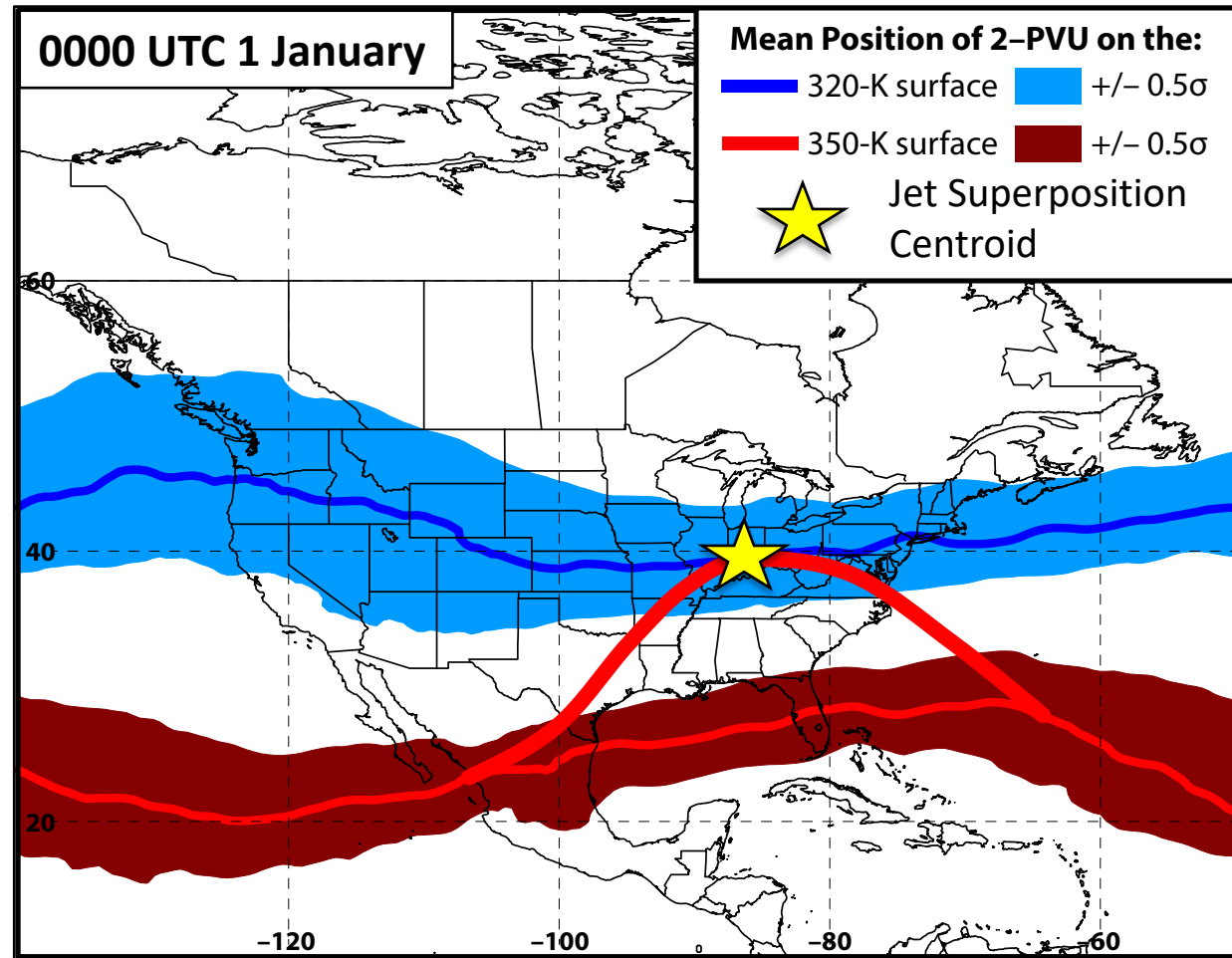
Jet Superposition Event Classification

1. Determined the mean position of the 2-PVU contour on the 320-K and 350-K surfaces at each analysis time in the CFSR.
 2. Compared the position of the jet superposition centroid at the start of each event against the climatological position of the 2-PVU contour.
- **Polar Dominant**



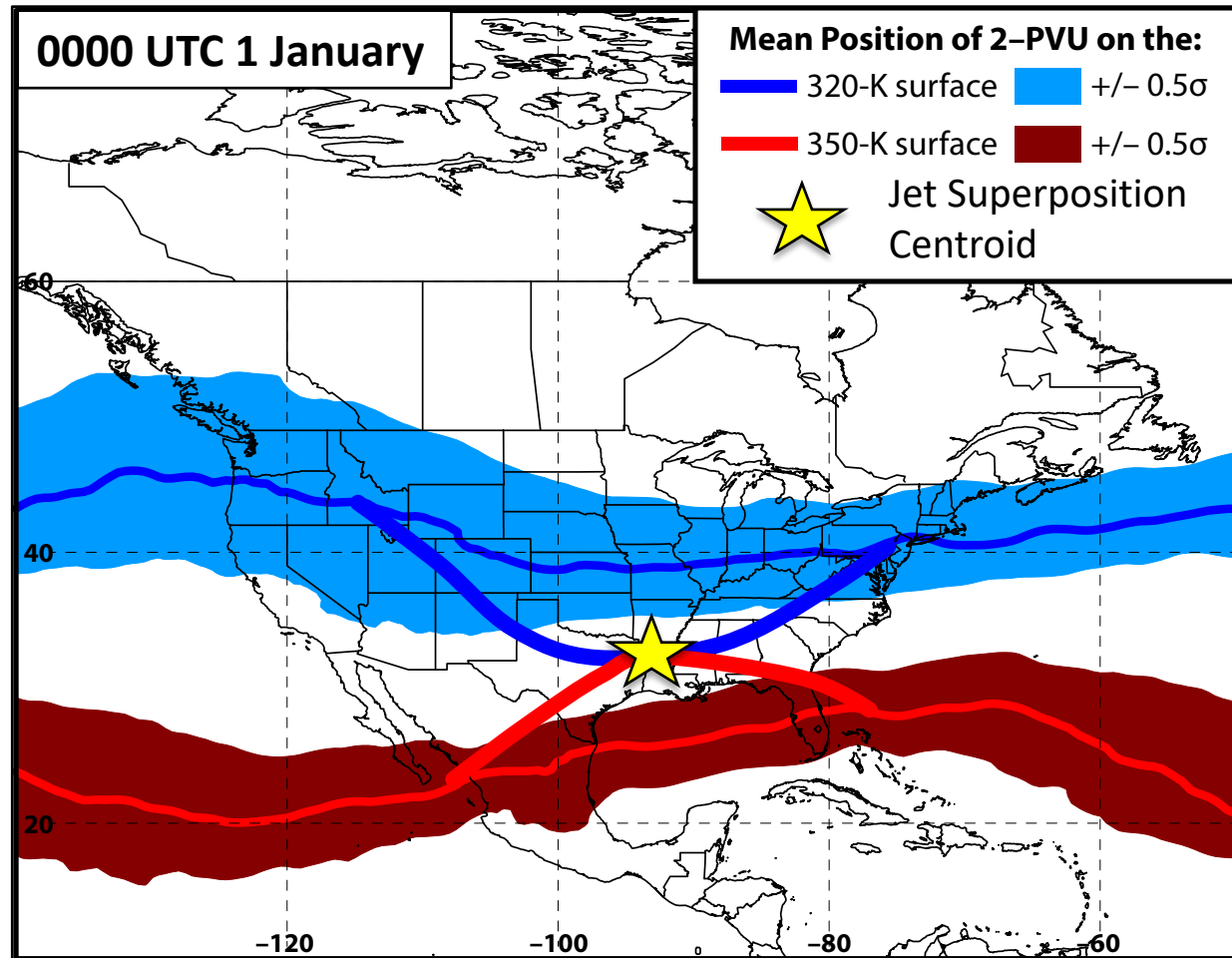
Jet Superposition Event Classification

1. Determined the mean position of the 2-PVU contour on the 320-K and 350-K surfaces at each analysis time in the CFSR.
 2. Compared the position of the jet superposition centroid at the start of each event against the climatological position of the 2-PVU contour.
- Polar Dominant
 - **Subtropical Dominant**

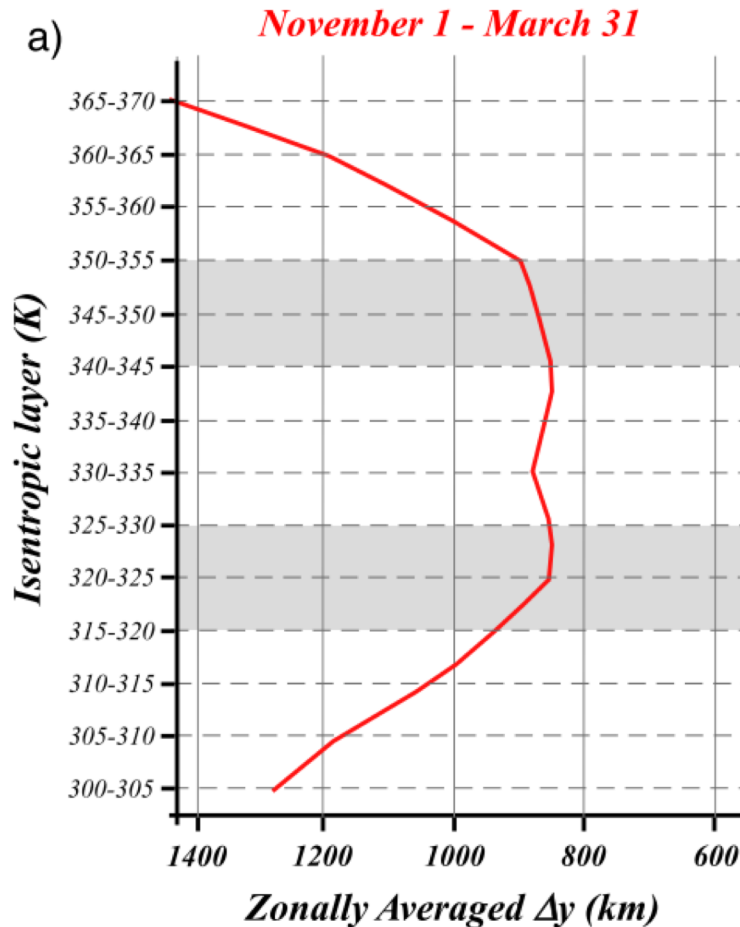


Jet Superposition Event Classification

1. Determined the mean position of the 2-PVU contour on the 320-K and 350-K surfaces at each analysis time in the CFSR.
 2. Compared the position of the jet superposition centroid at the start of each event against the climatological position of the 2-PVU contour.
- Polar Dominant
 - Subtropical Dominant
 - **Hybrid**



Background



Christenson et al. (2017)

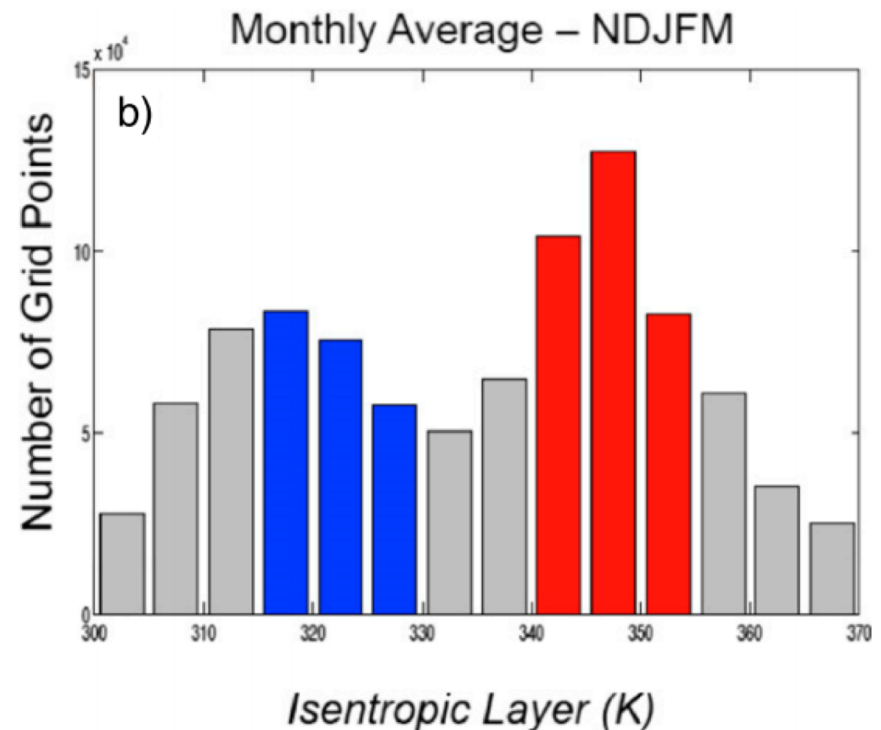
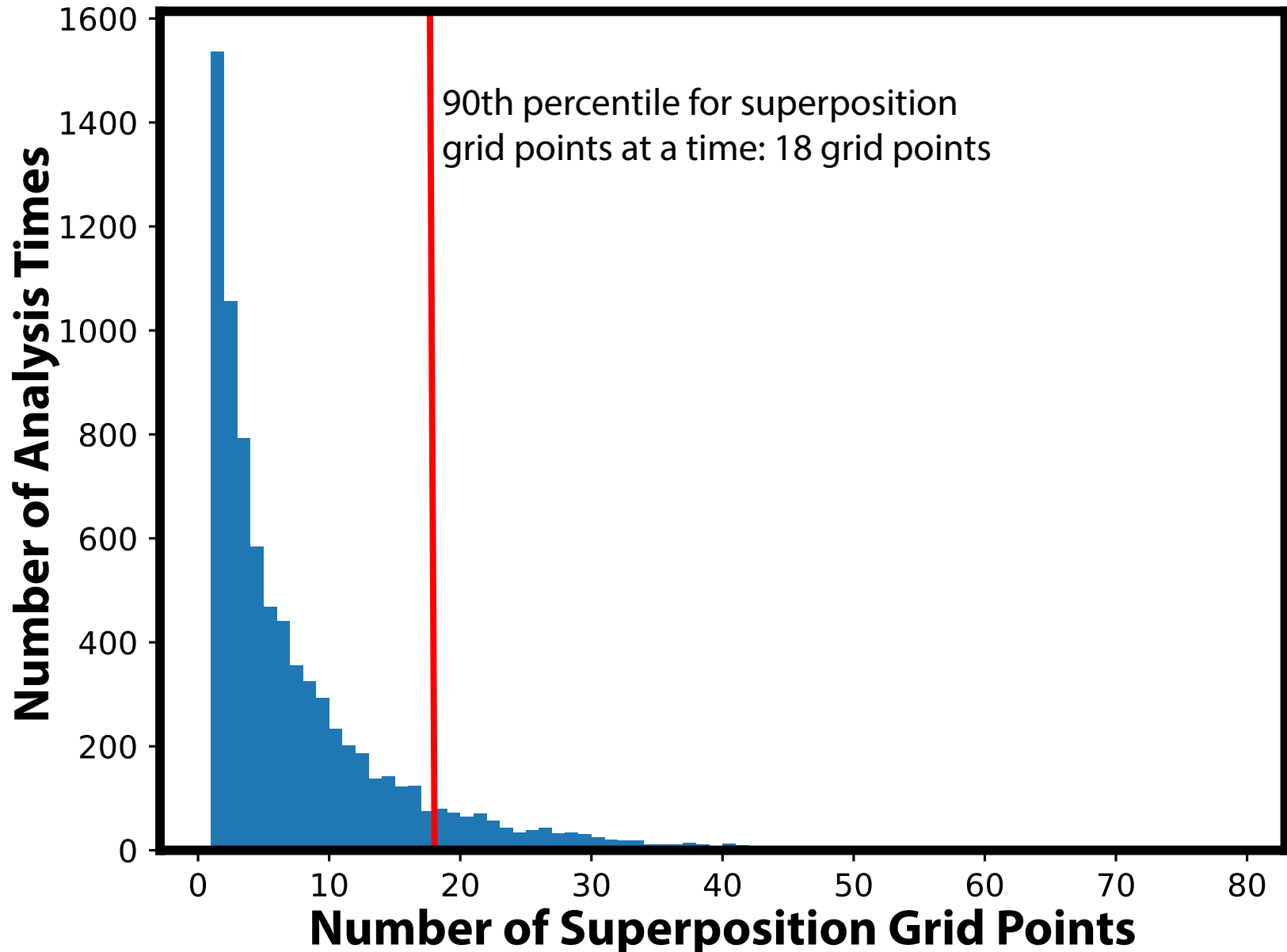


FIG. 2. (a) Cold season average of zonally averaged Δy (km) for 5-K isentropic layers ranging from 300–305 to 365–370 K. The 315–330- and 340–355-K layers are highlighted in light gray shading. (b) The average frequency of occurrence of grid points with a maximum wind speed value within the 5-K isentropic layers along the abscissa per cold season. The 315–330- and 340–355-K layers are shaded in blue and red, respectively.

Jet Superposition Event Identification

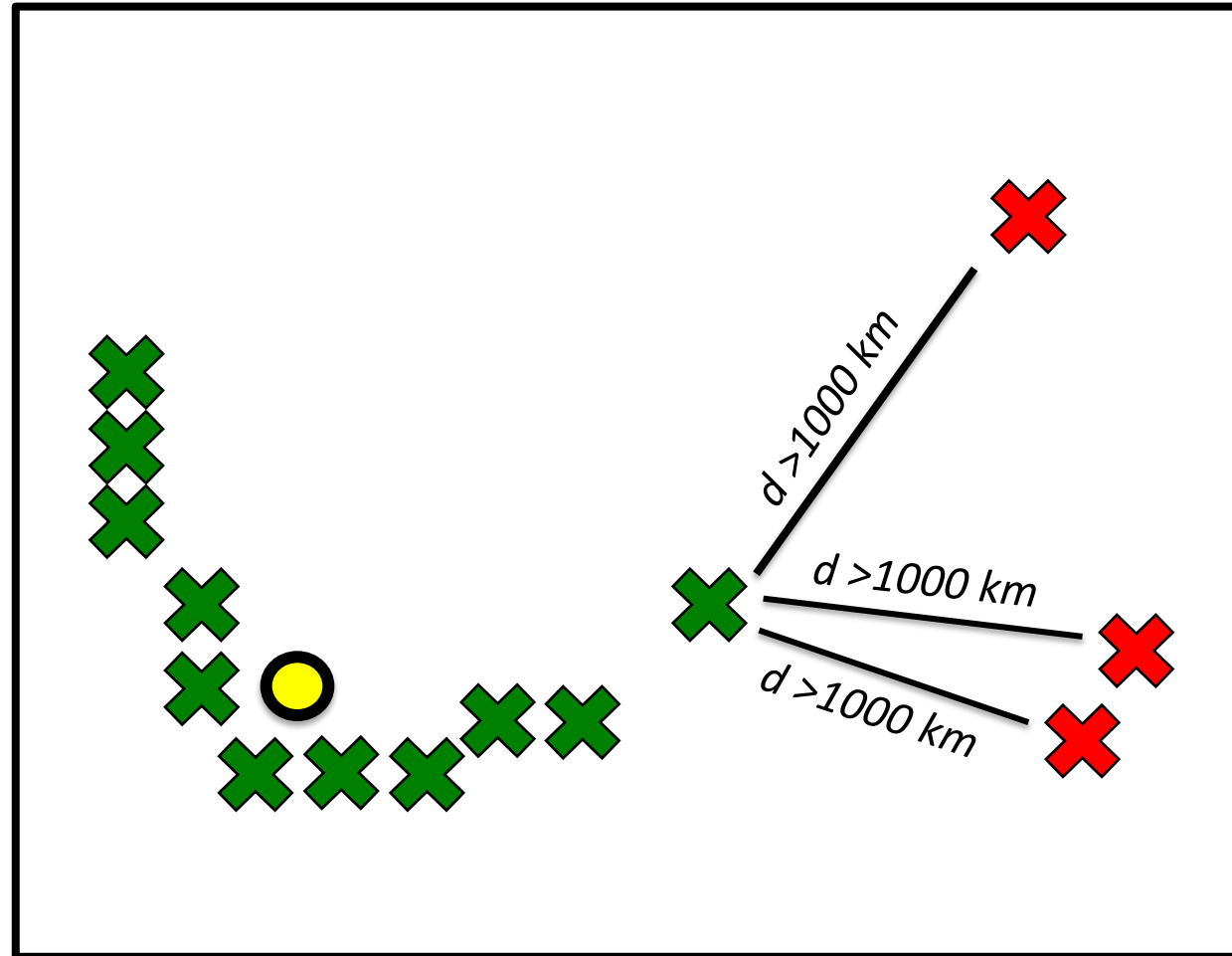


Jet Superposition Event Identification

Sample Jet Superposition Centroid Calculation

Calculated the centroid of each jet superposition based on all valid grid points at a particular analysis time.

To calculate the centroid, there must exist a group of 18 superposition grid points, of which no superposition grid point is >1000 km away from another superposition grid point.



✕ Used for calculation

✕ Not used for calculation

● Jet superposition centroid